The Thesis committee for Hyun Tae Yang

Certifies that this is the approved version of the following thesis

Development of Improved ASP Formulations for Reactive and Non-reactive Crude Oils

Approved by
Supervising Committee:

Gary A. Pope (Supervisor)

Chun Huh (Co-Supervisor)

Upali Weerasooriya

Development of Improved ASP Formulations for Reactive and Non-reactive Crude Oils

by

Hyun Tae Yang, B.S.

Thesis

Presented to the Faculty of the Graduate School of

The University of Texas at Austin

in Partial Fulfillment

of the Requirements

for the Degree of

Master of Science in Engineering

The University of Texas at Austin

December, 2010

Dedication

To God, my family and people who believe in this work

Acknowledgements

It is my honor to have been a student in the petroleum engineering graduate program at The University of Texas at Austin and I really appreciate all the people who helped me to learn and grow. First, I would like to mention my special thanks to Dr. Gary A. Pope for all his guidance and support. He has challenged me continuously to improve myself and be a real petroleum engineer and inspired me as a role model in this field. I can't express all my truthful appreciation for his supervision and support by words. Next I want to thank Dr. Chun Huh for his constant encouragement and mentoring and Dr. Upali Weerasooriya, Senior Research Fellow and Director of Surfactant Development, for his valuable suggestions and careful explanations of surfactants and surfactant behavior and also for reading and making useful suggestions to this thesis.

The research staff of the Center for Petroleum and Geosystems Engineering was especially helpful in providing direction and insight to this research. I am very thankful to Dr. Do Hoon Kim and Christopher Britton for their support and instruction in the laboratory. They provided persistent technical to help me accomplish my research. Thanks also go out to the research staff Pathma Jith Liyanage, Stephanie Adkins, Thilini Kuruwita-Mudiyanselage, Gayani Pinnawala, Gayani W. Kennedy and Erandimala Udamini Kulawardana for their valuable suggestions. I am grateful to Glen Baum, Tony Bermudez, Don Sorrel and Gary Miscoe who helped me install experimental instruments and made equipment for my research. I would like to thank Esther Barrientes, Shelette Paulino, Kiki Peckham, Joanna Castillo, Frankie Hart and Cheryl Kruize for their constant assistance.

I would also like to thank many graduate and undergraduate students past and present within the chemical EOR research group who shared their experience with me and assisted me with the experiments. I want to thank to Siamak Chabokrow, Robert Matthew Dean, Heesong Koh, Ahra Lee, Kyunghaeng Lee, Sukkyoon Choi, Amos Kim, Jun Lu, Vinay M. Sahni, Nitish Koduru, Faiz K. Veedu, Abhinav Sharma, Sriram Solairaj, Vikram Chandrasekar, and Alex Vyssotski for their friendship and consistent assistance at all times. I appreciate the support of other members of chemical EOR research group.

I would like to thank Chevron for their support of the UT-Chevron Alliance for EOR that provided part of the financial support for this research and to all of the industrial sponsors of the CPGE Chemical EOR industrial affiliates program for their support. I would also like to thank Stepan, Harcros, Shell Chemical, and Sasol for providing surfactant samples and SNF Floerger for supplying polymer samples. In particular, I would like to say thank to Vardarajan Dwarakanath Ping Zhao with Chevron, Jieyuan Zhang and Ravi Ravikiran with TIORCO, and Christopher Heinson with Oxy for their help and support.

Last, but not least, I would like to thank to family, Nakso Yang, Youngjin Ahn, Jaeyoon Shin, and Hyunmin Yang for their love, unconditional support and encouragement. Also I give many thanks to all the people around me for making me feel at home here. Everyone mentioned has contributed to my life I have had while completing my research at the University of Texas at Austin.

December 2010

Abstract

Development of Improved ASP Formulations for Reactive and Non-reactive Crude Oils

Hyun Tae Yang, M.S.E.

The University of Texas at Austin, 2010

Supervisor: Gary A. Pope

Co-Supervisor: Chun Huh

The ability to select low-cost, high-performance surfactants for a wide range of crude oils under a wide range of reservoir conditions has improved dramatically in recent years. Surfactant formulations (surfactant, co-surfactant, co-solvent, alkali, polymer, and electrolyte) were developed by using a refined phase behavior approach. Such formulations nearly always result in more than 90% oil recovery in core flood when good surfactants with good mobility control are used. The advances that have improved performance, reduced cost, increased robustness, and extended the range of reservoir conditions for these formulations are described in this work. There are thousands of

possible combinations of the chemicals that could be tested for each oil and each chemical combination requires many observations over a long time period at reservoir temperature for proper evaluation. It would take too long, cost too much and in many cases not even be feasible to test all combinations. In practice the scientific understanding is used to match up the surfactant/co-surfactant/co-solvent characteristics with the oil characteristics, temperature, salinity, hardness and so forth. Synthesized and new surfactants with much larger hydrophobes and more branching than previously available were tested. New classes of co-solvents and co-surfactants with superior performance were test to improve aqueous solubility. These new developments resulted in improved ASP formulations for both oils that react with alkali to make soap and oils that do not. Many of these developments are synergistic and taken together represent a breakthrough in reducing the cost of chemical flooding and thus its commercial potential.

Table of Contents

List of Tables

List of Figures

CHAPTER 1: INTRODUCTION

The research presented in this work was conducted to identify one or more low cost and high performance surfactant formulation for chemical enhanced oil recovery (EOR) based upon the phase behavior and core flood experiments. All the experiments have contributed to the ongoing chemical EOR research at The University of Texas at Austin. In this chapter, motivation and description of chapters will be discussed in subsequent sections.

1.1 MOTIVATION

In the previous studies, Austad and Milter showed that many mature reservoirs still contained more than half original oil in place (OOIP) after primary and secondary extraction (Austad and Milter, 1998). Besides, high oil price and high risk of discovering new reservoirs make EOR more economically attractive these days. However, many reservoirs used to have many limitations to be suitable candidates for chemical EOR and previous studies mainly focused on the ASP formulation designs for light and less difficult crudes. Recent research, including the development of new synthetic surfactants has enabled us to develop superior surfactant formulations (surfactant, co-surfactant, co-solvent, alkali, polymer, and electrolyte) for a wide range of crude oils under a wide range of reservoir conditions. It is well known that a surfactant formulation has to match up with the specific reservoir conditions, such as reservoir temperature, brine salinity, and equivalent alkane carbon number (EACN) of crude oils (Nelson and Pope, 1977; Lake, 1989; Falls *et al*., 1994, Austad and Milter, 1998; Jayanti *et al.*, 2002; Sanz and Pope, 1995; Zhang and Hirasaki., 2006). However, that would be too costly and time consuming to test all the combination of the parameters. The work performed in this

research demonstrates the feasible design of the formulation for reactive oil and non-reactive oil at different reservoir conditions based on the understanding of surfactant structure. A good understanding of surfactant structure assists understanding and prediction of surfactant behavior and performance for enhanced oil recovery. Selection of suitable surfactant, co-surfactant, and co-solvent systems is determined through phase behavior experiments and the formulation is verified with core flood experiments.

1.2 DESCRIPTION OF CHAPTERS

The literature review and background is described in Chapter 2. Chapter 3 describes experimental procedures, followed by the equipment and materials used in phase behavior, aqueous stability, and core flood experiments. Also, analytical calculation is discussed in Chapter 3. Phase behavior screening and optimization of the formulation for crudes as well as designing core flood are discussed in Chapter 4 and 5. Chapter 4 shows the results for non-reactive crudes and Chapter 5 shows the results for reactive crudes. In Chapter 6, the summary and conclusions are presented.

CHAPTER 2: LITERATURE REVIEW

2.1 Introduction

This chapter is a literature review and background discussion behind the research. It includes phase behavior patterns, classification, and characterization, followed by description of chemicals used in this research. The following chapter will discuss the procedures and methods used in this research.

2.2 Microemulsion Phase Behavior

The pattern of phase behavior for the mixture of oil/water/surfactant was described by Winsor (1954). Bourrel and Schechter defined a microemulsion as a thermodynamically stable phase under given conditions (Bourrel and Schechter, 1988). A distinct surfactant-rich phase, microemulsion, is fundamentally different from a macroemulsion, which is kinetically unstable, and these terminologies will be applied to describe the pattern of phase behavior experiments.

2.2.1 Microemulsion Screening

Winsor identified three types of phase equilibrium in microemulsion phase behavior as Type I, Type II, and Type III (Winsor, 1954). A Type I microemulsion is an oil-in-water microemulsion with an excess brine phase. It is also referred to as the lower phase microemulsion or Type II (-) because phase diagrams show a negative slope. In contrast, a Type II is a water-in-oil microemulsion with an excess oil phase also defined as the upper phase microemulsion or Type II (+). A portion of the water phase is dissolved in the oil phase by the surfactant. A Type III microemulsion exists as a distinct and bicontinuous third phase with excess oil and water phases. Usually Type III provides low interfacial tensions, especially where equal volumes of water and oil are solubilized

in the microemulsion. This condition is defined as optimal salinity which exhibits the lowest interfacial tension between the brine and the oil. Healy *et al.* described optimal salinity and optimal solubilization ratio as the intersection of the volume of oil (Vo) and water (Vw) solubilized in a given volume of surfactant (Vs) (Healy *et al.,* 1976). Also, optimal salinity can be expressed as the midpoint salinity where interfacial tension between microemulsion and water is same or nearly close to interfacial tension between microemulsion and oil.

2.2.2 Microemulsion Transition Parameters

A transition of phase behavior from Type I to Type II depends on surfactant type and conditions, such as salinity, temperature, pressure, and oil properties (Winsor, 1954; Bourrel and Schechter, 1988; Lake, 1989; Green and Willhite, 1998). Increasing the hydrophobicity of a surfactant causes a transition from lower phase microemulsion (Type I) to upper phase microemulsion (Type II). The hydrophobicity can be increased by increasing the alkyl chain length (carbon number or molecular weight), increasing propylene oxide (PO), or decreasing ethylene oxide (EO) in the surfactant. The same transition can be caused by increasing hardness or salinity and also temperature for most anionic surfactants but not all. Many co-solvents also cause the same transition, but there are exceptions if the co-solvent is very hydrophilic such as isopropyl alcohol. Pressure is a weak effect, but generally causes a Type II to I transition due to the increased density of the oil at fixed composition. The phase behavior is extremely sensitive to the oil composition. A type II to I transition is caused by decreasing the Equivalent Alkane Carbon Number (EACN) of the oil, for example, by adding methane or other light hydrocarbons typical of solution gas in live oils at high pressure.

2.2.3 Theory and Displacement Mechanism

The phenomena of the residual oil are well described by the generalized trapping number consisting of the capillary and Bond number (Pope *et al.*, 2000). Mathematically, trapping number can be expressed as follows:

$$N_{T_l} = \frac{\left|\vec{\vec{k}} \cdot (\vec{\nabla}\Phi_{l'} + g(\rho_{l'} - \rho_l)\vec{\nabla}D)\right|}{\sigma_{ll'}}$$

$$N_{c_l} = \frac{\left|\vec{\vec{k}} \cdot \vec{\nabla}\Phi_l\right|}{\sigma_{ll'}} \quad : \text{Capillary number}$$

$$N_{B_l} = \frac{kg(\rho_{l'} - \rho_l)}{\sigma_{ll'}} \quad : \text{Bond number}$$

Where, $\vec{\vec{k}}$ = permeability tensor, $\vec{\nabla}\Phi_{l'}$ = flow potential gradient, ρ_l = density of phase l, $\sigma_{ll'}$ = interfacial tension between phases l and l', l=displaced phase, and l'=displacing phase.

The Capillary Desaturation Curve (CDC) is defined as the residual oil saturation as a function of capillary number. From CDC experiments conducted using sandstones, the capillary number needs to be on the order of 10^{-3} or greater to mobilize the residual oil completely (Stegemeier, 1977; Pope *et al.*, 2000) This requires lowering the IFT to the order of 0.001 mN/m assuming a pressure gradient on the order of 1 psi/ft, which is typical of the pressure gradient in an oil reservoir far from the wells.

Healy and Reed first published an empirical correlation between IFT and solubilization ratios and later Huh developed a theoretical relationship (Healy and Reed, 1976; Huh, 1979). A simplified equation for IFT can be written as follows:

$$\gamma = \frac{C}{\sigma^2},$$

A typical value of C is about C=0.3 dynes/cm. The solubilization ratio (σ) is defined as the volume of oil or water divided by the volume of pure surfactant.

Consequently, IFT can be estimated from phase behavior screening experiments and the Chun Huh equation. Levitt *et al.* (2009) described the procedures and several benefits of IFT estimation from phase behavior data instead of measuring IFT directly, however, it is still a good idea to measure IFT directly after finding a good formulation of surfactants, co-surfactant, co-solvent, electrolytes, alkali and so forth.

2.3 Chemicals used for Enhanced Oil Recovery

2.3.1 Surfactants / Co-surfactants

Surfactants are surface-active agents. A surfactant consists of lipophilic moiety and hydrophilic moiety in a molecule. Typically surfactants can be categorized into four groups; anionic, cationic, non-ionic, and zwitterionic families depending on the charge of the head. Among these four groups, anionic surfactants and nonionic surfactants are widely used in chemical EOR. The balance of hydrophilic and lipophilic moieties (HLB) is one of the main characterizations of surfactants (Green and Willhite, 1998). A branched structure is also a desirable characteristic of EOR surfactants because the branched structure decreases ordered structures that form viscous gels. Co-solvents such as alcohol are not needed or less is needed when the surfactant is highly branched (Abe *et al.*, 1986, Levitt *et al.*, 2009). Co-surfactants with branched or different structures such as a twin tailed IOS is often used in the formulation to provide further disruption of arrangement of surfactant and match the crude oil properties at different conditions (Levitt *et al.*, 2009, Yang *et al.*, 2010).

Anionic surfactants

Anionic surfactants bear negative charge in the surface-active portion of the molecule in an aqueous solution. This type of surfactant is one of the most promising

primary surfactants in chemical EOR because of its excellent performance and minimal adsorption on the sandstone and limestone rocks. Silica exhibits negative charge at reservoir conditions and clays have negative charge at neutral pH for preventing ionic attractions (Levitt *et al*., 2009; Zhang and Hirasaki., 2004). Traditionally, sulfonate type surfactants are only considered for high temperature EOR application since ether sulfates were claimed to have poor hydrolytic stability at elevated temperatures (> 65C) (Talley, 1988). Recently, Adkins *et al.* (2010) described the new process of stabilizing of ether sulfate surfactant for chemical EOR and thermal stability of sulfates enable a wider selection of surfactant structures for use in high temperature reservoirs. The anionic surfactants used in this research are alkyl benzene sulfonates (ABS), internal olefin sulfonates (IOS), alcohol ethoxy sulfates (AES), alcohol propoxy sulfates (APS) and Guerbet alkoxy ether sulfates (GAS).

ABS surfactants are conventional surfactants broadly used in the past. Both of the structures contain a benzene aromatic ring and an alkyl chain contributing to the hydrophobicity. Typically these types of surfactants show high solubilization ratios with crudes and low optimal salinity because of the strong hydrophobicity. Another way to view this is they have poor aqueous solubility, low hardness tolerance (Jackson, 2006), and adsorption onto polar surface. Application of these types of surfactants is utilizing it with relatively high molecular weight crudes in fresh injected brine or employing it as a co-surfactant to provide extra hydrophobicity.

Internal olefin sulfonates (IOS) have been found to be excellent EOR surfactants from previous studies (Levitt, 2006; Jackson, 2006; Zhao *et al.*, 2008; Flaaten, 2008; Hirasaki *et al.*, 2008). Due to the deviation of double bond for internal olefin in the chain, twin hydrophobic tail has individual lengths and thus it can cover wide range of crude properties (Zhao, 2007; Sahni, 2009). Besides, IOS shows a superior compatibility of

surfactant and oil/water phase caused by structural heterogeneities and large hydrophobes.

AES and APS are commercially available, well-performed, and simply tailored surfactants in chemical EOR application. AES contains ethylene oxide (EO) and APS includes propylene oxide (PO) in a molecule and numbers of EO/PO characterize the properties of these types of surfactants. Further hydrophilicity and hydrophobicity for the surfactants depend on the numbers of EO and PO units respectively. Previous studies found that increasing numbers of EO increase aqueous solubility, calcium tolerance, and optimal salinity, whereas, increasing numbers of PO set off to opposite behaviors (Aoudia *et al.*, 1995; Austad and Milter, 1998; Bourrel and Schechter, 1988; Levitt, 2006; Flaaten, 2007; Zhao *et al.*, 2008). By varying PO and EO units, AES and APS can be tailored to fit specific EOR needs. Also Due to thermal stability of sulfate at high pH condition, AES and APS are now very promising, robust candidate surfactants in chemical EOR (Adkins *et al.*, 2010).

GAS surfactants are anionic surfactant containing mid-branched Guerbet alcohol with propylene oxide (PO) and ethylene oxide (EO) units, followed by sulfate. Very large hydrophobes and branched structures are required to achieve low interfacial tension and good fluidity for viscous oil containing over 12 EACN (Liu *et al.*, 2007). The Guerbet reaction is the only commercially viable process for producing very large hydrophobe structure. Previous studies on GAS surfactants showed the excellent performances of GAS surfactants (Varadaraj *et al.*, 1991; Aoudia *et al.*, 1995), however, the relatively high cost and thermal stability issues prohibited the usage of GAS surfactant in chemical EOR area. Due to new methods of manufacturing and stabilizing GAS surfactant, high performance and excellent GAS type surfactants are suitable options for high EACN crudes.

Nonionic surfactants

Alcohol ethoxylates are nonionic surfactants used as co-solvent to improve aqueous solubility of the formulation. These types of surfactant can be tailored easily for performance since the hydrophobe, hydrophile, and distribution of the ethylene oxide units can be varied. Another feature of alcohol ethoxylate is increased tolerance of high ionic strength and hardness over anionic surfactants. These surfactants are commercially available and show better performance than glycol and alcohols in some case studies. Case studies by Sahni showed that a small amount of alcohol ethoxylate used as co-solvent could replace large amounts of conventional co-solvents (Sahni *et al.*, 2010). Some field tests were conducted to form a single micellar solution by blending nonionic surfactant Neodol 25-12 with IOS surfactant to give sufficient hydrophilicity to the formation at White Castle field, Louisiana (Falls *et al.*, 1994). Also, the adsorption level for the non-ionic surfactants by hydrogen-bonding mechanism is comparable with adsorption of anionic surfactants (Trogus *et al.*, 1977). However, nonionic usage in the formulation is limited because of the cloud point where separation of the solution occurs due to the sharp increase in aggregation (Milton, 2004).

2.3.2 Co-Solvents

Co-solvent is low molecular weight water-miscible organic solvent used in the formulation to increase the solubility of poorly water-soluble compounds and enhance the chemical stability. Co-solvent maintains compatibility for surfactants/polymer in the aqueous phase by forming a thermodynamically stable mixture. Also, co-solvent reduces oil/water microemulsion viscosity and accelerates equilibrium time (Sanz and Pope, 1995, Levitt *et al*., 2009; Flaaten *et al*., 2008). The reduction of water/oil microemulsion viscosity is due to a reduction of rigidness in the surfactant films. Also, chemical gradients can be achieved by using co-solvents in chemical floods to create a robust

system (Dwarakanath *et al.*, 2008). However, the critical disadvantage of using co-solvent is that co-solvent reduces oil/water solubilization ratios and therefore decreases possible IFT reduction with a given surfactant (Salter, 1977). Also co-solvent destabilizes the foam which may be needed for mobility control in foam flooding. Thus, a compromise must be made between maximum solubilization ratio and low viscosity and the other critical factors needed for good transport under low pressure gradients in oil reservoirs (Levitt *et al.*, 2009).

Conventional co-solvents are small carbon chain (C3 to C5) alcohol molecules that act at the oil/water interface of microemulsion droplets (Levitt *et al*. 2009; Flaaten *et al*. 2008). The effect of branched structure co-solvents was investigated by Hsieh and Shah (Hsieh and Shah, 1977). Branched structure co-solvents tend to provide superior hydrophilicity than linear structure co-solvents for same molecular weight. Commercial alcohol type co-solvent includes Iso-propanol (IPA), Sec-butanol (SBA), etc. Also, glycol ether type co-solvents are extensively tested in chemical enhanced oil recovery recently. The advantage of this type of co-solvent is it has a higher flash point than its linear or branched counterpart (Jackson, 2006; Sahni *et al*., 2010). Commercial glycol ether co-solvents include Glycol Butyl Ether (EGBE), Diethylene Glycol Butyl Ether (DGBE), and Triethylene Glycol Butyl Ether (TGBE).

2.3.3 Alkali

Employing alkali in the formulation has several significant benefits, such as in situ soap generation with reactive crudes and reduced surfactant adsorption. High pH reduces surfactant adsorption by increasing negative charges on the sandstone rock (Nelson *et al*., 1984; Wessen and Harwell, 2000; Zhang and Somasundaran, 2006). Naphthalenic soaps generated by naphthalenic acid under alkali condition are anionic surfactants that are a mixture of salts formed by cyclo-alkyl carboxylic acids and other

organic acids (Jennings, 1975). Generally, three to five folds less surfactant volume is required for a robust EOR process for reactive crude compared to non-reactive crude. Conventionally the total acid number (TAN) is regarded as a good indicator of the activity of crude oil; however, a reactive crude oil requires the measurement of saponification number in order to determine the total amount of soap that can be generated by alkali reaction (Yang *et al.* 2010). The conventional alkali used for chemical EOR is sodium carbonate. However, in presence of gypsum and anhydrite, calcium dissolves and the carbonate ion precipitates as calcium carbonate (Labrid, 1991). Among several alternative novel alkali, sodium metaborate and tetrasodium Ethylenrdiamine Tetraacetate (EDTA) are the most promising alkali under divalent cations condition. The borate ions from sodium metaborate form complexes with dissolved divalent ions with small amount of usage under complex condition (Flaaten *et al.* 2008). Relatively expensive EDTA-Na_4 is a powerful chelating agent with an ability to sequester metal ions through its two amines and four carboxylates (Yang *et al.* 2010).

2.3.4 Polymers

The main objective for using polymer in chemical flooding is to provide enough viscosity to increase vertical/horizontal sweep efficiency and prevent fingering (Sorbie, 1991; Lake, 1989; Green and Willhite, 1998). Once high performance surfactants reduce IFT significantly, the slug starts to finger due to unfavorable mobility control (Green and Willhite, 1998). In order to avoid fingering and maintain favorable mobility control, water soluble polymer is added into the ASP/SP slug and polymer drive. A safe approach to maintain sufficient mobility control is used to reduce the mobility ratio to less than one (Gogarty *et al*., 1968). The mobility ratio is mobility of the chemical slug divided by the mobility of the oil bank. Mobility ratio can accurately and conveniently be measured during the core flood by taking the ratio of the pressure gradient in the clean oil bank

between closely spaced pressure taps along the core and the pressure gradient in the slug between closely spaced pressure taps (Yang *et al.* 2010). Hydrolyzed polyacrylamides (HPAM) are common polymers for EOR application. HPAM is a polyelectrolyte with negative charges on the carboxylate groups with an average molecular weight of HPAM in the range of 1 to 20 million. Levitt described the process of selection and screening of polymers for chemical EOR (Levitt *et al*. 2008).

CHAPTER 3: EXPERIMENTAL MATERIALS, METHODOLOGY, AND DATA ANALYSIS

The experimental equipment, methodology, and data analysis are presented in this chapter. To determine an appropriate formulation for a specific crude at different conditions, it is necessary to perform phase behavior screening tests and verify the formulation with core flood experiment. The equipment is described, and then followed by methodology and data analysis for phase behavior and core flood experiments.

3.1 EXPERIMENTAL EQUIPMENT

3.1.1 Phase Behavior

Equipment and materials for conducting aqueous solubility tests and microemulsion phase behavior tests are described in this section.

Water Deionizer

A Nanopure^{TM} filter system was used to remove ions, organics, and particles out of the water. Water was filtered by a 0.45 micron filter to eliminate particles and organics. The filter uses a recirculation pump and monitors the water resistivity to indicate when the ions have been removed. All the makeup brines and solutions are made using deionized (DI) water.

Borosilicate Pipettes

Microemulsion experiments were made in standard 5 mL Borosilicate pipettes with 0.1 mL graduations. After adding the crude and the surfactant solution to the pipette, the ends were sealed using a propane-oxygen torch.

Pipette Repeater

An Eppendorf Repeater Plus® dispenser was used for dispensing accurate volumes. The volumetric capability of this repeater for one dispense ranges from 25 microliters to 1 milliliter. Disposable tips are attached to the repeater for easy operation and to prevent any contamination.

Propane-oxygen Torch

Microemulsion phase behaviors in borosilicate glass pipettes were sealed by using a propane-oxygen torch. A high-intensity flame is created by a mixture of propane and oxygen through a Bernz-O-Matic flame nozzle.

Convection ovens

Blue M® and Tenney® convection ovens were set to the reservoir temperature to observe aqueous solubility and the microemulsion phase behavior. Core flood experiments are conducted in convection ovens to imitate reservoir temperature. A digital display on the convection ovens indicated the real-time temperature.

3.1.2 Core Flood Experimental Equipment

Once a good formulation for specific crude is found, a core flood experiment is conducted to check the performance of the formulation. Schematic of the setup to be used for the core flood experiment is shown in Figure 3.1. It shows the location of the different pressure transducers as well as the different sections of the core. This section describes the experimental equipments used in core flood experiments.

Glass Columns

The Kontes Chromaflex® columns were used to contain fluids to be injected for core floods experiments. These columns were 0.5 to 2 foot in length and 2 inch in outer

diameter. The end pieces include a Vitron O ring and washer to prevent leaking when hand tightened. These columns can withstand up to 50 psi; but usually, 20 psi is used as a safe guard.

Stainless Steel Columns

Whitey® stainless steel columns were used for fluid injection under higher pressures of up to 120 psi. These columns were 2 feet in length and 1 inch in outer diameter. The stainless steel columns were custom made from stainless steel tubing with Swagelok fittings used as end pieces. These steel columns were used in oil flood experiments involving high pressures.

Pumps

A Teledyne ISCO 5000 syringe pump was used to inject the fluids into the core at constant rate. The pump was filled with mineral oil to displace the fluid in the columns into core. Air bubbles should be purged prior to use and the flow rate should be checked by effluent volume.

Pressure Transducer

The pressure drops for different sections across the core are measured by pressure transducers. Measured pressure-drops by the transducers is converted into output voltage and then read by a data acquisition recorder on the computer. The signals were then converted to a calibrated pressure for recording. The lines connected to the core should be flushed with DI water in order to remove any air bubbles prior to core flood experiments and transducers should be calibrated prior to each experiment.

Data Acquisition Recorder

The signals from the pressure transducers are collected by National Instruments USB-6008 Multifunctional Data acquisition card and transferred to Lab View 7.0

software. Raw data were recorded as .DAT Microsoft Excel file with 1-30 second intervals.

Fraction Collector

An Instrument Specialties Company (ISCO) Retriever II fractional collector was used for collecting effluents from chemical ASP flooding. The collector can be programmed to collect the samples at fixed time intervals or fixed volume interval. System leaks can be detected by checking the volume of effluent in the fraction collector.

Filter Press

Solutions and stocks were filtered by using a stainless steel OFITE filter press. Polymer solutions are filtered by using a 1.2 μm Millipore™ hydrophilic cellulose filter paper. Oil and brine stocks were filtered through 0.45 μm filter paper.

Rheometer

The bulk viscosity measurements were conducted using a TA instrument ARES-LS1. ARES-LS1 is a rheometer optimized for inertia-free dynamic measurements of low viscosity fluids and measures the torque generated in response to a steady or constant shear strain applied to a sample. The instrument requires 8 ml samples for non-Newtonian fluid and 15 ml samples for Newtonian fluid to operate properly.

HPLC

HPLC is a chromatographic technique that can separate a mixture of compounds to identify the individual components of the mixture. Varian prostar 230® used in this research is a ternary solvent delivery module with microborn-to-analytical flows and the column was Acclaim ® surfactant having 250 mm in length and 4.6 mm in outer diameter. Effluent samples were measured on all even numbered samples by HPLC in order to determine surfactant retention in the porous medium.

3.2 METHODOLOGY

3.2.1 Phase Behavior Description

Phase behavior experiments consist of two parts: aqueous solubility tests and microemulsion phase behavior tests. An aqueous solubility experiment is conducted to evaluate aqueous solubility of the surfactants up to at least optimum salinity. The chemical slug should form a clear solution at injected salinity (usually optimal salinity). Microemulsion phase behavior experiments are fast and efficient screening method to determine surfactant/co-surfactant/co-solvent formulations for a specific crude at different conditions. There are several crucial criteria for a good surfactant formulation: low microemulsion viscosity, good fluidity, absence of gels, and short equilibrium time.

Procedure and description of crude evaluation, aqueous solubility and microemulsion phase behavior experiments are presented in this section. The crude was evaluated for the activity prior to aqueous solubility and microemulsion tests. An aqueous solubility experiment was conducted to evaluate aqueous solubility limitations by mixing surfactant stock, brine stock, and polymer stock solution over a range of salinities. With increasing salinity, the aqueous solution tends to become cloudy or phase separation occurs because, as previously mentioned, aqueous solubility decreases with salinity. After the aqueous solubility test, microemulsion experiments were performed in order to obtain IFT data by blending surfactant stock, brine stock, and crude over a range of salinities. Aqueous and microemulsion phase behavior components consist of surfactant stock, alkali stock, polymer stock, brine and crude oil. Stock solution was made with synthetic makeup brine.

Surfactant stock

Primarily a surfactant stock solution contains surfactant, co-surfactant, co-solvent and brine. Four times concentrated solution is made based on weight percent. Concentrated surfactant stock was diluted with makeup brine to achieve a desired concentration in aqueous solubility and microemulsion phase behavior experiments.

Polymer stock

Polymer stock solutions were prepared and diluted to the desired concentration later. Polymer stock was used for aqueous solubility experiment, but not for microemulsion phase behavior experiment. Polymer stocks were prepared by adding polymer powder to synthetic makeup brine slowly and mixed for two days to avoid gel formation. After mixing, polymer solution is filtered through 1.2 μm filter paper. Measured filtration ratio values using the following equation should be less than 1.2, indicating a homogenous polymer stock solution.

$$\text{Filtration ratio} = \frac{\Delta t_{180} - \Delta t_{160}}{\Delta t_{40} - \Delta t_{20}}$$

Δt_x = Measured time for collecting x ml of filtered polymer

Alkali stock

Sodium carbonate was used as the alkali for the aqueous solubility and microemulsion experiments. Alkali stocks were prepared by adding sodium carbonate to synthetic makeup brine. Because solubility of sodium carbonate is 22g/100 mL at room temperature, concentrated sodium carbonate stock solutions used in the experiments were in the 10-20wt% range. It is important to make a sodium carbonate stock daily because sodium carbonates form precipitation easily around the bottle neck, altering the composition of the mixture.

Crude activity evaluation

Saponification number (SAPN) experiments were conducted to evaluate oil properties for phase behavior experiments and core floods. First, crude was weighed and then toluene was added into the conical flask with a magnetic stir bar and mixed well until oil was completely diluted in toluene. Then, Isopropyl alcohol (IPA) was added to the same flask with an Argon blanket. Carefully, standard NaOH solution was added and covered with an Argon blanket. Next, the mixture was heated to 70 °C for 30 minutes and cooled down to room temperature. Then, the mixture was added to Molecular grade water, which was boiled to remove any dissolved CO_2, and a drop of phenolphthalein was added as an indicator. Finally, the crude oil mixture was titrated by standard HCl until it reached the end point. The amount of HCl added was measured to calculate the SAPN by converting the NaOH molecular weight to KOH value.

Aqueous solubility

Aqueous solubility experiments were performed to determine homogeneity and thermodynamic stability of the solution. It is crucial to form a single phase and clear solution for injection after it reaches equilibrium. Generally, 10 ml of solution containing surfactant, co-surfactant, and polymer in wide range of salinities was dispensed in 20 ml vials to check the compatibility of the components. Once all the components were added into vials, vials were gently shaken and set inside the convection oven at the reservoir temperature. After sufficient time to reach equilibrium (generally a couple of hours), the vials were checked visually and the salinity where cloudiness or phase separation occurred was recorded.

Microemulsion Phase Behavior

Microemulsion phase behavior experiments were performed to check the performance of a surfactant formulation with the specific crude. Due to the oil composition complexity, the formulation needed to be tested with each specific crude by conducting microemulsion phase behavior experiments. The benefits of microemulsion phase behavior tests are well described by Levitt (Levitt *et al.*, 2009). The procedure of microemulsion phase behavior experiments is similar to the aqueous solubility tests. Injected components into the pipettes consisted of brine stock, surfactant stock, electrolytes, and crude. Polymer was not added in microemulsion phase behavior tests because it has an insignificant effect on the phase behavior results and increases time to reach equilibrium. First, concentrated brine stock was added, followed by sodium carbonate stock, and surfactant stock. The order of addition is critical because the surfactant performance can be altered if surfactant stock contacts concentrated sodium carbonate. After injecting the aqueous components, the volume of the aqueous solution was recorded. Crude oil was added last. Pipettes were blanketed with argon gas to prevent reaction with oxygen and sealed using a propane-oxygen torch. Pipettes were shaken gently to verify that there are no leaks and then mixed thoroughly. The pipettes were placed in a convection oven at reservoir temperature. Solubilization ratio, fluidity of microemulsion, equilibrium time, droplet size and uniformity were observed over range of salinities and all information were recorded. Oil solubilization in microemulsion increased and water solubilization in microemulsion decreased as salinity increased, which was expected.

3.2.2 Core Flood Description

The core flood procedure includes the method of core preparation, core assembly, core saturation, ageing with brine or crude oil, brine flooding, oil flooding, water

flooding and chemical flooding, collecting and analyzing the effluent samples for cumulative oil recovery, pH, surfactant retention and adsorption. This section describes the flooding procedure.

Brine Flooding

After finishing core preparation, core assembly, core saturation, and aging, core was flushed with synthetic formation brine. The objective of this brine flooding was to determine absolute brine permeability. Several pore volume of formation brine was injected with flow rate 2-4 ml/min into the core until pressure stabilized. The pressure drop was recorded to determine the average absolute brine permeability of the core.

Oil Flooding

After brine flooding, oil flooding was conducted at high injection pressure at the reservoir temperature. The main purpose of the oil flooding is to determine initial oil saturation, residual water saturation, effective oil permeability, and relative oil permeability. Prior to oil flooding, the crude was filtered by 0.45 μm filter paper at the reservoir temperature. Oil flooding was conducted under a constant pressure (80-120 psi) to saturate the pore volume with oil and obtain accurate residual water saturation. Approximately, 1.5 PV of the oil was injected into the top end to consider density effect of oil and water. The effluent fluids were collected in 100 ml burettes and the volume of displaced water was the volume of saturated oil inside the core. Oil flooding was continued until water cut was less than 1% and pressure stabilized. The pressure drop was recorded during oil flooding in order to calculate the oil permeability.

Water Flooding

Water flooding with filtered synthetic injection brine was followed by oil flooding. Water flooding was conducted in order to determine residual oil saturation,

effective water permeability, and relative water permeability after water flooding. Approximately, 1.5 PV of synthetic injection brine was injected into the core at a low constant flow rate (0.4 - 0.5 ml/min) to achieve general residual oil saturation after water flooding. The effluent fluids were collected in a burette and water flooding was stopped when the oil cut was less 1% and pressure stabilized. The residual oil saturation was estimated based on the volumes of oil in a burette and effective brine permeability was calculated by the pressure drop across the core.

Chemical Flooding

Chemical slug was injected after water flooding in order to check performance of formulation and recover residual oil in the core as a tertiary recovery. Typically, 0.3-0.5 PV of ASP slug was injected into the core at reservoir temperature and followed by approximately 1.5-2.0 PV polymer drive. Chemical flooding was performed at a constant flow rate about 1-2 ft/day and the flooding was performed until no more emulsion produced. The effluent fluids were collected by fractional collector for further analysis. Oil recovery and residual oil saturation were determined after chemical flooding by material balance and measuring volumes of oil produced. After chemical flooding, effluent fluids were placed in the convection oven at the reservoir temperature and tubes were centrifuged for 1-2 min at 1000 rpm after 24 hours. Then, surfactant retention, viscosity, and pH data for the effluent fluids were analyzed to evaluate the performance of the formulation.

3.3 CALCULATIONS AND EQUATIONS

3.3.1 Microemulsion Phase Behavior Calculations

Theoretical equation and calculation for microemulsion phase behavior are described in this section. The trend of microemulsion phase behavior experiment was obtained through generating solubilization ratio of oil/water as increased salinity. Fluidity, droplet size and uniformity of microemulsion should be checked visually. Also aqueous solubility should be form a single and clear phase at the optimal salinity.

Solubilization Ratio Plots

The solubilization ratio of oil is defined as the volume of oil solubilized divided by the volume of active surfactant in the microemulsion phase. The volume of oil is estimated by the interval between initial aqueous level and top interface level. . Similarly water solubilization ratio is defined by the interval between initial aqueous level and bottom interface level. All the surfactants are assumed to be in microemulsion phase. Solubilization ratios for oil and water are calculated by following equations.

$$\sigma_o = \frac{V_o}{V_s}$$

$$\sigma_w = \frac{V_o}{V_s}$$

σ_w = Solubilization ratio of water

σ_o= Solubilization ratio of oil

Vo = Volume of oil solubilized in microemulsion

Vw = Volume of water solubilized in microemulsion

Vs= Volume of surfactant in microemulsion

Optimal salinity is the intersection where oil solubilization and water solubilization curves are crossed. As discussed in chapter 2, Healy and Reed presented the correlation between IFT and solubilization ratio and optimal salinity is the intersection where the lowest IFT is achieved. Once the formulation generates high solubilization ratio by calculation and good fluidity of microemulsion visually, activity diagram is tested by changing oil concentration to check the oil concentration sensitivity.

Activity Diagram

Activity diagram is conducted to ensure the sensitivity of oil concentration for reactive crude with the formulation. Reactive crudes contain naphthenic acids and considerable amount of in-situ soap (carboxylic soap) is generated under alkali conditions. Typically, in-situ soap is more hydrophobic than synthetic surfactant, hence optimal salinity shift to lower salinity as increasing oil concentration. For reactive crudes, generated in-situ soap is interacting with synthetic surfactant formulation and altering HLB of surfactant formulation. The activity diagram is a plot of oil concentration on the x-axis and sodium carbonate concentration on the y-axis. Oil scan is performed by changing oil concentration from 10% to 50% and ranges of type III region for different oil concentrations are plotted in the activity diagram. An activity diagram with broad type III regions and negative slope is desired for salinity gradient in ASP flooding. Negative slope of type III is effective propagation of slug in porous medium and the formulation has favorable HLB in the total system.

3.3.3 Core Flood Calculations

Theoretical calculations in core flood experiment include pore volume, porosity, effective permeability, phase saturation, fluid mobility, polymer resistance factor,

permeability reduction factor, and oil recovery. Calculations and parameters used are described in this section.

Pore Volume

The pore volume of core is calculated by mass balance. Calculated pore volume in core flood is mass of saturated brine divided by density of brine as follows:

$$V_p = \frac{M_{sat} - M_{dry}}{\rho_w}$$

V_p = pore volume

M_{sat} = mass of brine saturated core

M_{dry} = mass of evacuated core

Bulk Volume and Porosity

The porosity of the core is pore volume divided by bulk volume as follows:

$$\phi = \frac{V_p}{V_b} = \frac{V_p - V_s}{V_b}$$

And the bulk volume is calculated by total volume of the bare core.

$$V_b = \pi r^2 L$$

V_b = bulk volume

r = radius of core

L = length of core

Brine Permeability

After saturating the core with brine, a brine flood was conducted in order to measure pressure drop between inlet and outlet of the entire core. The brine permeability, or absolute permeability, was calculated based on Darcy's single phase, steady-state, and horizontal flow equation with laboratory. The permeability calculation for brine, effective oil, and effective water based on Darcy's law are described by Jackson (Jackson, 2006).

Effective Oil Permeability

The effective oil permeability was calculated from the oil flood. The pressure drop was measured throughout the flooding process; the stabilized portion of the pressure data was used to calculate the effective oil permeability.

Effective Water Permeability

After the water flood, the effective water permeability was calculated. Again, the pressure drop was measured across the core. When pressure stabilized and the oil cut was less than 1%, the pressure drop was recorded and used in Darcy's equation to calculate relative permeability. Flow at this end point was assumed to be steady state.

End Point Oil/Water Relative Permeability

After running the water flood, end point relative permeability for both oil and water were calculated. Relative permeability was used for removing pore size effect and normalization by using a base permeability in multiphase flow. End point oil permeability was calculated by dividing effective oil permeability by a base permeability such as brine permeability. End point water permeability was calculated in same manner.

$$k_{ro}{}^{o} = \frac{k_o}{k_{brine}}$$

$$k_{rw}{}^{o} = \frac{k_w}{k_{brine}}$$

Initial Oil Saturation

An oil flood was conducted in the brine saturated core until residual water saturation was reached. Mass balance was used to determine the initial oil saturation: the volume of produced water is the volume of oil saturated in the core. Initial oil saturation was estimated by dividing volume of produced water by the pore volume as follows:

$$S_{oi} = \frac{V_w}{V_p}$$

S_{oi} = initial oil saturation

V_w = volume of produced water from oil flood

Residual Oil Saturation

The residual oil saturation from the water flood was calculated after the oil cut from the water flood was less than 1%. The volume of oil produced during the water flood was the mobile oil saturation. Residual oil saturation was estimated using the following equation:

$$S_{orw} = \frac{V_w - V_o}{V_p}$$

S_{orw} = residual oil saturation after water flood

V_w = volume of produced water from oil flood

V_o = volume of produced oil from water flood

The residual oil saturation after the chemical flood is the difference between the volume of oil remaining after the water flood and the volume of oil produced after the chemical flood. Residual oil saturation after chemical flood can be calculated as follows:

$$S_{orc} = \frac{S_{orw} Vp - V_o}{V_p}$$

S_{orc} = residual oil saturation after chemical flood

V_o = volume of produced oil from chemical flood

Mobility ratio

Mobility control in a chemical flood is a crucial step to improve oil recovery. Gogarty suggested that minimum total mobility yield a favorable viscosity and improve sweep efficiency (Gogarty *et al.*, 1968). Relative permeability of oil and water at different water saturations could be calculated using Corey's equation as follows:

$$k_{rw} = k_{rw}{}^{o} S^{n}$$

$$k_{ro} = k_{ro}{}^{o} S^{m}$$

$$S = \frac{S_w - S_{wirr}}{1 - S_{wirr} - S_{or}}$$

$k_{rw}{}^{o}$ = Water end point relative permeability

$k_{ro}{}^{o}$ = Oil end point relative permeability

n = Exponent of water relative permeability from water cut in oil flood

m = Exponent of oil relative permeability from oil cut in water flood

Total mobility is the sum of water mobility and oil mobility as below:

$$\lambda_t = \left(\frac{K_w}{\mu_w} + \frac{K_o}{\mu_o} \right)$$

A plot of water saturation versus total relative mobility is made to find the minimum in the curve. For a stable displacement, the slug and drive viscosity must be equal or greater than the inverse total relative mobility of the oil bank as follows:

$$\mu s = \frac{1}{\lambda_{tmin}} = \frac{1}{\left(\frac{k_w}{\mu_w} + \frac{k_o}{\mu_o} \right)_{min}}$$

Polymer viscosity should be higher or equal to slug viscosity to prevent fingering effect. The concentration of polymer required to have such a viscosity was estimated by plotting viscosity versus different polymer concentration at identical conditions such as salinity, hardness, and temperature.

Polymer Resistance Factor

The polymer resistance factor is defined as the ratio of water mobility over polymer mobility as follows:

$$R_f = \frac{\lambda_w}{\lambda_p} = \frac{k_w \mu_p}{k_p \mu_w}$$

R_f = polymer resistance factor

The resistance factor can be determined from the pressure drop data by dividing the steady state polymer pressure drop by the steady state water pressure drop provided the flow rate and saturation are the same for both floods:

$$R_f = \left(\frac{\Delta P_p}{\Delta P_w} \right)_{q,sj}$$

Polymer Permeability Reduction Factor

The polymer permeability reduction factor indicated the effect of trapped or adsorbed polymer. This factor was the ratio of effective brine permeability to effective polymer permeability as follows:

$$R_k = \frac{k_w}{k_p} = R_f \frac{\mu_w}{\mu_p}$$

R_k = polymer reduction factor

Oil Recovery

Oil recovery can be estimated after chemical flood. Only free oil produced in tube was counted for the volume of recovered oil since oil in emulsion phase was assumed to be negligible. Oil recovery was calculated by dividing the sum of oil recovered from chemical flood by volume of residual oil after water flood as follows

$$f_{op} = \frac{\sum_{i=1} V_{opi}}{V_{or}}$$

f_{op} = fraction of oil produced

V_{opi} = volume of free oil produced in tube i

V_{or} = volume of residual oil after water flood

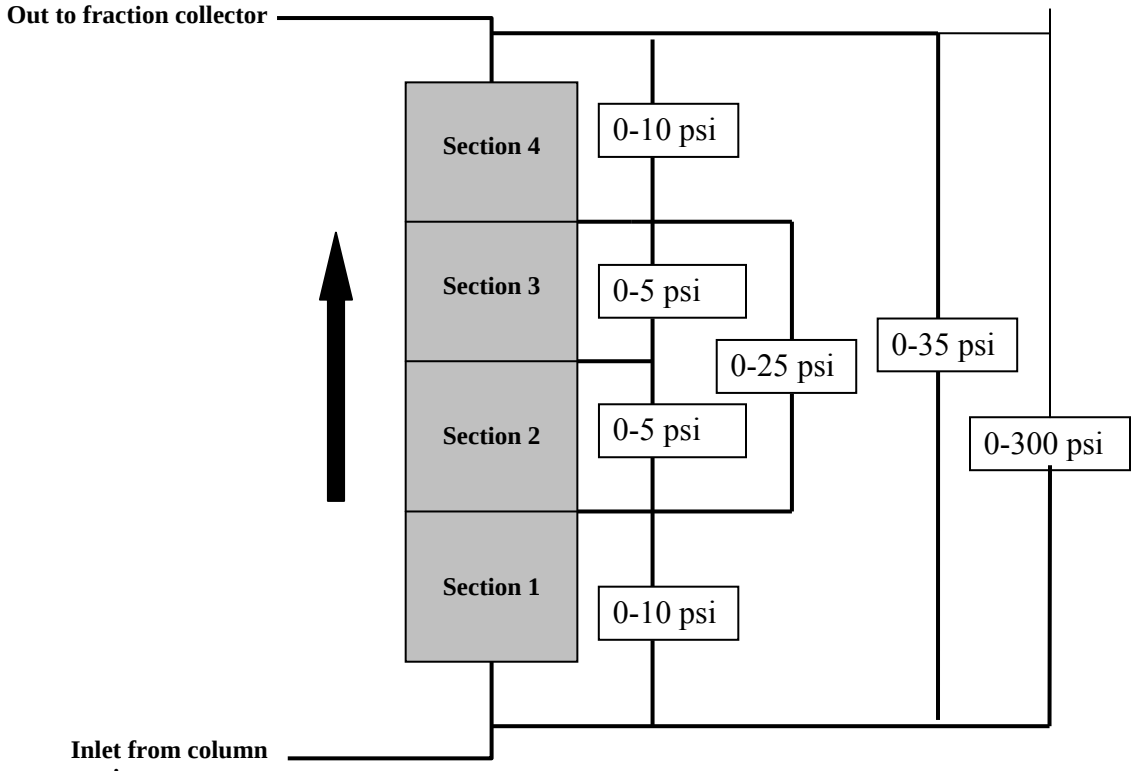

Figure 3.1 Schematic setup of ASP flood

CHAPTER 4: DESIGN OF HIGH PERFORMANCE ASP FORMULATIONS WITH LOW ACID NUMBER

This chapter describes the process for selection and testing of a formulation consisting of a primary surfactant, co-surfactant, co-solvent and polymer for a crude oil with a low acid number. The selection process is based upon careful observations of the aqueous and microemulsion phase behavior experiments and important physical properties such as viscosity. A summary of these observations is given in Tables 4.4 to 4.6.

4.1 DEVELOPMENT AND OPTIMIZATION OF ASP FORMULATIONS

4.1.1 Crude oil and brine

Table 4.1 shows the viscosity of several different samples of crude oil taken at different times. Zhao (2006) used crude oil sample number 3 with a viscosity of 3.4 cp in her phase behavior studies. This study used samples 4 to 7. The viscosity of sample 6 was 6.3 cp and the viscosity of sample 7 was 6.6 cp. All of these samples showed somewhat different phase behavior results. Although this is a light oil with an API gravity of 35, it has a high EACN (Jackson, 2006) so it acts like a heavy oil with respect to surfactant behavior.

The saponification number (SAPN) of sample 6 was measured to give some indication of how much soap might be generated from the reaction between the alkali and acid from the oil. The measured SAPN was 0.30 mg of KOH/g, which is a relatively low SAPN.

The phase behavior tests were done using the softened brine shown in Table 4.2. The hard brine shown in Table 4.2 was used in a core flood to water flood the core. All of the tests were done at the reservoir temperature of 85 °C.

4.1.2 Phase behavior optimization by testing diverse surfactants

Surfactant and co-surfactant selection

The summary of screening criteria for surfactant and co-surfactant is listed in Table 4.3. It is a guideline used in the laboratory for choosing surfactant and co-surfactant corresponding to diverse conditions. All the microemulsion phase behavior experiments were prepared with over 0.1 wt% active surfactant concentration, which is above the typical CMC of the surfactant (Bourrel and Schechter, 1988; Wu *et al.*, 2005).

Heavy IOS

Jackson (2006) and Zhao (2007) found that surfactants with large hydrophobes solubilized more of this heavy oil than short hydrophobes. Thus, C_{20-24} IOS and C_{24-28} IOS were tested with different co-surfactants and co-solvents and the results are listed in Table 4.4. Experiments from MN-304 to MN-363 were aimed to test IOS surfactants with different co-surfactants and co-solvents. It was observed that the HLB in the formulation with IOS surfactants is very sensitive for this crude oil. The phase behavior results demonstrated Type I easily with relatively hydrophilic co-surfactant/co-solvents, however, IOS surfactants with hydrophobic co-surfactants/co-solvents showed poor aqueous solubility such as cloudy phase or phase separation. Experiment MN-367 used 2 wt% C_{20-24} IOS (Petrostep S3A, batch # 18239-091907, called A in Table 4.4). It showed a low solubilization ratio of about 7 from 0% to 4% Na_2CO_3 concentration as shown in Figure 4.1. Therefore, C_{24-28} IOS (Shell batch #26445-63A) with a larger hydrophobe (longer carbon chain) was tested next. However, the specific C_{24-28} IOS batch (batch #:

26445-63A) that was used in this test was found to be more hydrophilic than the C_{20-24} IOS (A) (batch #: 18239-091907). The solubilization ratio of the formulation with 2% C_{24-28} IOS and 2% TEGBE was only 4.5 (see MN-374 in Table 4.4) Also, it should be addressed that aqueous solubility problems occurred for all phase behavior experiments with heavy IOS. It may be solved intramolecularly by substituting sulfate, maleic mono-ester, and sulfoacetate for a hydroxyl group in the IOS.

Ether sulfates

Adkins *et al.* (2010) showed that alcohol ether sulfates are stable at high temperatures for long periods of time when the pH is high. Exploiting this discovery, an alcohol ether sulfate was used in phase behavior studies at 85 °C. All these phase behavior results are summarized in Table 4.5. The first ether sulfate tested was C_{16-17}-7PO-sulfate. The formulation with C_{16-17}-7PO-sulfate showed promising microemulsion phase behavior. It generated a huge microemulsion and the fluidity of the microemulsion was good without any gels or liquid crystals. This ether sulfate is a commercial surfactant that has been successfully used for low temperature (less than 60°C) applications making it easier and less expensive to manufacture than ether sulfonate surfactants, especially the alkyl ether gylceryl sulfonates (Levitt *et al.*, 2009). However, it was observed that alcohol ether sulfate took a relatively long time to reach equilibrium. Figure 4.2 shows the phase behavior for experiment MN-411 (Table 4.5) for the 2% C_{16-17}-7PO-sulfate surfactant formulation with 2% TEGBE with crude #5. Several other PO sulfate surfactants with different hydrophobes and PO numbers were tested.

Guerbet alcohol (Larger hydrophobe structures) for ether sulfate

With the understanding that a high EACN crude oil requires surfactants with large hydrophobes, another approach was identified to meet this requirement, i.e., dimer of

linear alcohols to make inexpensive large hydrophobe Guerbet alcohols for which the condensation reaction does not have to go to completion, thereby leaving behind about 10-20% monomer alcohol. Thus, the final ether sulfate will contain 80-90% of Guerbet ether sulfate and 10-20% of linear alcohol ether sulfate (Adkins *et al.*, 2010). This technique coupled with the enhanced hydrolytic stability of ether sulfate will allow us to use Guerbet alkoxy sulfate in high temperature EOR applications wherein the hydrophobe size could be anywhere starting from 20-24 carbons (using C_{10-12} alcohols as monomer) to as large as 32-36 carbons (using C_{16-18} alcohols). The surfactants made in the initial effort to investigate this idea are based on C_{20} and C_{24} Guerbet alcohols commonly referred to as ISOFOL alcohols in pure commercial form. In order to mimic inexpensive Guerbet ether sulfate, ISOFOL ether sulfates were blended with minor amounts of monomer alcohol ether sulfates for the phase behavior studies.

Figure 4.3 shows that the larger hydrophobe structure ether sulfate, C_{20}-8EO-sulfate (a blend of C_{20}-6EO-sulfate and C_{20}-10EO-sulfate) without any co-solvent, gave a relatively high solubilization ratio and thus low interfacial tension (IFT) was achieved with crude M #5. In order to keep the cost structure down for these molecules, a low-cost Guerbet alcohol derivative was simulated by blending Guerbet ether sulfate with monomer alcohol ether sulfate in a 4:1 ratio and no co-solvent. Figure 4.4 shows that high solubilization ratios were also achieved with this mixture of 1.8% C_{24}-10EO-sulfate and 0.2% C_{12-15}-12EO-sulfate. These preliminary results indicate this approach was very promising. Although good phase behavior results were seen for several of these Guerbet ether sulfate surfactants, it is thought that even better interactions with oil and water could be obtained by adding a segment of PO incorporated between the hydrophobic and the hydrophilic parts of the molecule. Thus, the next series of Guerbet type sulfates containing PO in the molecules were studied and evaluated.

Various tests using both EO and PO sulfate surfactants have been conducted with two new batches of crude known as M #6 and #7. Generally, phase behavior tests with PO/EO sulfate surfactants showed high solubilization ratios, small droplet sizes in the microemulsions, nice fluidity, and low optimal salinity. It is believed that additional PO segments increase entropy and hydrophobicity in the microemulsion phase. Also containing PO/EO segments together in the molecules is more feasible to tailor the properties of surfactant by controlling PO numbers for hydrophobicity and EO numbers for hydrophilicity respectively. Consequently, the formulation could result in favorable performance.

Figure 4.5 to Figure 4.8 show oil scan phase behavior plots for 0.25% C_{32}-7PO-6EO Sulfate, 0.25% C_{20-24} IOS, 0.25% TEGBE, 0.4% Aerosol MA-80 used in a core flood experiment. However, a very hydrophilic solubilizer was needed to dissolve these large molecule surfactants in the aqueous phase as a tradeoff. So, Aerosol MA-80 was used. The functions and mechanism of Aerosol MA-80 are described in the sacrificial surfactant section in great detail. The summary for the Guerbet ether sulfate studies is listed in Table 4.6

4.1.3 Aqueous solubility improvement

Conventional glycol ether

First, new co-solvents were tested to modify the formulation containing 1.5% CS2000A and 0.5% IOS 6300 with 3% EGBE, which was considered before to be a robust solution (Zhao, 2007). The main purpose was to examine new chemicals for reducing chemical cost. Several alcohols and glycol ethers were evaluated in order to minimize the requirement of a co-solvent. Among the tested co-solvents, triethylene glycol ether (TEGBE) replaced 3% EGBE to 2% TEGBE by increasing the numbers of ethylene oxide present. Phase behavior for 1.5% CS2000A and 0.5% IOS 6300 with 2%

TEGBE (Figure 4.9) shows the optimum salinity of about 10,000 ppm Na_2CO_3, and the solubilization ratio of 8, which results in similar behavior to the experiment with the same surfactants and 3% EGBE co-solvent. The aqueous solubility limit of 12,500 ppm Na_2CO_3 is greater than the optimum salinity of 10,000 ppm in this particular experiment. However, similar experiments with surfactants and/or different oil samples showed aqueous solubility less than optimal salinity. So, this solution was not considered to be a robust solution and other alternatives were explored.

Alcohol ethoxylate surfactant

It is well documented that increasing the EO number increases the aqueous solubility of surfactants (Sahni *et al.*, 2010). As discussed in the literature review section, alcohol ethoxylate surfactants, namely non-ionic surfactants, are reactive when heated to a temperature known as the cloudy point due to the sharp increase in aggregation number of the micelles and decrease in intermicellar repulsion (Milton, 2004). When alcohol ethoxylate surfactants are being used in the formulation, the cloudy point is a key parameter to be considered.

Further studies based on structure of alcohol ethoxylate surfactants were performed for better co-solvent selection and optimization of co-solvent usage. A 1% C_{20-24} IOS was tested with various alcohol ethoxylate surfactants as shown in Figure 4.10. Several significant observations were found. First, a small change in the carbon number from C_{10} to C_{13} showed very similar results in aqueous solubility as if EO numbers had changed. It is believed that the ability to resist electrolyte and hardness depends mainly on the numbers of EO in an alcohol ethoxylate surfactant with a short carbon chain range (C_{10}-C_{13}). Second, the alcohol ethoxylate surfactant needs to have at least 8 EOs to function as a co-solvent for the C_{20-24} IOS surfactant used in many case studies as the primary surfactant. Third, the Na_2CO_3 solubility increases rapidly from 8 EOs to 18EOs.

However, the observed aqueous solubility increase is minimal beyond 18EOs. This observation gives reason for designing the phase behavior formulation with non-ionic surfactants because optimal salinity shifts drastically as the number of EOs increases. Figure 4.11 shows that at a low surfactant concentration, these non-ionic surfactants were more effective than TEGBE, making them the best co-solvent found to date. Also, the aqueous solubility (clear solution) can be achieved by a co-solvent/alcohol ethoxylate surfactant combination in order to minimize the co-solvent usage and reduce the chemical cost.

Adding oil

A way to avoid slug phase separation by including a paraffinic white oil or crude oil was tested in the Loudon field many years ago (Maerker and Gale, 1992). It was thought that adding small amounts of either mineral oil (an idea advocated by Rice University at the time based upon making a Type I microemulsion using a more hydrophobic oil) or crude oil to some of the more promising surfactant solutions would help overcome the phase separation problem. This was an old idea to avoid problems of cloudy aqueous solutions and phase separation. A 2.0% C_{20-24} IOS, 2.0% TEGBE, and 2.0% Na_2CO_3 surfactant solution was clear with about 1% oil shown in Figure 4.12. However, the results were very sensitive to the volume of oil added to the solution and sometimes changed after a few days making the results inconsistent. Consequently, this approach also did not appear to be a robust solution to the aqueous solubility problem.

Sacrificial surfactants

Given the extreme difficulty of reducing the expensive co-solvent concentration in formulations effective for crude oils with low acid numbers, a completely new approach was considered and the concept of sacrificial surfactants was introduced in our

laboratories. The reason why it is called a sacrificial surfactant is because it provides aqueous stability temporarily and later hydrolyses. A sacrificial surfactant is used to get the primary surfactant into solution temporarily i.e. a clear, stable aqueous solution including polymers for a limited duration. An even more elegant approach is to make new surfactants that are difunctional where-in the functional group that gave extra aqueous solubility could be destroyed under controlled conditions.

With this concept in mind, TDA-9EO-sulfate with C_{20-24} IOS was evaluated because TDA-9EO-sulfate is very hydrophilic and thought to be reactive at 85 °C. However, under the alkali conditions used in the experiments, the sulfate group did not hydrolyze as expected and TDA-9EO-sulfate increased optimal salinity higher than improved aqueous solubility.

Aerosol MA-80 was tested as another sacrificial surfactant. Aerosol MA-80 is sodium dihexyl sulfosuccinate and its structure is shown in Figure 4.13. The Aerosol MA-80 is very hydrophilic and acts as a powerful solubilizer to give enhanced aqueous solubility even at very low concentrations. The Aerosol MA-80 molecule is highly branched and short, it was expected to disturb the order of arrays and provide a low solubilization ratio. Furthermore, it is highly reactive at high temperatures. Various aqueous tests were done to determine the concentration of Aerosol MA-80 needed for a clear solution and how long the solution would remain clear at 85 °C. Figure 4.14 through Figure 4.17 show some of the test results when C_{16-17}-7PO-sulfate was the primary surfactant for various concentrations of co-solvent and sodium carbonate of interest for the formulations. These results indicate that Aerosol MA-80 hydrolyzes too fast for use in the field, but it is suitable for use in core floods to verify the sacrificial surfactant concept. After testing concentrations of Aerosol MA-80 needed for a clear solution for certain time period, various microemulsion phase behavior tests were

performed to evaluate the effect of Aerosol MA-80 on phase behavior and surfactant performance in the formulation. Figure 4.18 compares the phase behavior result after 21 days with the phase behavior result after 270 days. It is observed that optimal salinity decreased about 0.8 wt% from 4.0 wt% to 3.2 wt%. Two iso-hexanol molecules functioned as a heavy co-solvent that shifted the phase behavior in the direction of lower to middle to upper phase microemulsion. Furthermore, hydrolyzed dihexyl sulfosuccinate provided extra hydrophobicity in the formulation. So microemulsion phase behavior was improved during decomposition of Aerosol MA-80. This could be a proper interpretation for improved microemulsion phase behavior tests with Aerosol MA-80 over time. All the phase behavior results with Aerosol MA-80 are listed in the summary tables as a co-solvent.

4.1.4 M-9 Core Flood Experiment

The ASP formulation developed using surfactant phase behavior experiments was tested in a Berea core flood experiment at the reservoir temperature of 85 °C. The purpose of the core flood experiment was to test the performance of the Guerbet alkoxy and heavy IOS surfactant with sacrificial surfactant (Aerosol MA-80) as a solubilizer. The ASP formulation showed excellent performance in the core flood. A relatively small amount of ASP slug was used (% pore volume* % surfactant concentration, PV*C, = 15) and the oil recovery was 97.6% and the final residual oil saturation was 0.8%.

M-9 Core Data

Core M-9 is Berea sandstone with a length of 28.58 cm and a diagonal of 5.03 cm. 5-minute epoxy was used to affix the two end pieces. The core was then placed inside a homemade Teflon mold and cast in slow-setting epoxy with a 1:2 ratio of

hardener to epoxy at 85 °C oven. Table 4.7 below shows the core properties of the M-9 core flood experiment.

The permeability values are listed in Table 4.8. These values are calculated from pressure data and flow rates after flooding experiments. The flooding experiments consisted of brine flooding, oil flooding, water flooding, chemical flooding (ASP flooding), and finally followed by polymer flooding. Then, the oil permeability and relative oil permeability, 208 md and 0.58 respectively, are acquired after the oil flood at the residual water saturation. Initial oil saturation of 0.61 is calculated using the volume of oil from the core. After water flooding with synthetic softened brine, water permeability of 356 md and relative water permeability of 0.056, and residual oil saturation of 0.335 are rendered. Oil saturation data for the M-9 core are shown in Table 4.9.

M-9 Brine flood

Initially M-9 core was saturated with SMB and then flooded with SMB to measure the brine permeability. SSMB was used for the chemical flood. The compositions of the SMB as well as the SSMB used in the chemical flood are listed in Table 4.2. The brine flood was done at a rate of 3 ml/min and the pressure data measured is shown in Figure 4.19. The measured absolute permeability is 356 md.

M-9 Oil flood

The crude was filtered through a 0.45 micron filter under a pressure of 50 psi at reservoir temperature (85 °C). Prior to the oil flood, filtered oil viscosity was measured by a rheometer at the reservoir temperature (6.6 cP at 10 s^{-1}). Then, the oil flood experiment was conducted with 1.5-2 pore volumes of filtered oil. The flood was continued until the water cut of effluent was less than 1%. The oil permeability to

residual water was calculated to be 208 md and the relative permeability endpoint of oil was 0.58. The initial oil saturation (S_{oi}) after the oil flood was 0.61, for a residual water saturation of 0.39. The pressure data is shown for the M-9 oil flood in Figure 4.20.

M-9 Water Flood

The core was water flooded with SMB (2865 ppm) at a flow rate of 0.4 ml/min (5 ft/day) at 85 °C until the produced oil cut of effluent was less than 1%. The pressure data for the M-9 water flood is illustrated in Figure 4.21. After 1.4 PV of water flood, residual oil saturation (S_{or}) was obtained to be 0.335. The permeability of water was evaluated to be 19.94 md, corresponding to the end-point relative permeability of 0.056.

M-9 Chemical flood design

The chemical flood is designed using data from the phase behavior, aqueous solubility, activity diagram, and polymer viscosity. The solubilization plots for different oil concentrations with 0.25% C_{32}-7PO-6EO Sulfate, 0.25% C_{20-24} IOS, 0.25% TEGBE, and 0.4% Aerosol MA-80 are illustrated from Figure 4.5 to Figure 4.8. Activity diagram shown in Figure 4.22 determines the salinity of injected chemical slug and polymer drive for designing sufficient driving force. Also, since Aerosol MA-80 hydrolyzes at a high temperature as discussed above, the aqueous stability test was conducted to confirm that the injection solution stayed in a clear, stable single phase until it reached the core from the injector. The ASP solution was clear for 40 minutes with MA-80 at the reservoir temperature of 85 °C. So, it was suitable for use in core floods to verify the sacrificial surfactant concept. The aqueous experiment was conducted with Floppam^{TM} 3630S polymer (SNF Floerger, Cedex, France). The designed viscosity was estimated from the inverse of the minimum total mobility with Corey relation as described in Chapter 3. The concentrations of polymer for the ASP slug and polymer drive were determined based on

the polymer viscosity experiments at reservoir temperature shown in Figure 4.23. All of the measured fluid viscosities at reservoir temperature are listed in Table 4.10. Characteristics and chemical composition for the ASP slug and polymer drive for core flood experiment M-9 are tabulated in Tables 4.11 and Table 4.12 correspondingly.

M-9 Chemical Flood recovery

A 0.3 PV ASP slug with 2000 ppm FP 3630S polymer concentration (16 cp) was injected at 1 ft/D followed by a polymer drive with 1150 ppm FP 3630S polymer concentration (18 cp) at the same rate. Figure 4.24 shows the pressure data across the whole core, section 1 (inlet), section 2&3, and section 4 (outlet) versus the pore volumes injected. The oil breakthrough occurred at 0.31 PV and the emulsion breakthrough occurred at 0.84 PV. The total oil recovery was calculated to be 97.6 % of residual oil. A high oil cut (around 55%) was observed and most of the free oil was recovered before emulsion breakthrough. The residual oil saturation after the chemical flood (Sorc) was 0.8 %. Figure 4.25 shows the oil recovery data for the M-9 core flood. Surfactant concentration was measured on all even numbered samples by HPLC so that the retention could be determined. The surfactant adsorption/retention value was 0.01 mg/g rock shown in Figure 4.26, indicating that PV*C= 15% was just sufficient enough to satisfy retention requirements. The result of the M-9 core flood is tabulated in Table 4.13.

Table 4.1 Viscosity of Crude Oil Samples Received at Different Times

Time period	oil sample	Viscosity (filtered)
January, 2008- February, 2008	3	3.4 cp
March, 2008 - June, 2008	4	Not measured
June, 2008 - January, 2009	5	Not measured
January, 2009 - March, 2009	6	6.3
March, 2009 - Present time	7	6.6

Table 4.2 Composition of Synthetic Brines and Synthetic Soften brine

Concentration (ppm)	SMB	SSMB
Na	900	932
Ca	20	0
Mg	5	0
K	15	15
Cl	800	800
SO4	18	18
HCO3	1100	1100
TDS	2858	2865

*SMB: Synthetic Brine
*SSMB: Synthetic Soften Brine

Table 4.3 Summary of Phase Behavior Screening criteria

Performance Characteristic	**Corresponding chemical**
Less surfactant adsorption in formation	Anionic surfactants
Low EACN crude oil / Low IFT at high salt (TDS)	Light GAS surfactant, IOS, AES (HLB > ~ 11)
High EACN crude oil / Low IFT at low salt (TDS)	Heavy GAS surfactant, IOS, APS, ABS, AOS (HLB < ~ 11)
Stable at high reservoir temperature	Sulfonate group at any condition / Sulfate group at pH 10-11
Sequestering hardness in brine	Strong sequestering agent, EDTA
Surfactant performance validation in core flood	Powerful solubilizer, MA 80-I
Improve aqueous solubility at low surfactant concentration, low temperature	Non-ionic surfactant
Reduce liquid crystals, viscous gel and multi phases	Branched hydrophobes / surfactants with multiple chemical structure / Mixture of surfactants / Conventional co-solvent

Table 4.4 Summary of Phase Behavior Experiments with IOS surfactants

	Primary surfactant	wt (%)	co- surfactant	wt (%)	Co-solvent	Wt (%)	Aqueous limit (wt% Na_2CO_3)	Optimum wt% Na2CO3	Solubilization ratio at optimum	Oil sample number	Comment
MN-304	C20-24 IOS (A)	0.2	-	-	C12-15 12EO	0.10	1.5	-	1.5	4	phase behavior: all type 1, sol.ratio at aqueous limitation
MN-305	C20-24 IOS (A)	0.2	-	-	C12-15 12EO	0.20	2.0	-	2.0	4	phase behavior: all type 1, sol.ratio at aqueous limitation
MN-319 A	C24-28-IOS	0.50	-	-	C12-15 12EO	0.60	1.50	-	2	4	phase behavior: all type 1, sol.ratio at aqueous limitation
MN-320 A	C24-28-IOS	0.50	C12-15 12EO	0.10	TEGBE	1.00	2.50	-	8	4	phase behavior: all type 1, sol.ratio at aqueous limitation
MN-330	C20-24 IOS (A)	0.25	C16-18 AXS	0.25	C12-15 12EO	0.10	NC	-	-	4	0.5-1% cloudy, 1.5-5% phase separation
MN-331	C20-24 IOS (A)	0.25	C16-18 AXS	0.25	C12-15 12EO	0.20	NC	-	-	4	0.5-1.5% cloudy, 2-5% phase separation
MN-332	C20-24 IOS (A)	0.25	C16-18 AXS	0.25	C12-15 12EO	0.30	0.5	-	-	4	1.0% cloudy, 1.5-5% phase separation
MN-333	C20-24 IOS (A)	0.25	C16-18 AXS	0.25	TEGBE	1.00	NC	-	-	4	0.5.1% cloudy, 1.5-5% phase separation
MN-334	C20-24 IOS (A)	0.25	C14 ABS	0.25	C12-15 12EO	0.10	NC	-	-	4	0.5-5% phase separation
MN-335	C20-24 IOS (A)	0.25	C14 ABS	0.25	C12-15 12EO	0.20	0.5	-	-	4	1-5% phase separation
MN-336	C20-24 IOS (A)	0.25	C14 ABS	0.25	C12-15 12EO	0.30	1.0	-	-	4	1.5% cloudy and some precipitation, 2-5% phase separation
MN-337	C20-24 IOS (A)	0.25	C14 ABS	0.25	TEGBE	1.00	NC	-	-	4	0.5.1% cloudy, 1.5-5% phase separation
MN-338	C20-24 IOS (A)	0.25	C14 ABS	0.25	C12-15 12EO	0.10	0.5	-	-	4	1-2% cloudy, 2.5-5% phase separation
MN-339	C20-24 IOS (A)	0.25	C14 ABS	0.25	C12-15 12EO	0.20	0.5	-	-	4	1-5% cloudy
MN-340	C20-24 IOS (A)	0.25	C14 ABS	0.25	C12-15 12EO	0.30	1.0	-	-	4	1.5-2% cloudy, 2.5-5% phase separation

Table 4.4 Summary of Phase Behavior Experiments with IOS surfactants (Cont.)

	Primary surfactant	wt (%)	co- surfactant	wt (%)	Co-solvent	Wt (%)	Aqueous limit (wt% Na_2CO_3)	Optimum wt% Na2CO3	Solubilization ratio at optimum	Oil sample number	Comment
MN-341	C20-24 IOS (A)	0.25	C14 ABS	0.25	TEGBE	1.00	NC	-	-	4	0.5-5% phase separation
MN-342	C20-24 IOS (A)	0.25	C16 ABS	0.25	C12-15 12EO	0.10	NC	-	-	4	0.5-3% cloudy, 3.5-5% phase separation
MN-343	C20-24 IOS (A)	0.25	C16 ABS	0.25	C12-15 12EO	0.20	0.5	-	-	4	1-2.5% cloudy, 3-5% phase separation
MN-344	C20-24 IOS (A)	0.25	C16 ABS	0.25	C12-15 12EO	0.30	0.5	-	-	4	1% cloudy but not crystal clear, 1.5 % cloudy, 2-5% phase separation
MN-345	C20-24 IOS (A)	0.25	C16 ABS	0.25	TEGBE	1.00	NC	-	-	4	0.5-2% cloudy, 2.5-5% phase separation
MN-346	C20-24 IOS (B)	0.25	C16 ABS	0.25	C12-15 12EO	0.20	0.5	-	-	4	1% cloudy but not crystal clear, 1.5-5% phase separation
MN-347	C20-24 IOS (B)	0.25	C16 ABS	0.25	C12-15 12EO	0.20	0.5	-	-	4	1% cloudy, 1.5-5% phase separation
MN-348	C20-24 IOS (A)	1.00	-	-	TEGBE	2.00	-	-	-	4	C20-24 IOS (A) solubilze more oil than C20-24 IOS (B), not accurate sigma
MN-349	C20-24 IOS (B)	1.00	-	-	TEGBE	2.00	-	-	-	4	C20-24 IOS (A) solubilze more oil than C20-24 IOS (B)
MN-350	C20-24 IOS (A)	1.00	C12-15 12EO	0.30	TEGBE	1.00	NC	-	-	4	1% cloudy, 2-5% phase separation
MN-351	C20-24 IOS (B)	1.00	C12-15 12EO	0.30	TEGBE	1.00	2.0	-	-	4	2.5-5% phase separation
MN-353	C20-24 IOS (A)	0.20	-	-	C12-15 12EO	0.10	1.0	3.5	17	4	not accurate sigma
MN-354	C20-24 IOS (A)	0.20	-	-	C12-15 12EO	0.20	1.5	3.7	15	4	not accurate sigma
MN-355	C20-24 IOS (B)	0.20	-	-	C12-15 12EO	0.10	2.5	>5	12	4	not accurate sigma, sol.ratio at aqueous limitation
MN-356	C20-24 IOS (B)	0.20	-	-	C12-15 12EO	0.20	2.5	>5	11	4	not accurate sigma, sol.ratio at aqueous limitation

Table 4.4 Summary of Phase Behavior Experiments with IOS surfactants (Cont.)

	Primary surfactant	wt (%)	co- surfactant	wt (%)	Co-solvent	Wt (%)	Aqueous limit (wt% Na_2CO_3)	Optimum wt% Na2CO3	Solubilization ratio at optimum	Oil sample number	Comment
MN-357	C20-24 IOS (A)	2.00	C12-15 12EO	0.10	TEGBE	1.00	1.0	ABOVE 5	2	4	ALL TYPE 1, at 1% Sol. Ratio is 2
MN-358	C20-24 IOS (A)	2.00	C12-15 12EO	0.10	TEGBE	1.50	1.0	ABOVE 5	1.8	4	ALL TYPE 1, at 1% Sol. Ratio is 1.8. (at 1.5% clear but not crystal clear)
MN-359	C20-24 IOS (A)	2.00	C12-15-3EO-sulfonate	0.10	TEGBE	1.00	0.5	ABOVE 5	0.5	4	at 0.5% Sol. Ratio is 0.5
MN-360	C20-24 IOS (A)	2.00	C12-15-3EO-sulfonate	0.10	TEGBE	1.50	1.0	ABOVE 5	1.5	4	ALL TYPE 1, at 1% Sol. Ratio is 1.5
MN-361	C20-24 IOS (A)	2.00	C12-15-3EO-sulfonate	0.05	C12-15 12EO	0.05	NC	-	-	4	no phase behavior, AQ is all cloudy
MN-362	C20-24 IOS (A)	2.00	C12-15-3EO-sulfonate	0.10	C12-15 12EO	0.10	NC	-	-	4	no phase behavior, AQ is all cloudy
MN-363	C20-24 IOS (A)	2.00	C12-15-3EO-sulfonate	0.30	C12-15 12EO	0.30	NC	-	-	4	no phase behavior, AQ is all cloudy
MN-364	C24-28-IOS	1.00	C12-15 12EO	0.10	TEGBE	1.50	4.0	ABOVE 5	6	4	at 4% Sol. Ratio is 6
MN-365	C24-28-IOS	2.00	C12-15 12EO	0.10	TEGBE	1.50	2.5	ABOVE 5	2	4	at 2.5% Sol. Ratio is 2
MN-367	C20-24 IOS (A)	2.00	-	-	-	-	NC	3.3	7	5	Aqueous stability is all cloudy
MN-368	C20-24 IOS (B)	2.00	-	-	-	-	1.0	ABOVE 4	4	5	at 1% oil solubilization ratio is 4
MN-369	C20-24 IOS (A)	1.00	TDA 9EO sulfate	0.50	-	-	1.0	-	-	5	no phase behavior
MN-370	C20-24 IOS (A)	1.00	TDA 9EO sulfate	1.00	-	-	2.0	ABOVE 4	-	5	all type 1
MN-371	C20-24 IOS (A)	1.00	TDA 9EO sulfate	0.50	TEGBE	0.50	2.0	-	-	5	all type 1
MN-372	C20-24 IOS (A)	2.00	TDA 9EO sulfate	2.00	-	-	2.0	ABOVE 4.5	-	5	all type 1

Table 4.4 Summary of Phase Behavior Experiments with IOS surfactants (Cont.)

	Primary surfactant	wt (%)	co- surfactant	wt (%)	Co-solvent	Wt (%)	Aqueous limit (wt% Na_2CO_3)	Optimum wt% Na2CO3	Solubilization ratio at optimum	Oil sample number	Comment
MN-373	C24-28-IOS	2.00	-	-	-	-	NC	-	-	5	only aqueous stability was tested
MN-374	C24-28-IOS	2.00	-	-	TEGBE	2.00	4.5	2.2	4	5	Low oil solubilization ratio
MN-375	C24-28-IOS	1.33	C15+ bABS	0.67	TEGBE	2.00	4.0	-	5	5	all type 1, at 4.0% sol.raio is 5
MN-376	C24-28-IOS	1.33	CS2000A	0.67	TEGBE	2.00	1.0	3.5	10	5	Poor aqueous stability-
MN-377	C24-28-IOS	1.00	CS2000A	1.00	TEGBE	2.00	0.5	2.5	8	5	Poor aqueous stability-
MN-378	C24-28-IOS	1.33	C16 bABS	0.67	TEGBE	2.00	2.5	4.6	9	5	Poor aqueous stability , high optimum salinity
MN-379	C24-28-IOS	1.33	C20-24 IOS (A)	0.67	TEGBE	2.00	4.0	-	4	5	all type 1, at 4.0% sol.raio is 4
MN-382	C24-28-IOS	0.50	C20-24 IOS (A)	1.50	EGBE	2.00	1.0	4.2	4	5	Poor aqueous stability-, high optimum salinity
MN-383	C20-24 IOS (A)	2.00	-	-	TEGBE	2.00	1.5	4.6	5	5	Poor aqueous stability , high optimum salinity
MN-390	C24-28-IOS	1.50	C16 bABS	0.50	TEGBE	2.00	3.0	4.6	6	5	Poor aqueous stability , high optimum salinity
MN-400	C20-24 IOS (A)	1.50	C16-17-9PO-sulfonate	0.50	TEGBE	2.00	2.0	-	0.5	5	all Type1
MN-401	C20-24 IOS (A)	1.50	C16-17 3PO-sulfonate	0.50	TEGBE	2.00	2.0	-	1.9	5	all Type1
MN-402	C24-28-IOS	1.50	C16-17-9PO-sulfonate	0.50	TEGBE	2.00	2.0	-	2.4	5	all Type1, 4.0% Type3 starts

Table 4.5 Summary of Phase Behavior Experiments with Ether sulfate with 50% oil

	Primary surfactant	wt (%)	co-surfactant	wt (%)	Co-solvent	wt (%)	Aqueous limit (wt% Na2CO3)	Optimum wt% Na2CO3	Solubilization ratio at optimum	Oil sample number	Comment.
MN-411	C16-17-7PO-sulfate	2.00	-	-	TEGBE	2.00	1.50%	3.40%	20	5	-
MN-412	C16-17-7PO-sulfate	2.00	-	-	TDA 12EO TDA 30EO	0.28 0.22	0.50%	3.30%	21	5	Multiphase in middle phase
MN-414	C14-15-9PO-sulfate	2.00	-	-	TDA 12EO TDA 30EO	0.28 0.22	0.50%	2.75%	14	5	Multiphase in middle phase
MN-415	C13-13PO-sulfate	2.00	-	-	TEGBE	2.00	0.50%	1.45%	11	5	-
MN-416	C13-13PO-sulfate	2.00	-	-	TDA 12EO TDA 30EO	0.28 0.22	0.50%	3.50%	24	5	Multiphase in middle phase
MN-418	C14-15-9PO-sulfate	0.30	-	-	Butanol 3.5EO	0.30	0.50%	1.25%	17	5	-
MN-419	C14-15-9PO-sulfate	0.30	-	-	-	-	0.50%	2.30%	10	5	-
MN-420	C14-15-9PO-sulfate	0.30	-	-	TEGBE	0.30	0.50%	1.25%	15	5	-
MN-421	C13-9PO-sulfate	0.30			Butanol 3.5EO	0.30	1.00%	2.10%	20	5	-
MN-424	C16-17-7PO-sulfate	2.00	-	-	-	-	Not measured	2.65%	26	5	-
MN-430	C16-17-7PO-sulfate	2.00	-	-	MA-80-I	0.50	Not measured	2.80%	28	5	-
MN-431	C14-15-9PO-sulfate	2.00	-	-	MA-80-I	0.50	Not measured	2.15%	27	5	-
MN-432	C16-17-7PO-sulfate	1.00	C14-15-9PO-sulfate	1.00	-	-	Not measured	1.95%	19	5	-
MN-433	C16-17-7PO-sulfate	1.00	C13-13PO-sulfate	1.00	-	-	Not measured	1.60%	24	5	-
MN-437	C16-17-7PO-sulfate	1.00	-	-	-	-	Not measured	2.05%	9	5	-
MN-438	C14-15-9PO-sulfate	1.00	-	-	-	-	Not measured	1.85%	17	5	-

Table 4.5 Summary of Phase Behavior Experiments with Ether sulfate with 50% oil (Cont.)

	Primary surfactant	wt (%)	co-surfactant	wt (%)	Co-solvent	wt (%)	Aqueous limit (wt% Na2CO3)	Optimum wt% Na2CO3	Solubilization ratio at optimum	Oil sample number	Comment.
MN-451	C13-7PO-sulfate	1.00	-	-	-	-	Not measured	3.50%	14	5	-
MN-452	C13-9PO-sulfate	1.00	-	-	-	-	Not measured	2.00%	16	5	-
MN-453	C13-13PO-sulfate	1.00	-	-	-	-	Not measured	0.70%	20	5	Viscous Type 2
MN-456	C13-7PO-sulfate	1.00	-	-	MA-80-I	0.40	Not measured	4.20%	28	5	-
MN-457	C13-9PO-sulfate	1.00	-	-	MA-80-I	0.40	Not measured	2.80%	16	5	-
MN-458	C13-13PO-sulfate	1.00	-	-	MA-80-I	0.40	Not measured	0.75%	13	5	Viscous Type 2
MN-489	C14-15-9PO-sulfate	1.00	-	-	TEGBE	0.50	Not Measured	2.50%	50	6	viscous gels
MN-492	C13-9PO-sulfate	1.00	TEGBE	0.50	MA-80-I	0.20	Not Measured	2.30%	11	6	
MN-498	C13-9PO-sulfate	0.50	C13-7PO-sulfate	0.50	TEGBE	0.50	Not Measured	4.50%	15	6	-
MN-499	C13-9PO-sulfate	0.75	C13-7PO-sulfate	0.25	TEGBE	0.50	Not Measured	4.20%	10	6	-
MN-500	C13-9PO-sulfate	1.00	-	-	TEGBE	0.50	Not Measured	3.40%	7	6	-
MN-502	C16-17-7PO-sulfate	1.00	-	-	TEGBE	1.00	Not Measured	3.70%	12	6	-
MN-504	C16-17-7PO-sulfate	1.00	TEGBE	0.50	MA-80-I	0.70	Not measured	3.60%	16	6	-

Table 4.5 Summary of Phase Behavior Experiments with Ether sulfate with oil scans (Cont.)

	Primary surfactant	wt (%)	co-surfactant	wt (%)	Co-solvent	wt (%)	Aqueous limit (wt% Na2CO3)	Optimum wt% Na2CO3	Solubilization ratio at optimum	Oil sample number	Comment.
MN-505	C16-17-7PO-sulfate	1.00	TEGBE	0.50	MA-80-I	0.20	Not measured	3.70%	30	6	50% oil
MN-506	C16-17-7PO-sulfate	1.00	TEGBE	0.50	MA-80-I	0.20	Not measured	4.20%	12	6	20% oil scan
MN-507	C16-17-7PO-sulfate	1.00	TEGBE	0.50	MA-80-I	0.30	Not measured	3.80%	24	6	50% oil
MN-508	C16-17-7PO-sulfate	1.00	TEGBE	0.50	MA-80-I	0.40	Not measured	3.40%	12	6	50% oil
MN-509	C16-17-7PO-sulfate	1.00	TEGBE	0.50	MA-80-I	0.20	Not measured	2.80%	7	6	50% oil, Type II Gels
MN-510	C16-17-7PO-sulfate	1.00	TEGBE	0.50	MA-80-I	0.20	Not measured	3.40%	20	6	40% oil, Type II Gels
MN-511	C16-17-7PO-sulfate	1.00	TEGBE	0.50	MA-80-I	0.20	Not measured	3.60%	20	6	30% oil, Type II Gels
MN-512	C16-17-7PO-sulfate	1.00	TEGBE	0.50	MA-80-I	0.20	Not measured	3.70%	10	6	20% oil, Type II Gels
MN-513	C16-17-7PO-sulfate	1.00	TEGBE	0.50	MA-80-I	0.20	Not measured	3.85%	25	6	10% oil, Type II Gels
MN-514	C16-17-7PO-sulfate	0.75	C14-15-9PO-sulfate	0.25	TEGBE MA-80-I	0.50 0.20	Not measured	1.80%	4	6	Type II Gels
MN-515	C16-17-7PO-sulfate	0.75	C20-24 IOS (A)	0.25	TEGBE MA-80-I	0.50 0.20	Not measured	3.90%	9	6	50% oil
MN-516	C16-17-7PO-sulfate	0.75	C24-28 IOS (A)	0.25	TEGBE MA-80-I	0.50 0.20	Not measured	3.50%	7	6	50% oil
MN-517	C16-17-7PO-sulfate	0.75	C24-10EO-sulfate	0.25	TEGBE MA-80-I	0.50 0.20	Not measured	3%	0	6	Type II Gels 50% oil
MN-518	C16-17-7PO-sulfate	0.50	C14-15-9PO-sulfate	0.50	TEGBE MA-80-I	0.50 0.20	Not measured	3.90%	8	6	20% Oil
MN-519	C16-17-7PO-sulfate	0.75	C14-15-9PO-sulfate	0.25	TEGBE MA-80-I	0.50 0.20	Not measured	3.4%?	24	6	50% oil

Table 4.5 Summary of Phase Behavior Experiments with Ether sulfate with oil scans (Cont.)

	Primary surfactant	wt (%)	co-surfactant	wt (%)	Co-solvent	wt (%)	Aqueous limit (wt% Na2CO3)	Optimum wt% Na2CO3	Solubilization ratio at optimum	Oil sample number	Comment.
MN-520	C16-17-7PO-sulfate	0.50	C14-15-9PO-sulfate	0.50	TEGBE MA-80-I	0.50 0.20	Not measured	3.1%?	24	6	50% oil
MN-522	C16-17-7PO-sulfate	0.75	C20-24 IOS (A)	0.25	TEGBE MA-80-I	0.50 0.20	Not measured	5.00%	10	6	50% oil
MN-527	C16-17-7PO Sulfate	0.66	C20-24 IOS (A)	0.33	TEGBE MA-80-I	0.50 0.30	Not measured	>4%	~10	6	50% oil
MN-528	C16-17-7PO Sulfate	0.75	C24-28-IOS (new)	0.25	TEGBE MA-80-I	0.50 0.30	Not measured	2.75%	22	6	Type II Gels, 50% oil
MN-530	C16-17-7PO Sulfate	0.75	C20-24 IOS (A)	0.25	TEGBE	0.50	Not measured	3.90%	18	6	50% oil

Table 4.6 Summary of Phase Behavior Experiments with Guerbet ether sulfate

	Primary surfactant	wt (%)	Co- surfactant	wt (%)	Co-solvent	wt (%)	Aqueous limit (wt% Na2CO3)	Optimum wt% Na2CO3	Solubilization ratio at optimum	Oil sample number	Comment.
MN-428	C20-10EO-sulfate	1.00					Not measured	3.20%	8.5	5	-
MN-429	C20-10EO-sulfate	1.00	C20-10EO-sulfate	1.00	-	-	Not measured	2.90%	6	5	Solids in Type II
MN-439	C20-6EO Sulfate	1.00	C20-10EO-sulfate	1.00	-	-	Not measured	2.50%	6	5	-
MN-439-1	C20-6EO Sulfate	1.00	C20-10EO-sulfate	1.00	-	-	Not measured	3.30%	10	5	-
MN-440	C20-6EO Sulfate	1.50	C20-14EO Sulfate	0.50	-	-	Not measured	3.10%	5	5	-
MN-447	C20-2EO Sulfate	1.00	C20-6EO Sulfate	1.00	-	-	Not measured	0.85%	9	5	-
MN-448	C20-2EO Sulfate	1.00	C20-6EO Sulfate	1.00	-	-	Not measured	1.15%	6	5	-
MN-455	C20-2EO Sulfate	1.25	C20-10EO Sulfate	0.75	-	-	Not measured	1.70%	6	5	-
MN-459	C20-10EO Sulfate	0.50	C20-6EO Sulfate	0.50	-	-	Not measured	3.80%	9	5	-
MN-460	C20-10EO Sulfate	0.50	C20-6EO Sulfate	0.50	MA-80-I	0.40	Not Measured	~4.5%	Unknown	5	-
MN-461	C20-2EO Sulfate	1.50	C20-6EO Sulfate	0.50	-	-	Not Measured	< 0%	Unknown	5	Type 2 w/ Macroemulsion
MN-462	C24-10EO Sulfate	2.00	-	-	-	-	Not Measured	1.00%	Unknown	5	Type 2 Macroemulsion
MN-463	C24-14EO Sulfate	2.00	-	-	-	-	Not Measured	2.90%	13	5	-
MN-467	C24-10EO Sulfate	1.80	C12-15-12EO Sulfate	0.20	-	-	Not Measured	1.30%	17	5	-
MN-470	C24-10EO Sulfate	1.60	C12-15-12EO Sulfate	0.40	-	-	Not Measured	2.30%	4	5	Viscous Type 2
MN-472	C24-10EO Sulfate	1.00	C20-10EO Sulfate	0.10	MA-80-I	0.40	Not Measured	2.70%	4	5	

Table 4.6 Summary of Phase Behavior Experiments with Guerbet ether sulfate (Cont.)

	Primary surfactant	wt (%)	Co- surfactant	wt (%)	Co-solvent	wt (%)	Aqueous limit (wt% Na2CO3)	Optimum wt% Na2CO3	Solubilization ratio at optimum	Oil sample number	Comment.
MN-474	C24-2EO Sulfate	0.50	C20-6EO Sulfate	0.50	MA-80-I	0.40	Not Measured	1.95%	18	5	Viscous Type 2
MN-475	C24-10EO Sulfate	0.90	C12-15-12EO Sulfate	0.10	MA-80-I	0.40	Not Measured	2.25%	<10	5	Viscous Type 2
MN-476	C24-10EO Sulfate	0.90	C12-15-12EO Sulfate	0.10	-	-	Not Measured	2.40%	6	5	Solids
MN-477	C24-10EO Sulfate	0.30	C12-15-12EO Sulfate	0.03	-	-	Not Measured	1.80%	10	5	Solids
MN-486	C20-2EO Sulfate	0.90	C20-6EO Sulfate	0.90	(C12-15-10EO Sulfate)	0.20	Not Measured	3.40%	5	6	-
MN-488	C20-2EO Sulfate	0.90	C20-6EO Sulfate	0.90	(C12-15-3EO Sulfate)	0.20	Not Measured	3.60%	9	6	-
MN-490	C20-2EO Sulfate	0.45	C20-6EO Sulfate	0.45	C12-15-3EO-Sulfate	0.10	Not Measured	3.40%	4	6	-
MN-491	C20-2EO Sulfate	0.45	C20-6EO Sulfate	0.45	C12-15-3EO-Sulfate	0.10	Not Measured	3.70%	4	6	1.5% MA-80-I
MN-495	C20-2EO Sulfate	0.45	C20-6EO Sulfate	0.45	C12-15-3EO-Sulfate	0.10	Not Measured	-	-	6	.5% TEGBE
MN-496	C20-2EO Sulfate	0.45	C20-6EO Sulfate	0.45	C12-15-3EO-Sulfate	0.10	Not Measured	-	-	6	1% TEGBE
MN-523	C20-7PO Sulfate	1.00	-	-	TEGBE	0.50	Not measured	-	-	6	Type I Gel
MN-524	C20-7PO Sulfate	0.50	C16-17-7PO Sulfate	0.50	TEGBE	0.50	Not measured	-	-	6	Type I Gel
MN-525	C20-7PO Sulfate	1.00	-	-	TEGBE	0.50	Not measured	-	-	6	Type I Gel
					MA-80-I	0.20					
MN-526	C20-7PO Sulfate	0.50	C16-17-7PO Sulfate	0.50	TEGBE	0.50	Not measured	-	-	6	Type I Gel
					MA-80-I	0.20					
MN-529	C20-7PO-10EO Sulfate	1.00	-	-	TEGBE	0.50	Not measured	>5%	-	6	Type I Gel
MN-535	C20-7PO-6EO Sulfate	1.00	-	-	TEGBE	0.50	Not measured	2.00%	5.8	6	GEL

Table 4.6 Summary of Phase Behavior Experiments with Guerbet ether sulfate (Cont.)

	Primary surfactant	wt (%)	Co- surfactant	wt (%)	Co-solvent	wt (%)	Aqueous limit (wt% Na2CO3)	Optimum wt% Na2CO3	Solubilization ratio at optimum	Oil sample number	Comment.
MN-536	C20-7PO-6EO Sulfate	1.00	C20-24 IOS (A)	0.50	TEGBE	0.50	Not measured	4.50%	9.5	6	-
MN-537	C20-7PO-14EO Sulfate	1.00	-		TEGBE	0.50	Not measured	All I	0.5	6	Gel
MN-538	C20-7PO Sulfate	0.50	C20-24 IOS (A)	0.50	TEGBE	0.50	Not measured	3-4%	8.7	6	-
MN-539	C20-7PO Sulfate	0.50	C15-18 IOS	0.50	TEGBE	0.50	Not measured	All I	3	6	Little gel
MN-540	C20-7PO Sulfate	0.50	C15-18 IOS	0.50	-	-	Not measured	All I	3	6	Little gel
MN-541	C20-7PO-6EO Sulfate	1.00	-		TEGBE	0.50	Not measured	-	-	6	-
MN-542	C20-7PO-6EO Sulfate	0.50	C20-24 IOS (A)	0.50	TEGBE	0.50	Not measured	-	-	6	-
MN-543	C-20-7PO-6EO Sulfate	0.50	C15-18 IOS	0.50	TEGBE	0.50	Not measured	-	-	6	-
MN-544	C-28-7PO-2EO Sulfate	0.50	C20-24 IOS (A)	0.50	TEGBE	0.50	Not measured	3%	15.2	6	-
MN-544-1	C28-7PO-2EO Sulfate	0.50	C20-24 IOS (A)	0.50	TEGBE	0.50	Not measured	2.75	-	6	Oil Scan
MN-545	C28-7PO-2EO Sulfate	0.25	C20-24 IOS (A)	0.75	TEGBE	0.50	Not measured	3-4%	6.1	6	-
MN-547	C28-7PO-2EO Sulfate	0.50	C20-24 IOS (A)	0.50	TEGBE	0.50	Not measured	2-3%	7.3	6	-
MN-548	C28-7PO-2EO Sulfate	0.50	C20-7PO Sulfate	0.50	TEGBE	0.50	Not measured	All II	-	6	GEL
MN-549	C28-7PO-2EO Sulfate	0.25	C20-7PO Sulfate	0.25	TEGBE	0.50	Not measured	All II	-	6	All II Gel
MN-556	C28-7PO-2EO Sulfate	0.30	C20-6EO Sulfate	0.30	TDA 30	0.30	0%	All I	8	6	All I
MN-557	C28-7PO-2EO Sulfate	0.30	C20-6EO Sulfate	0.30	C24-26-26EO	0.30	Not measured	-	-	7	-

Table 4.6 Summary of Phase Behavior Experiments with Guerbet ether sulfate (Cont.)

	Primary surfactant	wt (%)	Co- surfactant	wt (%)	Co-solvent	wt (%)	Aqueous limit (wt% Na2CO3)	Optimum wt% Na2CO3	Solubilization ratio at optimum	Oil sample number	Comment.
MN-558	C28-7PO-2EO Sulfate	0.30	C20-6EO Sulfate	0.30	TDA-12	0.30	None	3.50%	40.7	7	-
MN-559	C28-7PO-2EO Sulfate	0.30	C20-6EO Sulfate	0.30	TDA 30	0.10	None	>3.5%	20.1	7	-
MN-560	C32-7PO-6EO Sulfate	0.30	C20-24 IOS (A)	0.30	TDA 30	0.20	4%	>4.5%	7	7	-
MN-561	C32-7PO-6EO Sulfate	0.30	C20-24 IOS (A)	0.30	TDA 30	0.10	1.5%	~4.5%	10.7	7	20% Oil
MN-561	C32-7PO-6EO Sulfate	0.30	C20-24 IOS (A)	0.30	TDA 30	0.10	1.5%	~4.5%	7.9	7	50% Oil
MN-562	C32-7PO-6EO Sulfate (85% comm blend)	0.30	C20-24 IOS (A)	0.30	-	-	0.5%	0.2-2.5%	10-20'	7	-
MN-563	C32-7PO-6EO Sulfate	0.30	C20-24 IOS (A)	0.30	-	-	0.5%	3%	158	7	Gel at high Na2CO3
MN-564	C32-7PO-6EO Sulfate	0.45	C20-24 IOS (A)	0.15	-	-	None	3-3.5%	6.3	7	GEL
MN-565	C32-7PO-6EO Sulfate	0.40	C20-24 IOS (A)	0.20	-	-	0%	2%	15.1	7	-
MN-566	C32-7PO-6EO Sulfate (85% comm blend)	0.40	C20-24 IOS (A)	0.20	-	-	0.5%	2.50%	25.6	7	-
MN-567	C32-7PO-6EO Sulfate	0.50	C20-24 IOS (A)	0.50	TEGBE	0.50	1%	3.75-4%	23.3	7	-
MN-568	C32-7PO-6EO Sulfate	0.42	C20-24 IOS (A)	0.18	-	-	None	2%	9.5	7	gel
MN-569	Isocarb C-24-COOH	0.30	C20-24 IOS (A)	0.30	-	-	None	-	-	7	Cloudy 0-1.4% TDA30 at 2% Na2CO3
MN-570	Isocarb C-24-COOH	0.30	C15-18 IOS	0.30	TDA 30	0.30	0.5-3%	-	All I	7	0% Na2CO3 HAZY All type I
MN-571	Isocarb C-24-COOH	0.30	C15-18 IOS	0.30	-	-	Not measured	~3%	7-10	7	-

Table 4.6 Summary of Phase Behavior Experiments with Guerbet ether sulfate (Cont.)

	Primary surfactant	wt (%)	Co- surfactant	wt (%)	Co-solvent	wt (%)	Aqueous limit (wt% Na2CO3)	Optimum wt% Na2CO3	Solubilization ratio at optimum	Oil sample number	Comment.
MN-572	Isocarb C-24-COOH	0.30	C20-10EO Sulfate	0.30	-	-	Not measured	3%	39.7	7	-
MN-576	C32-7PO-6EO Sulfate	0.50	C20-2EO	0.5	-	-	Not measured	2.5-3%	2.4	7	No type III Gel forms
MN-577	C32-7PO-6EO Sulfate	0.50	C-20-6EO	0.50	-	-	Not measured	all II	-	7	No type III Gel forms
MN-578	C32-7PO-6EO Sulfate	0.50	C-20-6EO sulfate	0.5	-	-	Not measured	>4.5%	4.3	7	Gel
MN-579	C28-7PE-2EO Sulfate	0.50	C20-24 IOS (A)	0.50	TEGBE	0.50	Not measured	4.5-5%	15.2	7	20% Oil
MN-580	C32-7PO-6EO Sulfate	0.50	C20-24 IOS (C)	0.50	TEGBE	0.50	Not measured	All I	2	7	20% Oil
MN-581	C28-7PE-2EO Sulfate	0.50	C20-24 IOS (C)	0.50	TEGBE	0.50	Not measured	>5%	15.4	7	20% Oil
MN-582	C32-7PO-6EO Sulfate	0.30	Petrostep S-3A C20-24 IOS	0.30	-	-	Not measured	3.25%	28	7	20% Oil
MN-583	C32-7PO-6EO Sulfate	0.30	C20-24 IOS (C)	0.30	-	-	Not measured	$\geq$4%	22.7	7	20% Oil
MN-584	C32-7PO-6EO Sulfate	0.30	C20-2EO Sulfate	0.30	-	-	Not measured	All II	-	7	GEL 20% Oil
MN-585	C32-7PO-6EO Sulfate	0.30	C24-28 IOS	0.30	-	-	Not measured	All II	-	7	20% Oil
MN-586	C28-7PE-2EO Sulfate	0.67	C20-24 IOS (A)	0.33	TEGBE	0.50	Not measured	2%	-	7	Gel
MN-587	C32-7PO-6EO Sulfate	0.50	C20-24 IOS (A)	0.50	MA-80-I	0.50	Not measured	2.75%	14	7	Oil Scan 10% Oil
MN-587	C32-7PO-6EO Sulfate	0.50	C20-24 IOS (A)	0.50	MA-80-I	0.50	Not measured	3.05%	15	7	20% Oil
MN-587	C32-7PO-6EO Sulfate	0.50	C20-24 IOS (A)	0.50	MA-80-I	0.50	Not measured	3.00%	15	7	30% Oil
MN-587	C32-7PO-6EO Sulfate	0.50	C20-24 IOS (A)	0.50	MA-80-I	0.50	Not measured	3.00%	18	7	40% Oil

Table 4.6 Summary of Phase Behavior Experiments with Guerbet ether sulfate (Cont.)

	Primary surfactant	wt (%)	Co- surfactant	wt (%)	Co-solvent	wt (%)	Aqueous limit (wt% Na2CO3)	Optimum wt% Na2CO3	Solubilization ratio at optimum	Oil sample number	Comment.
MN-587	C32-7PO-6EO Sulfate	0.50	C20-24 IOS (A)	0.50	MA-80-I	0.50	Not measured	3.00%	20	7	50% Oil
MN-588	C32-7PO-6EO Sulfate (repeat)	0.50	C20-24 IOS (A)	0.50	MA-80-I	0.50	Not measured	3.50%	90	7	50% Oil
MN-589	C32-7PO-6EO Sulfate (repeat)	0.50	C20-2EO Sulfate	0.50	TEGBE	0.50	Not measured	All II	-	7	Gel
MN-590	C32-7PO-6EO Sulfate (repeat)	0.50	C20-2EO Sulfate	0.50	TDA 30	0.50	Not measured	3-3.5%	2	7	No type III
MN-591	C32-7PO-6EO Sulfate (repeat)	0.50	C20-24 IOS (A)	0.50	TEGBE	0.50	Not measured	3.25%	13	7	50% Oil
MN-592	C32-7PO-6EO Sulfate (repeat)	0.50	C20-24 IOS (A)	0.50	TEGBE	0.50	Not measured	4.25%	8	6	50% Oil
MN-593	C28-7PE-2EO Sulfate	0.50	C20-24 IOS (A)	0.50	TEGBE	0.50	Not measured	2.5%	13	7	(originally 4.6 then 3.4%) need lower tubes for type I
MN-594	C28-7PE-2EO Sulfate	0.50	C20-24 IOS (A)	0.50	TEGBE	0.50	Not measured	3.30%	17	6	Opt lower than last weekHigher than previous (3%)
MN-595	C32-7PO-6EO Sulfate	0.50	C20-24 IOS (A)	0.50	TEGBE MA-80-I	0.5 0.4	4.5%	3.60%	7	7	Oil Scan 10% Oil
MN-595	C32-7PO-6EO Sulfate	0.50	C20-24 IOS (A)	0.50	TEGBE MA-80-I	0.5 0.4	4.5%	3.25%	8	7	20% Oil
MN-595	C32-7PO-6EO Sulfate	0.50	C20-24 IOS (A)	0.50	TEGBE MA-80-I	0.5 0.4	4.5%	3.85%	9	7	30% Oil
MN-595	C32-7PO-6EO Sulfate	0.50	C20-24 IOS (A)	0.50	TEGBE MA-80-I	0.5 0.4	4.5%	4%	9.5	7	40% Oil
MN-595	C32-7PO-6EO Sulfate	0.50	C20-24 IOS (A)	0.50	TEGBE MA-80-I	0.5 0.4	4.5%	4.00%	10	7	50% Oil
MN-596	C32-7PO-6EO Sulfate	0.25	C20-24 IOS (A)	0.25	MA-80-I	0.50	Not measured	2.75%	13	7	Oil Scan 10% Oil
MN-596	C32-7PO-6EO Sulfate	0.25	C20-24 IOS (A)	0.25	MA-80-I	0.50	Not measured	3.10%	11	7	20% Oil

Table 4.6 Summary of Phase Behavior Experiments with Guerbet ether sulfate (Cont.)

	Primary surfactant	wt (%)	Co- surfactant	wt (%)	Co-solvent	wt (%)	Aqueous limit (wt% Na2CO3)	Optimum wt% Na2CO3	Solubilization ratio at optimum	Oil sample number	Comment.
MN-596	C32-7PO-6EO Sulfate	0.25	C20-24 IOS (A)	0.25	MA-80-I	0.50	Not measured	3.25%	16	7	30% Oil
MN-596	C32-7PO-6EO Sulfate	0.25	C20-24 IOS (A)	0.25	MA-80-I	0.50	Not measured	3.12%	18	7	40% Oil
MN-597	C32-7PO-6EO Sulfate	0.25	C20-24 IOS (A)	0.25	TEGBE MA-80-I	0.25 0.4	Not measured	3.00%	10	7	Oil Scan 10% Oil
MN-597	C32-7PO-6EO Sulfate	0.25	C20-24 IOS (A)	0.25	TEGBE MA-80-I	0.25 0.4	Not measured	3.50%	11	7	20% Oil
MN-597	C32-7PO-6EO Sulfate	0.25	C20-24 IOS (A)	0.25	TEGBE MA-80-I	0.25 0.4	Not measured	3.50%	11	7	30% Oil
MN-597	C32-7PO-6EO Sulfate	0.25	C20-24 IOS (A)	0.25	TEGBE MA-80-I	0.25 0.4	Not measured	2.75-3%	12.5	7	40% Oil
MN-598	C32-7PO-6EO Sulfate	0.10	C20-24 IOS (A)	0.10	MA-80-I	0.50	Not measured	0.5-1.5%	-	7	50% Oil
MN-599	C32-7PO-6EO Sulfate	0.10	C20-24 IOS (A)	0.10	TEGBE MA-80-I	0.1 0.4	Not measured	1-1.5%	-	7	50% Oil
MN-600	C32-7PO-6EO Sulfate	0.15	C20-24 IOS (A)	0.15	TEGBE MA-80-I	0.15 0.4	Not measured	-	-	7	50% Oil
MN-600	C32-7PO-6EO Sulfate	0.15	C20-24 IOS (A)	0.15	TEGBE MA-80-I	0.15 0.4	Not measured	2.20%	15	7	40% Oil
MN-600	C32-7PO-6EO Sulfate	0.15	C20-24 IOS (A)	0.15	TEGBE MA-80-I	0.15 0.4	Not measured	2.40%	13	7	30% Oil
MN-600	C32-7PO-6EO Sulfate	0.15	C20-24 IOS (A)	0.15	TEGBE MA-80-I	0.15 0.4	Not measured	2.30%	10	7	20% Oil
MN-600	C32-7PO-6EO Sulfate	0.15	C20-24 IOS (A)	0.15	TEGBE MA-80-I	0.15 0.4	Not measured	2.30%	11	7	10% Oil

Table 4.7 Berea core properties for core flood M-9

Rock Type	Berea
Mass (g)	1198
Porosity	0.201
Length (cm)	28.575
Diagonal (cm)	5.03
Area (cm^2)	19.86
Temperature (°C)	85
Pore volume (ml)	114

Table 4.8 Permeability and relative permeability values of Berea core M-9

Absolute brine permeability, k_{brine} (md)	356
Oil permeability, k_{oil} (md)	208
Water permeability, k_{water} (md)	19.94
Relative oil permeability, k_{ro}	0.58
Relative water permeability, k_{rw}	0.056

Table 4.9 Saturation data for the Berea core M-9

Initial oil saturation, S_{oi}	0.61
Rediual oil saturation, S_{orw}	0.335

Table 4.10 Viscosity of fluid measured at 85°C, and measured at values are at 10 sec^{-1}

Brine viscosity (cp)	0.37
CrudeM viscosity (cp)	6.6
ASP slug viscosity (cp)	16
Polymer drive viscosity (cp)	18

Table 4.11 Alkali surfactant polymer slug data M-9

Pore Volume Injected (PV)	0.3
C_{32}-7PO-6EO-sulfate	0.25%
C_{20-24} IOS (Petrostep S-3A)	0.25%
TEGBE	0.25%
MA-80-I	0.40%
PV*C	15
Sodium Carbonate (ppm)	35000
Total Dissolved solid (ppm)	37865
Floppam 3630S (ppm)	2000
Front Adv. Rate [ft/day]	1
Viscosity [cP @ 10s-1]	16

Table 4.12 Polymer drive data for M-9

Pore Volume Injected (PV)	1.7
Total Dissolved solid (ppm)	2865
Floppam 3630S (ppm)	1150
Front Adv. Rate [ft/day]	1
Viscosity [cP @ 10s-1]	18

Table 4.13 Core flood results for M-9

S_{orc} [%]	0.8
Oil Recovery [%]	97.6
Oil Breakthrough, [PV]	0.31
Emulsion Breakthrough, [PV]	0.84
Surf. Retention [mg/g]	0.01

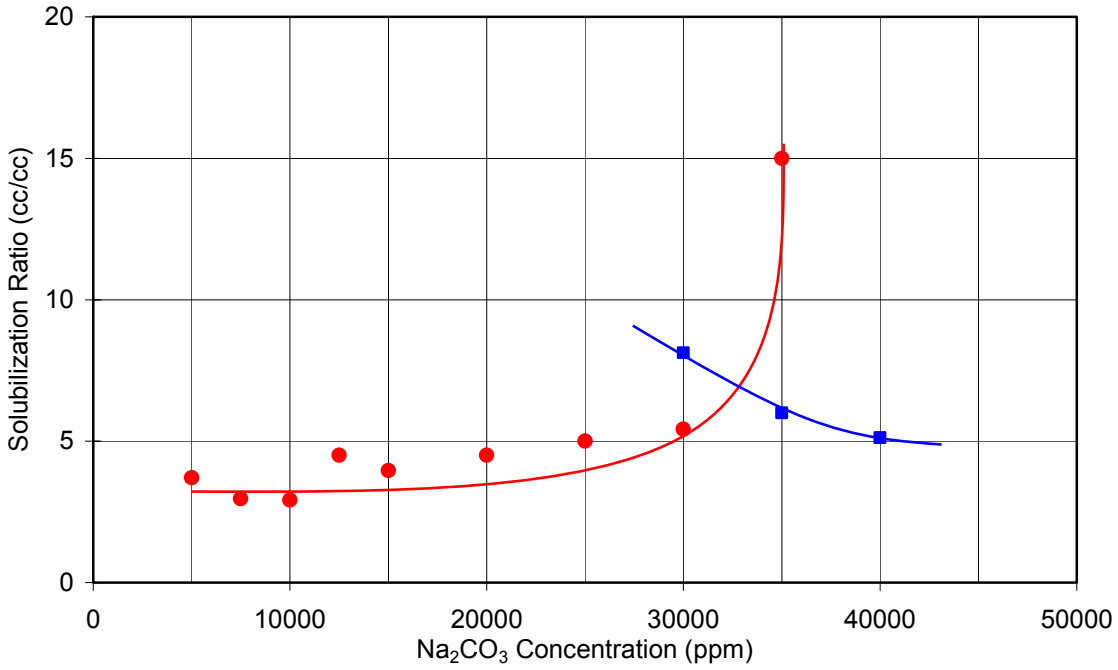

Figure 4.1 Solubilization ratio plot of phase behavior with 50% crude M #5 after 8 days. MN-367: C_{20-24} IOS (A) in SSMB

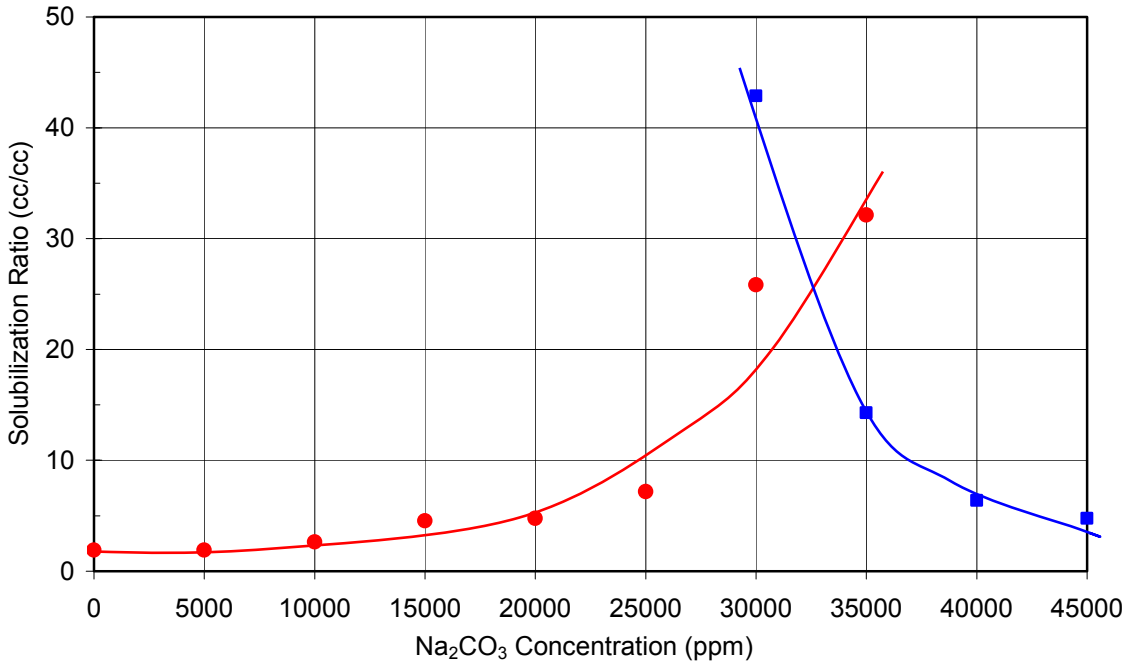

Figure 4.2 Solubilization ratio plot of phase behavior with 50% crude M #5 after 95 days. MN-411: 2.0% $C_{16\text{-}17}$-7PO-sulfate, 2.0% TEGBE in SSMB

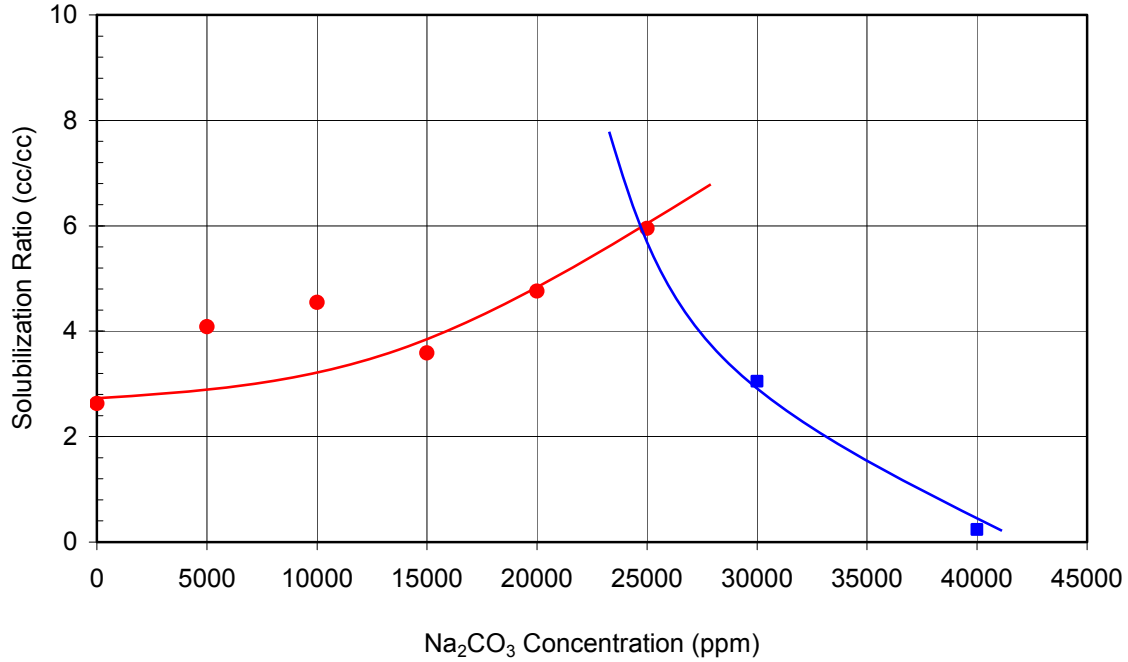

Figure 4.3 Solubilization ratio plot of phase behavior with 50% crude M #5 after 59 days. MN-439: 1.0% C_{20}-10EO-sulfate, 1% C_{20}-6EO-sulfate in SSMB

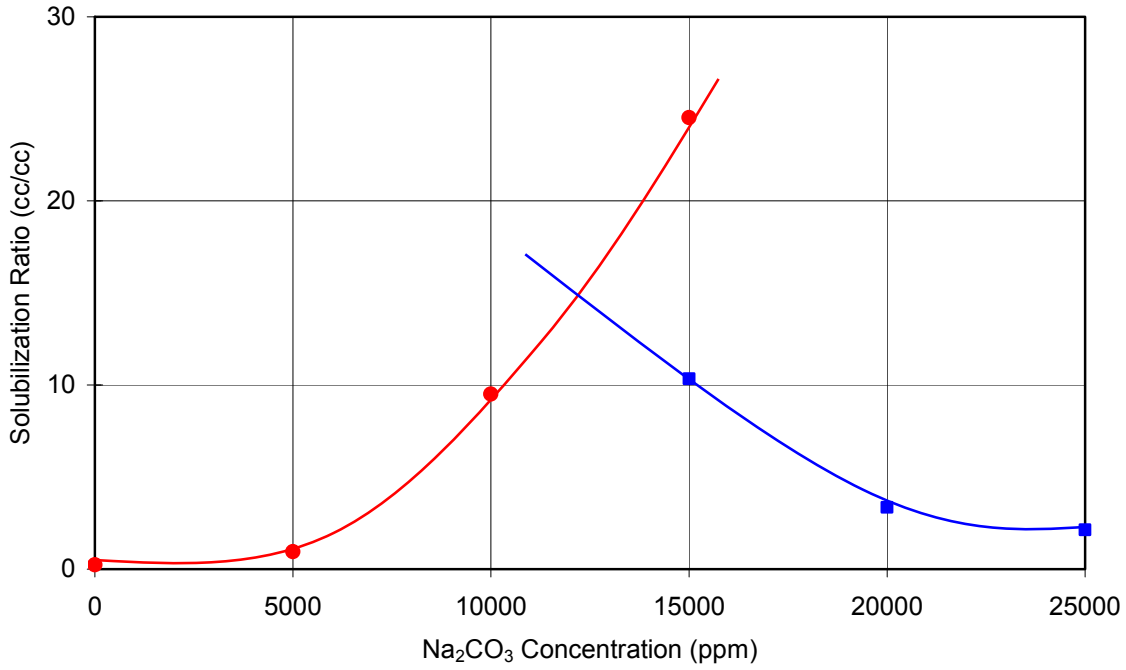

Figure 4.4 Solubilization ratio plot of phase behavior with 50% crude M #5 after 35 days. MN-467: 1.8% C_{24}-10EO-sulfate and 0.2% $C_{12\text{-}15}$-12EO-sulfate in SSMB

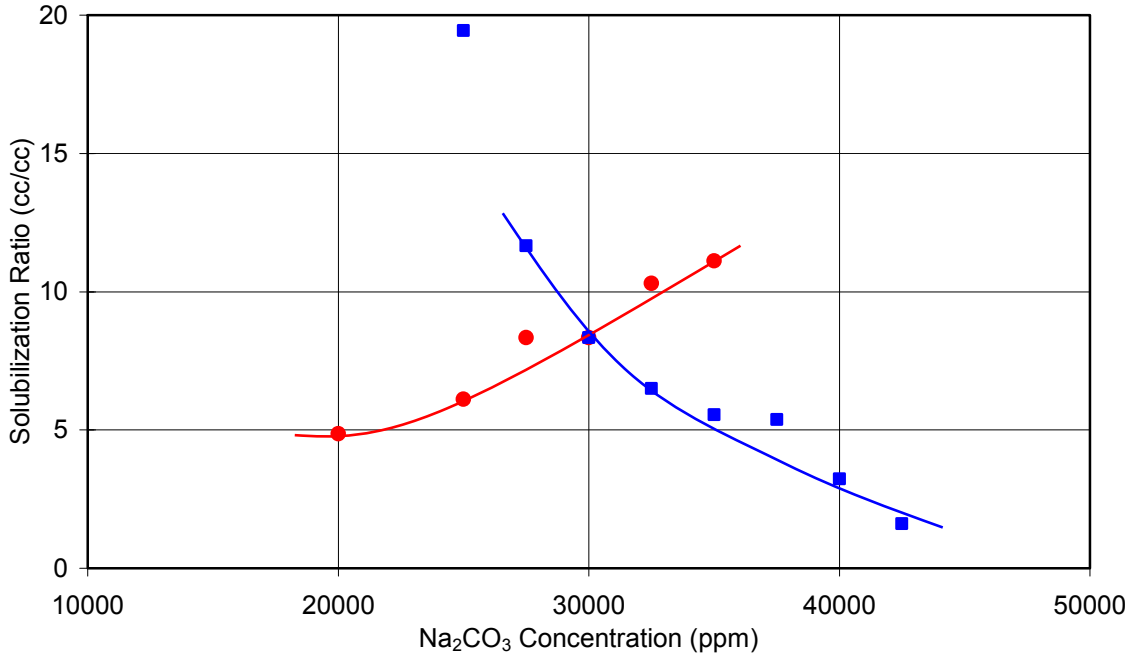

Figure 4.5 Solubilization ratio plot of phase behavior with 10% crude M #7 after 6 days. MN-597: 0.25% C_{32}-7PO-6EO Sulfate, 0.25% C_{20-24} IOS, 0.25% TEGBE, 0.4% Aerosol MA-80 in SSMB

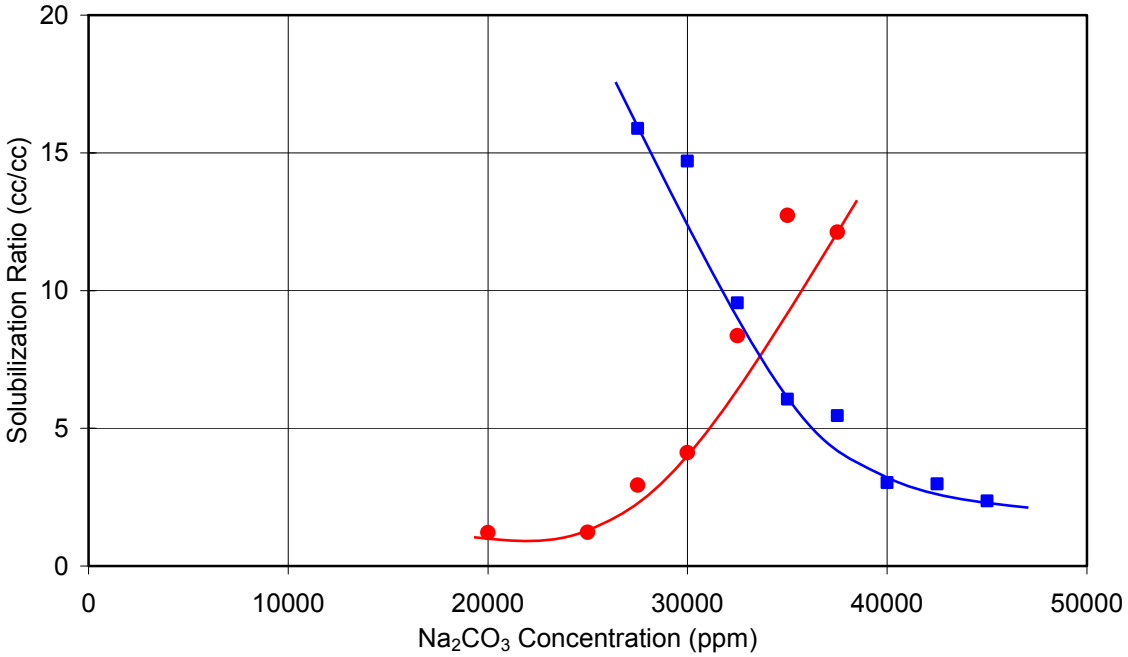

Figure 4.6 Solubilization ratio plot of phase behavior with 20% crude M #7 after 6 days. MN-597: 0.25% C_{32}-7PO-6EO Sulfate, 0.25% C_{20-24} IOS, 0.25% TEGBE, 0.4% Aerosol MA-80 in SSMB

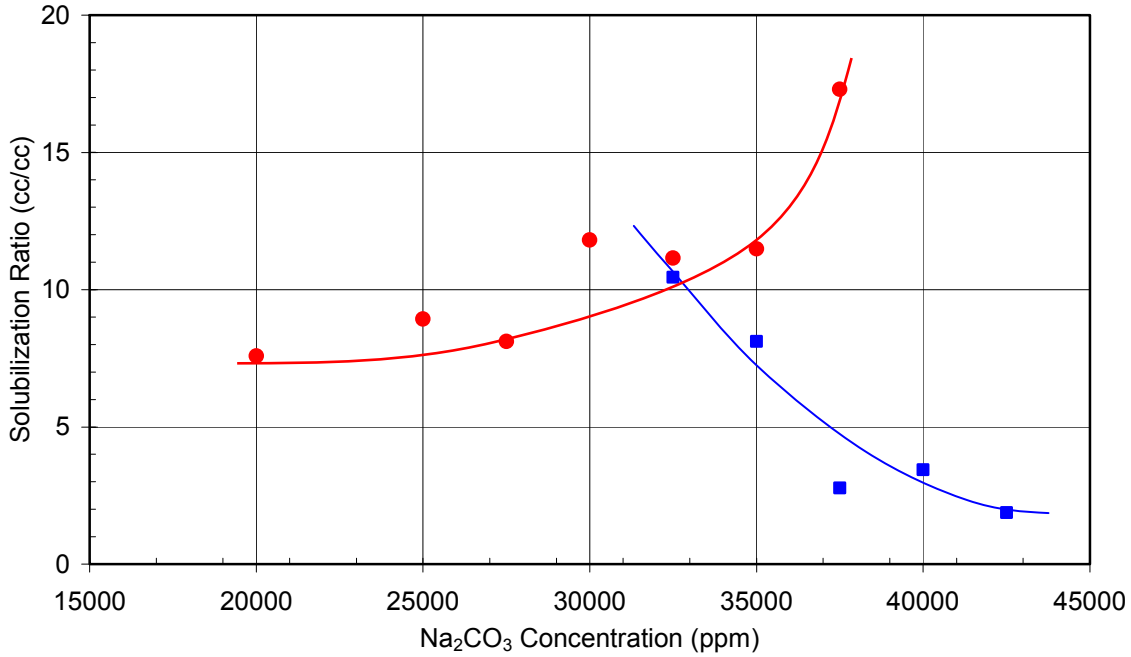

Figure 4.7 Solubilization ratio plot of phase behavior with 30% crude M #7 after 6 days. MN-597: 0.25% C_{32}-7PO-6EO Sulfate, 0.25% C_{20-24} IOS, 0.25% TEGBE, 0.4% Aerosol MA-80 in SSMB

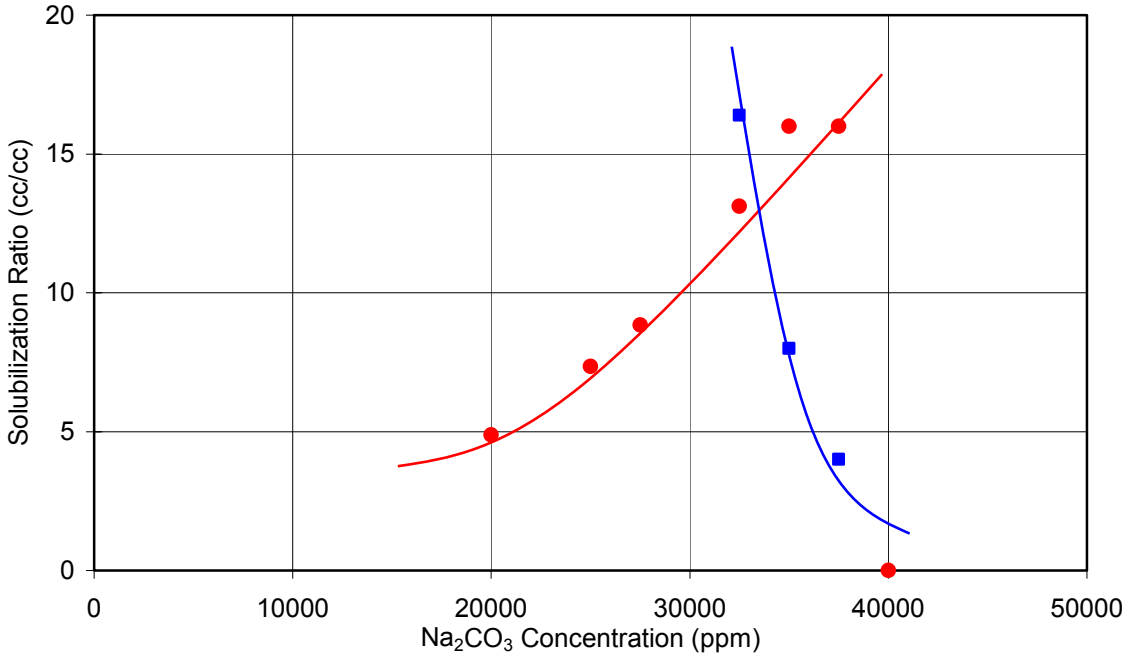

Figure 4.8 Solubilization ratio plot of phase behavior with 40% crude M #7 after 6 days. MN-597: 0.25% C_{32}-7PO-6EO Sulfate, 0.25% C_{20-24} IOS, 0.25% TEGBE, 0.4% Aerosol MA-80 in SSMB

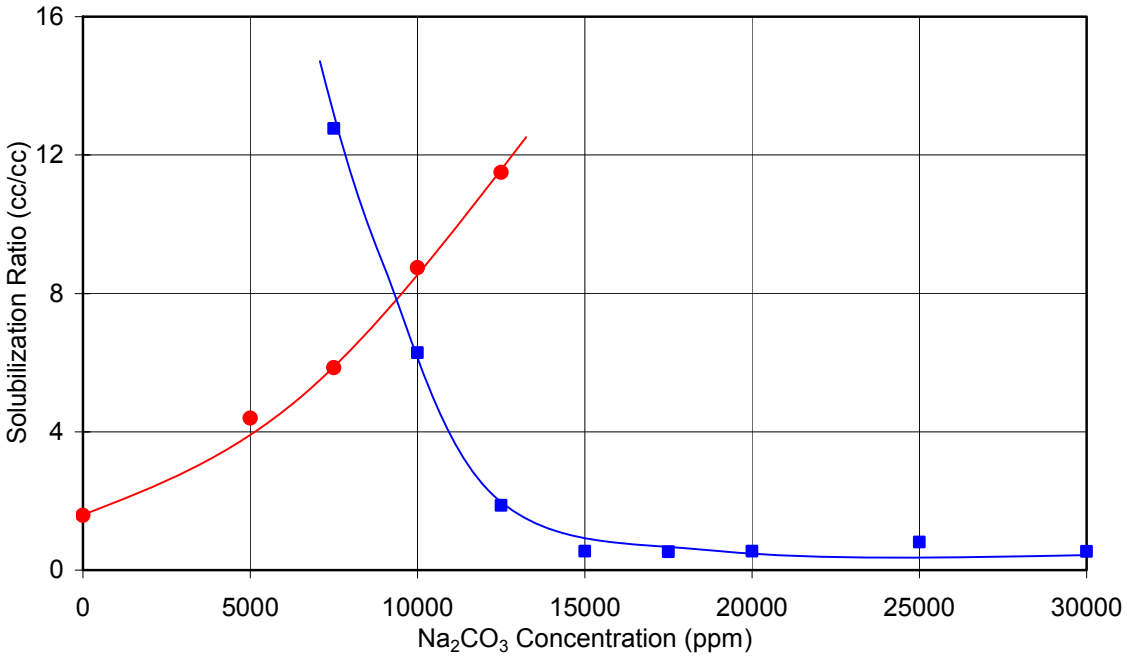

Figure 4.9 Solubilization ratio plot of phase behavior with 50% crude M #4 after 269 days. MN-210(a): 1.5% CS2000A, 0.5% IOS (6500) Blend, 2% TEGBE , in SSMB

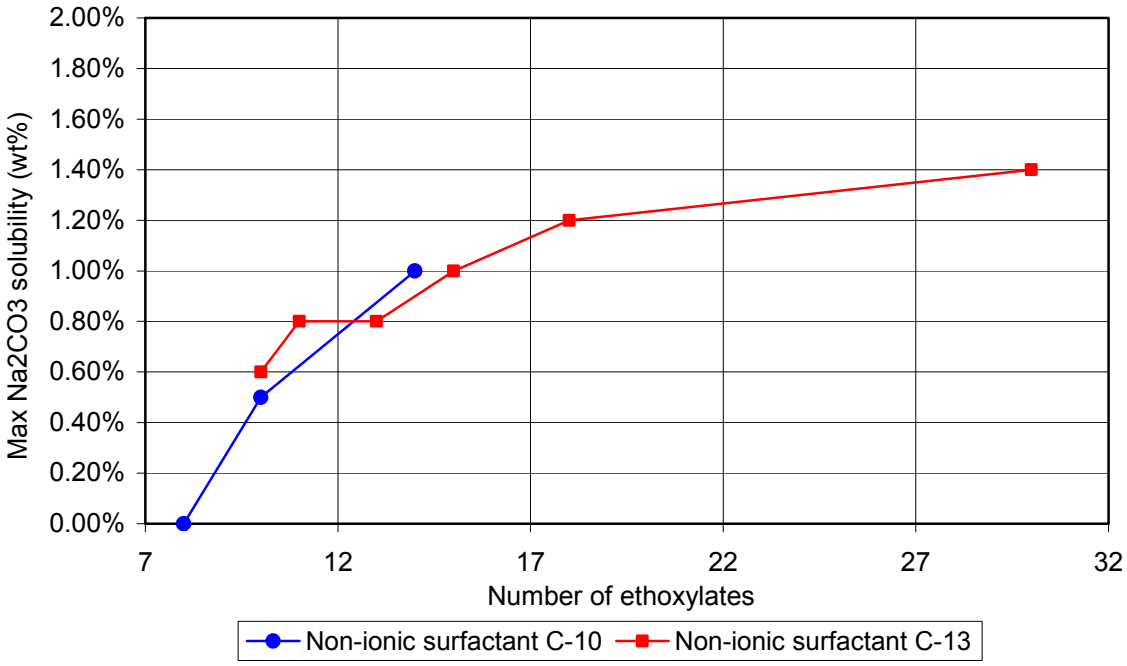

Figure 4.10 Effect of ethoxylate number on aqueous solubility: 1.0% C_{20-24} IOS with 0.5% alcohol ethoxylate in SSMB

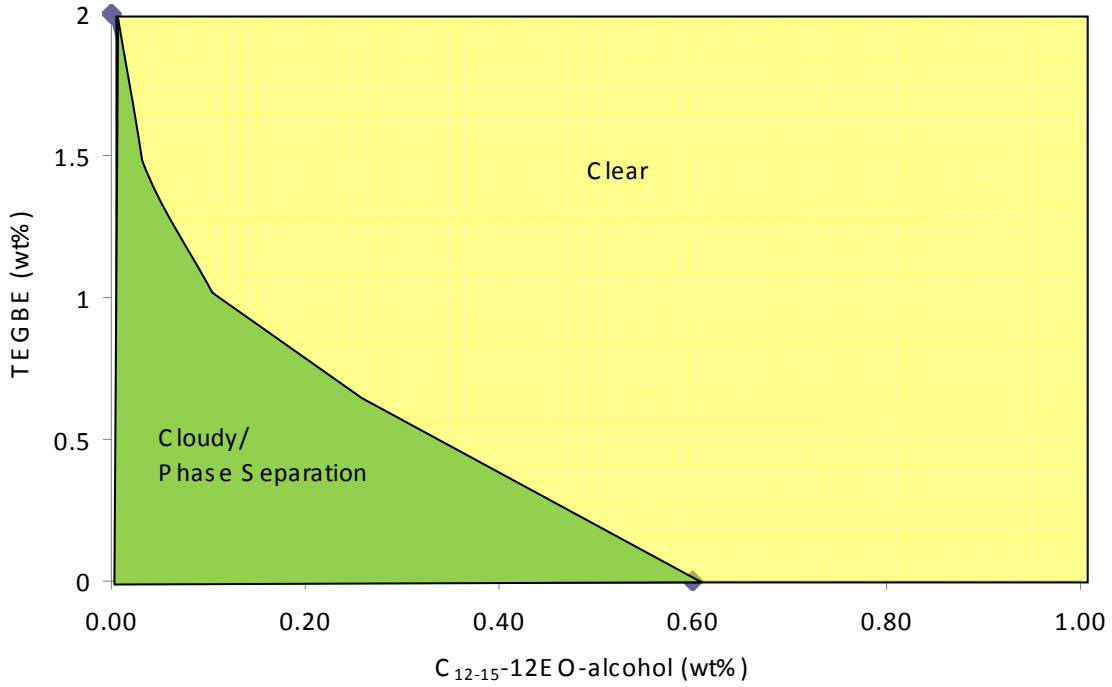

Figure 4.11 Effect of glycol ether/alcohol ethoxylate mixture on aqueous solubility: 0.5% C_{24-28}-IOS with 1.0% Na_2CO_3e in SSMB

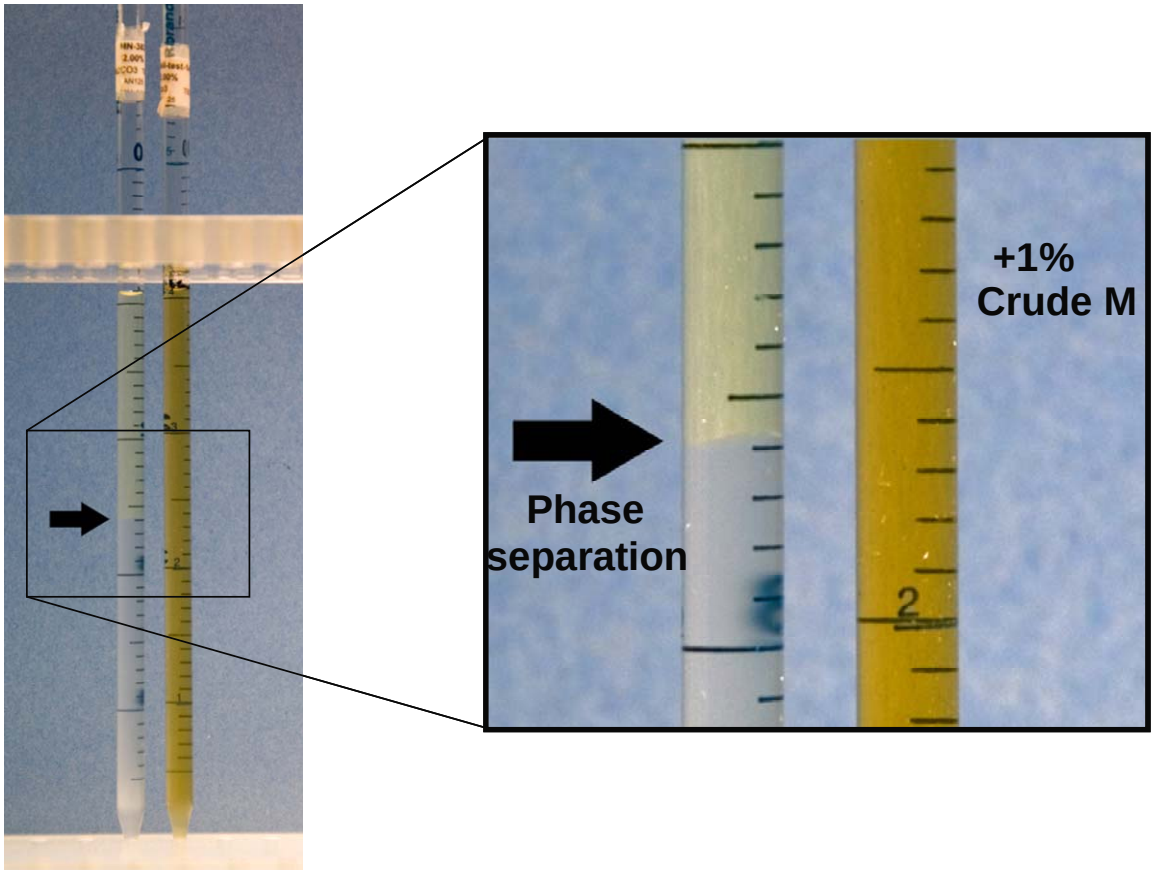

Figure 4.12 Comparison of aqueous solubility with and without adding crude M: 2.0% $C_{20\text{-}24}$ IOS, 2.0% TEGBE, and 2.0% Na_2CO_3

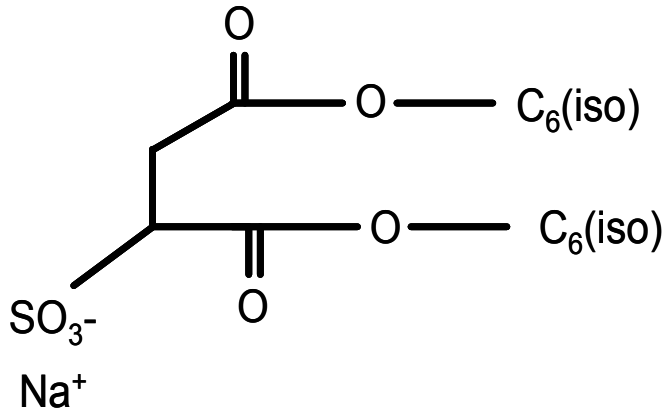

Figure 4.13 Structure of Aerosol MA-80

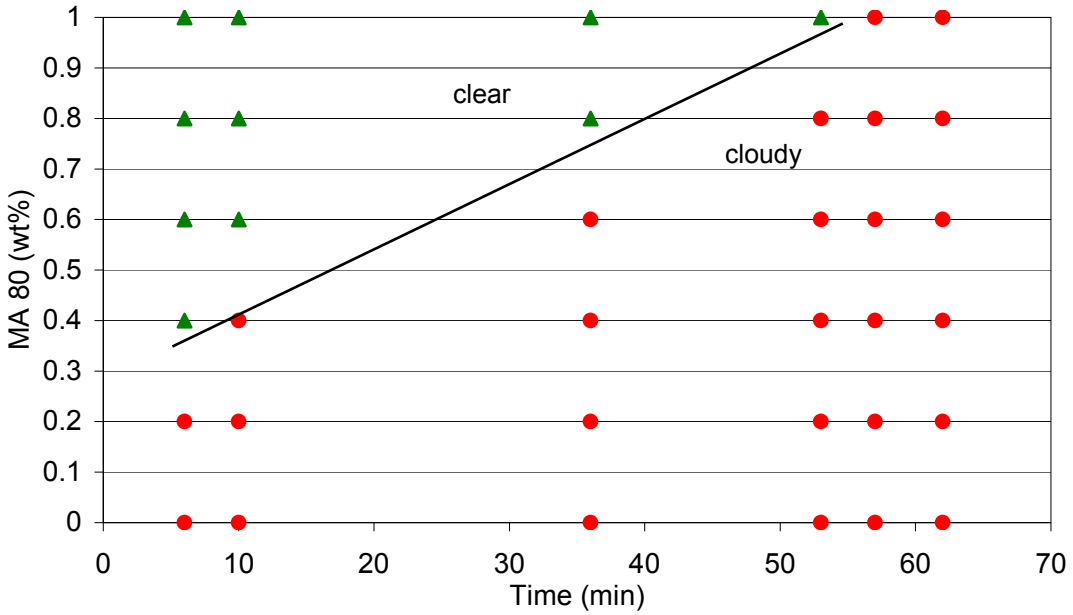

Figure 4.14 Aerosol MA-80 stability experiments at 85°C: 2% $C_{16\text{-}17}$-7PO-sulfate with 2.5% Na_2CO_3

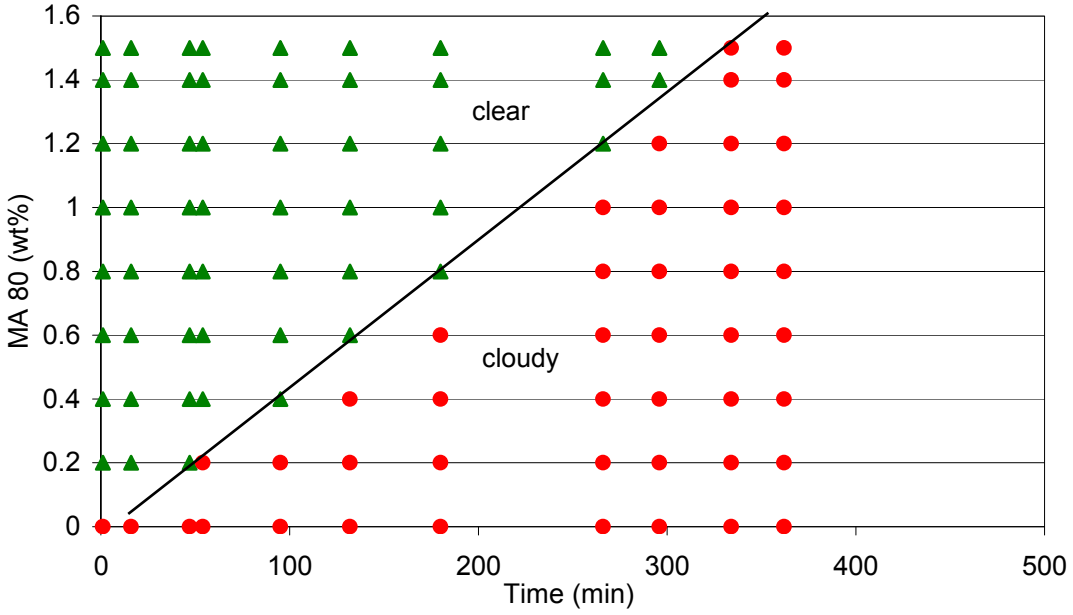

Figure 4.15 Aerosol MA-80 stability experiments at 85°C: 2% $C_{16\text{-}17}$-7PO-sulfate, 2% TEGBE with 2.5% Na_2CO_3

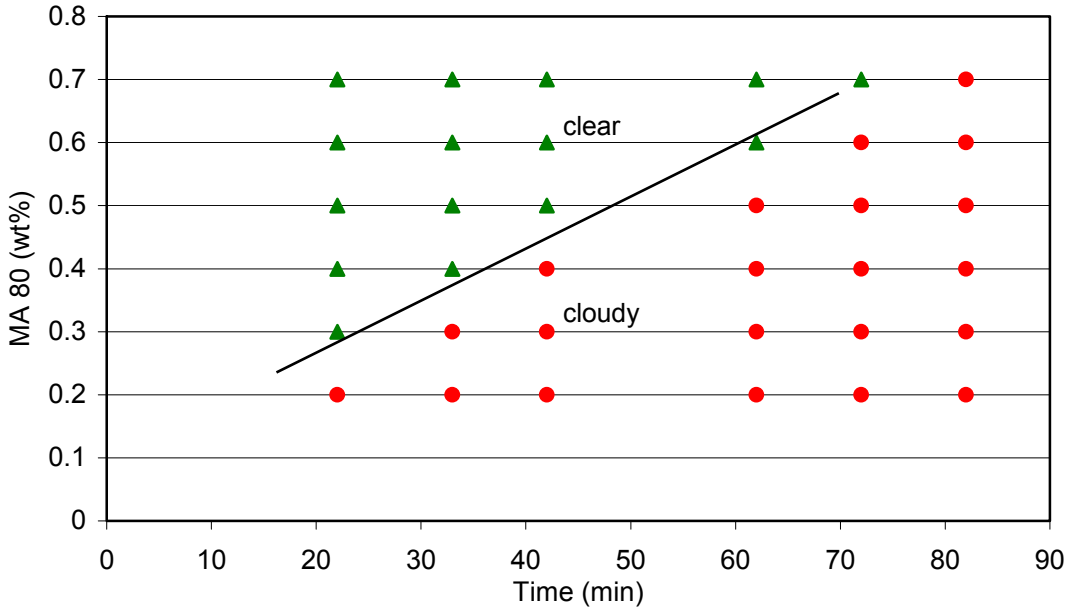

Figure 4.16 Aerosol MA-80 stability experiments at 85°C: 1% $C_{16\text{-}17}$-7PO-sulfate, 0.5% TEGBE with 3.0% Na_2CO_3

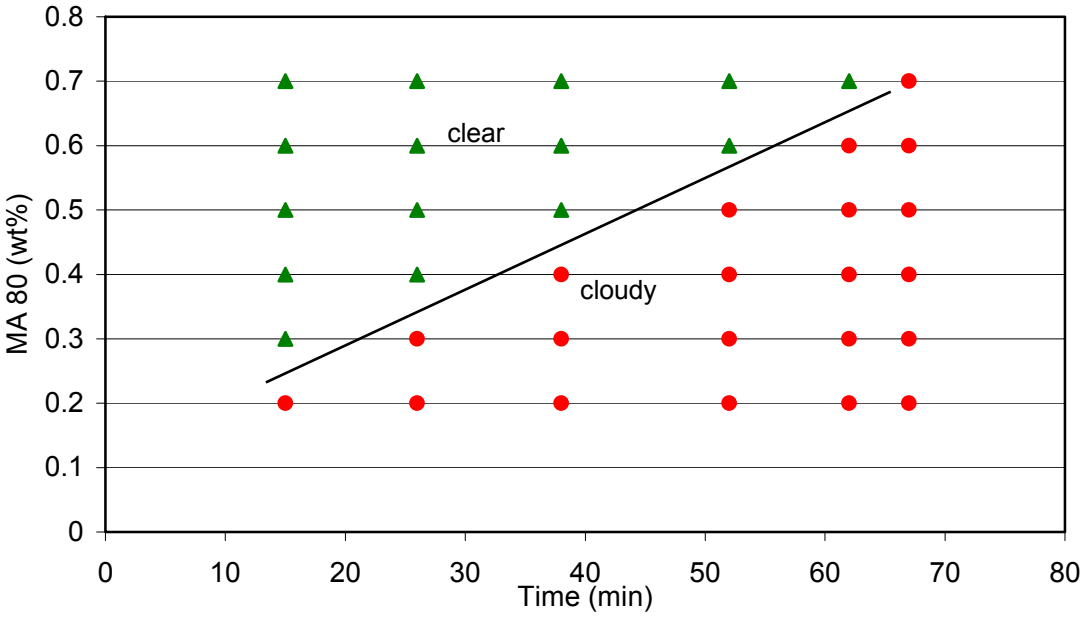

Figure 4.17 Aerosol MA-80 stability experiments at 85°C: 1% $C_{16\text{-}17}$-7PO-sulfate, 0.5% TEGBE with 3.5% Na_2CO_3

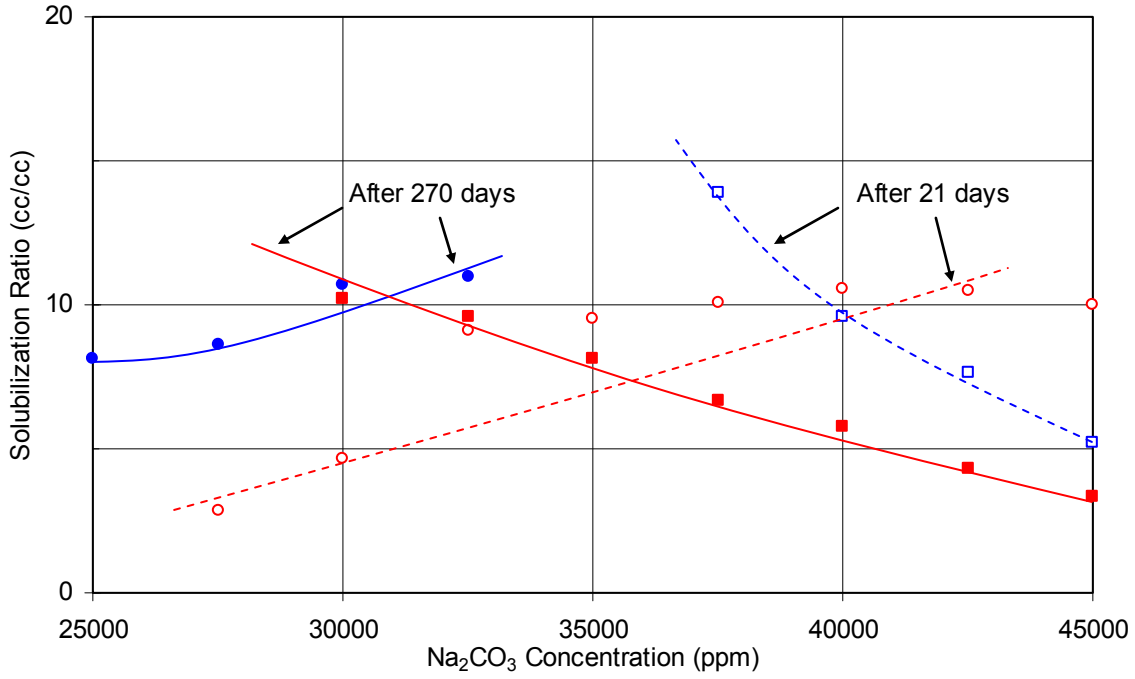

Figure 4.18 Effect of Aerosol MA-80 on microemulsion phase behavior test at 85°C: 0.5% C_{32}-7PO-6EO Sulfate, 0.5% C_{20-24} IOS with 0.5%TEGBE & 0.4% Aerosol MA-80 in SSMB with crude M #7 after 21 days and 270 days.

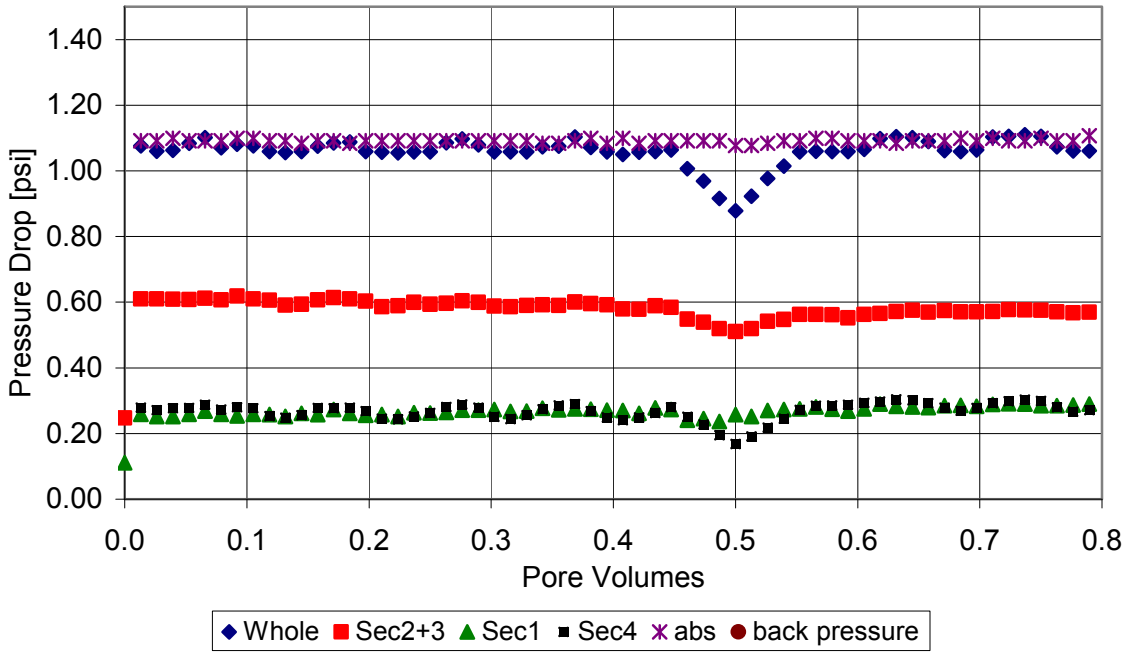

Figure 4.19 M-9 Brine Flood pressure

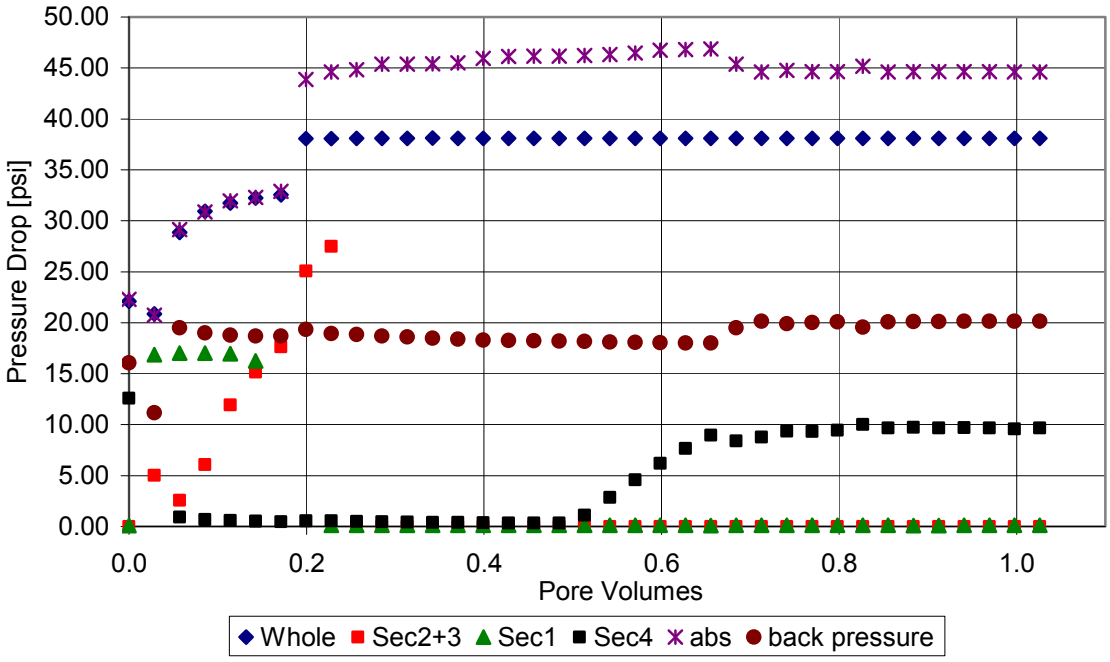

Figure 4.20 M-9 Oil Flood pressure

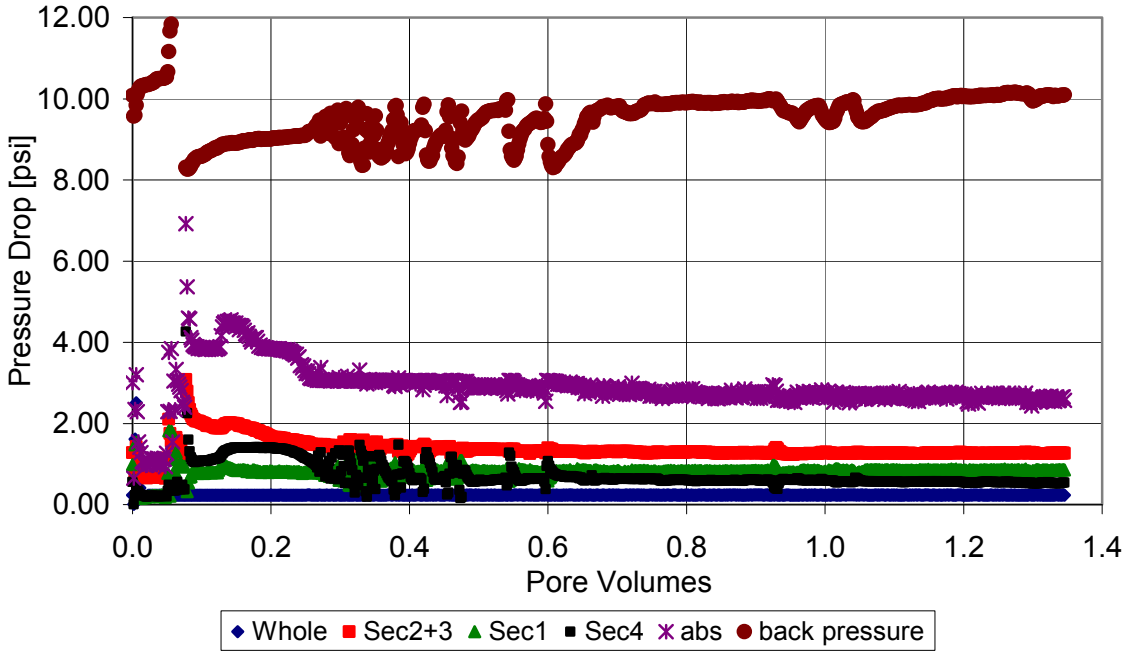

Figure 4.21 M-9 Water Flood pressure

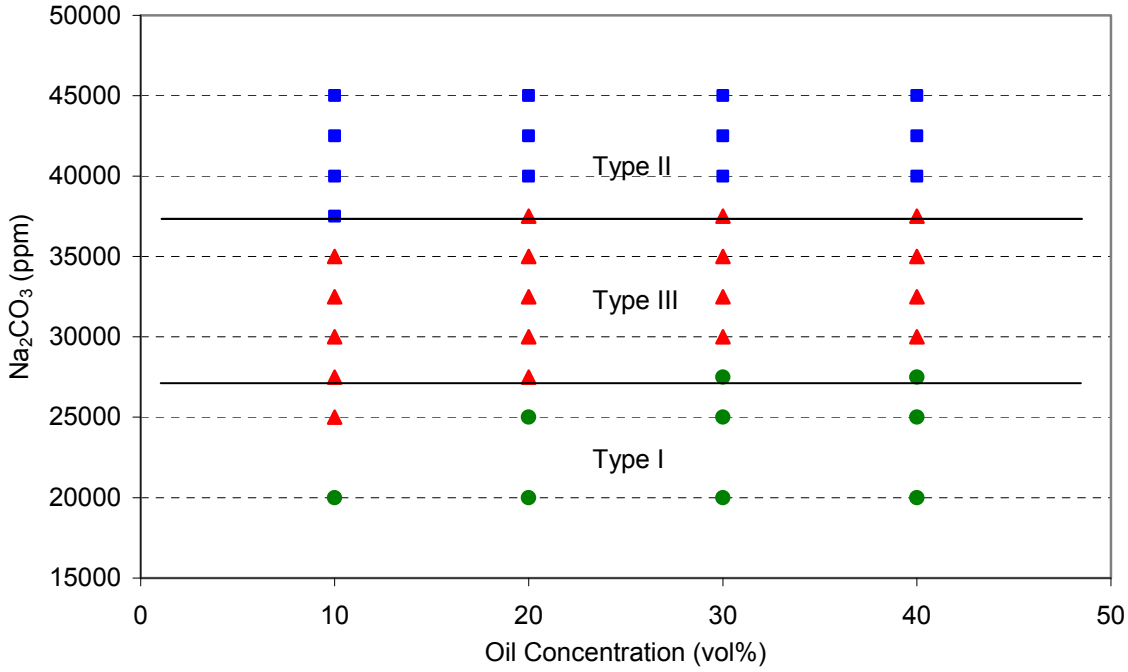

Figure 4.22 Activity diagram for 0.25% C_{32}-7PO-6EO Sulfate, 0.25% C_{20-24} IOS, 0.25% TEGBE and 0.4% MA 80I with crude M #7

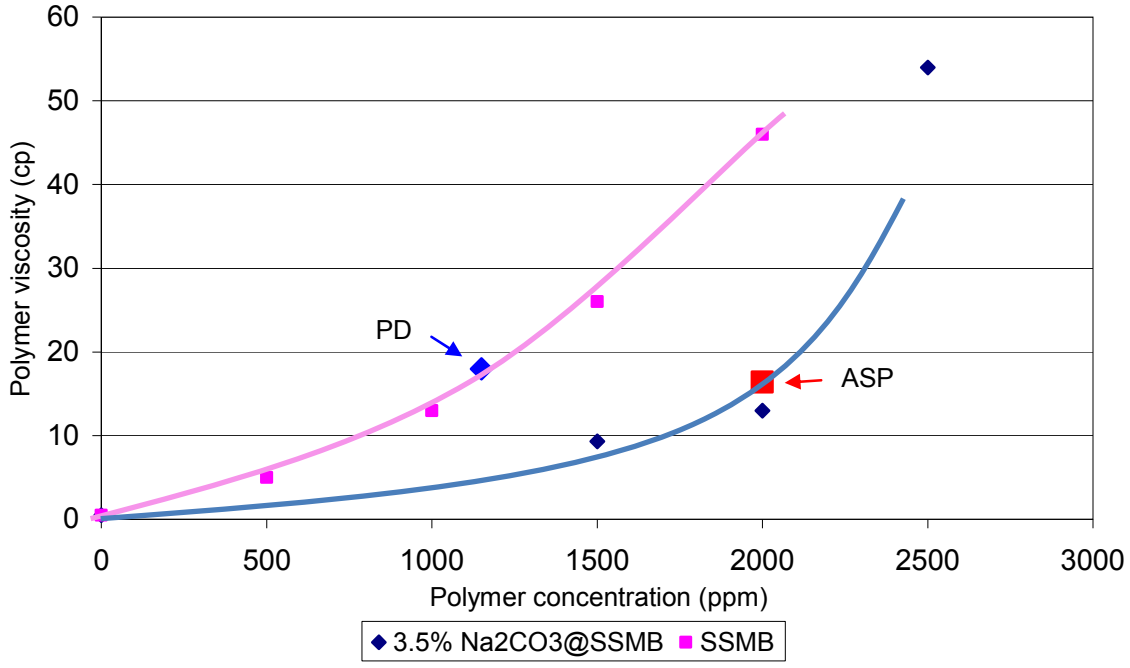

Figure 4.23 Polymer viscosities for M-9 at 85 °C and 10 s^{-1}

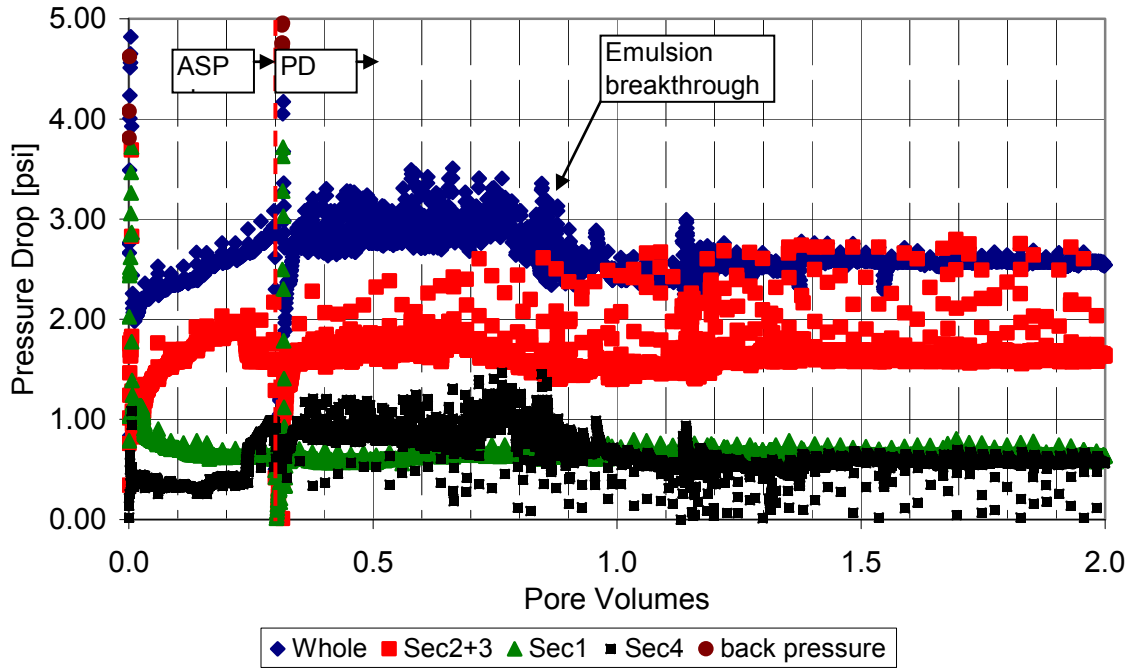

Figure 4.24 M-9 ASP Pressure

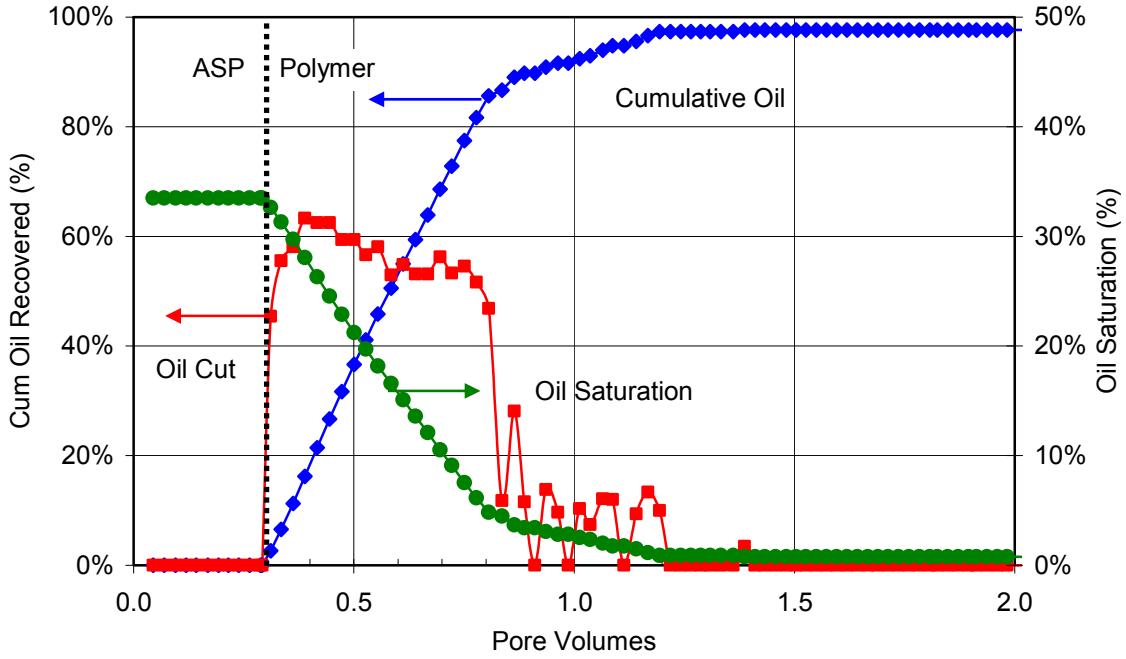

Figure 4.25 M-9 Oil Recovery

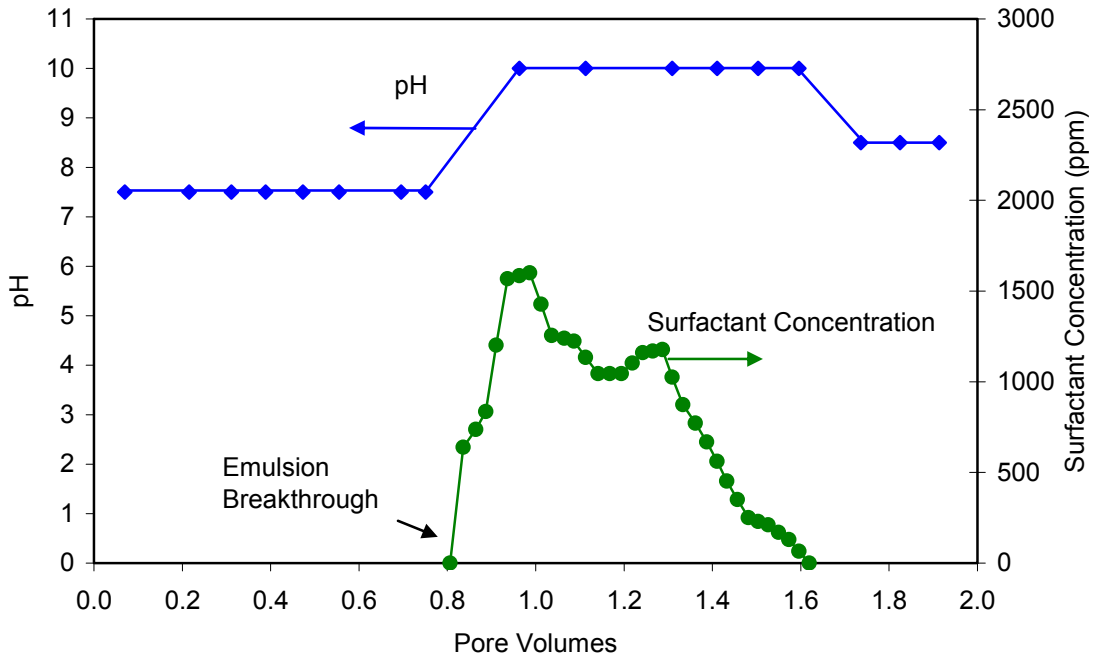

Figure 4.26 M-9 Surfactant Concentration

CHAPTER 5: DESIGN OF HIGH PERFORMANCE ASP FORMULATIONS FOR A REACTIVE CRUDE

This chapter describes the process for selection and testing of a formulation consisting of a primary surfactant, co-surfactant, co-solvent and polymer for a crude oil with a high acid number. The goal was to develop a formulation to work in conjunction with the natural soap from a reactive crude oil. Since the reactive oil contained Naphthalenic carboxylic acids that can generate soaps under basic conditions, it was beneficial to employ alkali in the formulation. Initially highly surface active formulations were faced with aqueous solubility issues that were solved by the use of high levels of co-solvents. Later on, lower cost formulations were developed that met the aqueous stability requirements with minimal or no use of co-solvents. The performance of one such formulation was tested in a core flood experiment with excellent results.

5.1 DEVELOPMENT OF ASP FORMULATION FOR REACTIVE CRUDE

5.1.1 Crude oil and brine

Crude L is a light oil (38 degrees API gravity) with a low viscosity (4.6 cP) at the reservoir temperature of 69 °C. The reservoir is a low permeability (5-10 md) limestone formation with a high-salinity formation brine. All experiments were conducted at reservoir temperature. Table 5.1 shows the composition of the formation brine, produced brine, a source or makeup brine F and the softened brine F used to develop the ASP formulation. The measured saponification number (SAPN) of the oil was 2.49 mg of KOH/g of oil. Macroemulsions formed when the oil was mixed with aqueous solutions of sodium carbonate. The slope of the activity diagram (Figure 5.1) is consistent with the formation of hydrophobic soap.

Primary surfactant selection

Initial surfactant screening was done in synthetic soft F brine (SSFB). Table 5.2 is a summary of the phase behavior experiments. Experiments L-001 to L-016 were the initial surfactant screening experiments. The phase behavior with oil was done using a range of 0.5 - 5.0 wt % Na_2CO_3. The aqueous tests had the range of 0- 7.0 wt % Na_2CO_3. The initial screening experiments were done by using 2 wt% TEGBE as the co-solvent. The purpose was to identify a primary surfactant with correct HLB. From initial screening tests, C_{15+} ABS seemed to be the most promising surfactant in terms of microemulsion phase behavior criteria. The L-001 scan containing 0.5% C_{15+} ABS and 2% TEGBE showed a high optimum solubilization ratio of 33, low optimal salinity and excellent fluidity. However, the aqueous solubility of the ABS was found to be too poor.

Co-surfactant screening

Next the C_{15+} ABS was blended with more hydrophilic surfactants for the purpose of raising its aqueous solubility to higher levels. Experiments L-027 to L-034 shown in Table 5.3 show the results of several phase behavior tests using this ABS with different co-surfactants. The mixture of C_{20-24} IOS and C_{15+} ABS showed an improvement in the aqueous solubility from the C_{15+} ABS experiment with 2% TEGBE. However, the aqueous solubility was still too low at the optimum salinity. Since the IOS series appeared to function well with C_{15+} ABS in terms of both aqueous solubility improvement and high solubilization ratio, more phase behavior and aqueous stability tests were conducted with mixtures of ABS and IOS surfactants.

Desirable phase behavior results with a single surfactant formulation are rarely found. Rather than a single component, mixtures of surfactants (co-surfactants) are preferred in order to match the crude oil properties under different conditions. The additional components enhance the phase behavior performance due to synergistic effects

among surfactants. One possible explanation could be that the varying chains of hydrophobic backbones in the blends match up well with the different components in the crude oil. As discussed in chapter 4, the specific new C_{24-28} IOS batch showed more hydrophilic behavior than C_{20-24} IOS (A) as shown in L-005, 0.5% C_{24-28} IOS and 2% TEGBE, resulted in a clear single phase up to 7 wt% Na_2CO_3 concentration in 10,693 ppm SSFB. This is presumably due to higher sulfonation level during the manufacture of the C_{24-28} IOS compared to the C_{20-24} IOS resulting in higher solubility for the heavier IOS. Based on this data, favorable result (see L-055 in Figure 5.2) was achieved by 0.5% C_{24-28} IOS, 0.25% C_{15+} ABS and 2% TEGBE in 10,693 ppm SSFB.

5.1.2 Aqueous solubility improvement

Co-solvents

To improve aqueous solubility, several alcohols and glycols were tested with the C_{15+} ABS. The alcohol evaluated included tri-ethylene glycol butyl ether (TEGBE), ethylene glycol butyl ether (EGBE), iso-butanol (IBA), t-pentanol (t-AA), sec-butanol (SBA). The results show that the TEGBE as co-solvent resulted in favorable aqueous solubility in the initial screenings, as shown in Table 5.4. A 0.5% C_{15+} ABS and 2% TEGBE aqueous solution was clear up to 1% Na_2CO_3 in 10,693 ppm SSFB. Another co-solvent, EGBE, provided the similar aqueous solubility. Additional tests indicate that as the ethylene oxide mole content of the glycol ether co-solvent increased from 1 (EGBE) to 3 (TEGBE), less co-solvent was required for a clear aqueous surfactant solution. Based on this observation, TEGBE was used extensively as a co-solvent in subsequent experiments.

Alcohol ethoxylates

The characterization of alcohol ethoxylates classified as non-ionic surfactants was described by Sahni (2009). Based on his findings, alcohol ethoxylates C_{12-15}-12EO, TDA-18EO, TDA-6EO, TDA-12EO, and TDA-30EO were evaluated for experiments L-046 through L-051 at low concentrations as shown in Table 5.5. A 0.5% C_{15+} ABS and 0.2% TDA-30EO provided a clear solution with 0% Na_2CO_3 in 10,693 ppm SSFB. From the explanation given for the structure of alcohol ethoxylate surfactants in chapter 2, the aqueous solubility increase is minimal beyond 18 EOs as shown in Figure 4.10. However, TDA-30EO shows a slightly better aqueous solubility with the C_{15+} ABS surfactant. This demonstrates that TDA-30EO is a promising non-ionic surfactant for improving aqueous solubility of anionic surfactants in this formulation.

5.1.3 Phase behavior optimization

The goal of further optimization was to reduce the cost of the ASP formulation by lowering the concentration of co-solvent or using a less expensive co-solvent. Experiments L-055 to L-069 were conducted to satisfy these objectives as shown in Table 5.6. Since the mixture of C_{20-24} IOS and C_{15+} ABS gave the most favorable results from the surfactant and co-surfactant screening tests, additional experiments were carried out with this formulation by changing the ratio of surfactant/co-surfactant and co-solvent concentrations. The first approach was to reduce the concentration of TEGBE to just above the aqueous limitation. Thus, L-068 containing 0.5% C_{24-28} IOS, 0.25% C_{15+} ABS and 1.4% TEGBE resulted in a solubilization ratio of 15 at 1.5% Na_2CO_3 optimal salinity with 3.5% Na_2CO_3 aqueous solubility as shown in Figure 5.3. Another approach was to test non-ionic surfactants as co-solvents. Compared to glycol ethers and alcohols, the requirement of concentrations needed to achieve similar or better aqueous limitation was very low. However, it drastically increased the optimal salinity. Several alcohol

ethoxylates were scanned with the formulation and TDA-30EO resulted in a high oil solubilization ratio, low IFT and good fluidity. L-069 containing 0.5% C_{24-28} IOS, 0.25% C_{15+} ABS and 0.3% TDA-30EO resulted in a solubilization ratio of 23 at 3.5% Na_2CO_3 optimal salinity with 3.5% Na_2CO_3 aqueous solubility (Figure 5.4).

Additional experiments with Guerbet alkoxy surfactants and sacrificial surfactants were conducted with the goal of lowering the surfactant concentration and cost. The phase behavior experiment results with Guerbet alkoxy sulfates are listed in Table 5.7. Initially, C_{28}-7PO-2EO-sulfate was tested. A viscous emulsion formed. Several experiments were performed in attempt to prevent this from happening, such as mixing different Guerbet alkoxy sulfates and PO sulfates. The best formulations were mixtures of Guerbet alkoxy sulfate and IOS. Sacrificial surfactants were used to solubilize the mixture in the aqueous phase by improving aqueous solubility.

A mixture of Guerbet alkoxy sulfate (C_{32}-7PO-6EO sulfate) and IOS (C_{20-24} IOS) was used to achieve high oil solubilization and microemulsion formation. Small amounts of alcohol ethoxylates were added for improving the compatibility between surfactant/polymer and also for lowering the microemulsion viscosity. Aerosol MA-80 was used to provide a temporary, clear solution for the formulation. The solubilization ratio was 30 for 20% oil concentration at optimum salinity (2.5% Na_2CO_3, and 1% NaCl). A solution containing surfactant and polymer was clear up to optimum salinity (3.5% TDS) for 30 minutes at the reservoir temperature (69 °C). Figures 5.5 to 5.9 show the phase behavior plots for the formulation with Crude L. The activity diagram illustrated in Figure 5.10 showed a negative and relatively flat slope which is desirable to give a salinity gradient during ASP flooding.

5.1.4 L-7 Core Flood Experiment

The ASP formulation 0.3% C_{32}-7PO-6EO sulfate, 0.3% C_{20-24} IOS (A), 0.1% TDA-30EO, 0.4% Aerosol MA-80 showed the best behavior so its performance was tested in a Berea core flood. The core flood was run in a convection oven that was set at the reservoir temperature of 69 ºC. The goal of this experiment was to demonstrate the efficacy of the formulation (L-018 (G)) that generated excellent microemulsions in the phase behavior experiments. Final oil recovery for the L-7 core flood experiment was 97.1% of the water flood residual oil saturation with a final oil saturation of 1.1%.

L-7 Core Data

The L-7 core flood was set up using Berea sandstone (length 11.44" and diameter 1.99") instead of the reservoir rock to prove the performance of the formulation with Crude L as well as minimize any errors from the reservoir rock. The Berea sandstone was placed inside a 7.5 cm diameter Lexan™ tube and cast in slow-setting epoxy with a hardener to epoxy ratio of 1:2. The core properties are given in Table 5.8. Other properties including permeability and saturation values are summarized in Table 5.9 and 5.10.

L-7 Brine flood

Initially the core was saturated with 1% NaCl which is similar to SSFB. Then 1% NaCl (0.48 cp) brine was injected at a flow rate of 5.0 ml/min until the equilibrium state was reached. The brine flood was conducted for 2.4 pore volumes through the core and the pressure data were recorded for each section as shown in Figure 5.11. The brine permeability was measured to be 587md.

L-7 Oil flood

The L-7 oil flood was done with filtered Crude L. The filtration process was conducted in 0.45 micron cellulose filter paper under a pressure of 40 psi at the reservoir temperature (69 ^{o}C). The oil flood was conducted at a constant pressure of about 60 psi and the measured viscosity of Crude L was 3 cp at 69 ^{o}C. The oil permeability to residual water was calculated to be 506 md and the relative permeability was 0.862. The initial oil saturation after the oil flood was 0.65 and residual water saturation was 0.35. The pressure data along with the L-7 oil flood are shown for the L-7 oil flood in Figure 5.12.

L-7 Water Flood

The core was water flooded with 1% NaCl at a flow rate of 0.5 ml/min (6 ft/day) at 69°C until the oil cut of the effluent was less than 1% with stabilized pressure drops. The pressure data for the L-7 water flood are illustrated in Figure 5.13. After the water flood, the residual oil saturation (S_{or}) was 0.366. The water permeability was 20 md and the end-point relative permeability was 0.035.

L-7 Chemical flood design

Chemical flood was designed based on the phase behavior, aqueous solubility, activity diagram, and polymer viscosity experiment. The formulation of 0.3% C_{32}-7PO-6EO sulfate, 0.3% C_{20-24} IOS (A), 0.1% TDA-30EO, 0.4% Aerosol MA-80 exhibited excellent phase behavior (Figure 5.5 to Figure 5.9) and activity diagram (Figure 5.10). The solubilization ratios at optimal salinity are above 17 even at 10% oil concentration. The ASP slug containing Aerosol MA-80 was tested at the reservoir temperature (69 °C) for 30 minutes to confirm the stability of the formulation at the optimum salinity (2.5% Na_2CO_3 and 1% NaCl). The ASP slug was clear and a single phase during the test. The aqueous experiment was conducted with Floppam^{TM} 3330S polymer. Another key factor

in designing the chemical flood was polymer viscosity. Desirable viscosities were calculated using the equations explained in chapter 3. The viscosities of the ASP slug and polymer drive were measured at 69 °C with varying shear rates. The ASP slug viscosity was measured to be 13.6 cp and the polymer drive was 14.9 cp at 10 s^{-1}. Viscosity data of fluids utilized for the L-9 core flood are listed in Table 5.11.

A 0.3 PV ASP slug was injected at a rate of 2 ft/D (= 0.167 ml/min) followed by a polymer drive at the same velocity until less than 1% of oil was produced in the effluent samples. The characterization and quantitative values for the ASP slug and polymer drive are tabulated in Table 5.12 and 5.13 respectively. The final oil recovery, residual oil, oil breakthrough, and emulsion breakthrough after chemical flood are tabulated in Table 5.14. The pressure drop for the chemical flood is illustrated in Figure 5.14 and the oil recovery for L-7 is shown in Figure 5.15 Final oil recovery for the L-7 core flood experiment was 97.1% of the water flood residual oil saturation with a final oil saturation of 1.1%.

5.2 OPTIMIZATION OF ASP FORMULATION FOR REACTIVE CRUDE WITH HIGH SALINITY

5.2.1 Brines

Two formulations have been developed for Crude L, one in the low salinity injection water (F brine) and the other in the high salinity produced brine. The procedure for developing the best formulation in high salinity brine (197,000 ppm TDS) and the results are discussed in this section. The reservoir was considered one of the most challenging targets for chemical flooding since permeability is low and the formation brine salinity is extremely high.

5.2.2 Phase behavior experiments

Primary surfactant/Co-surfactant selection

High salinity brines require extremely hydrophilic surfactants. Most surfactants with long carbon chains cause phase separation in high salinity brine, which makes them unsuitable for injection. Shorter carbon chain surfactants on the other hand have more salt tolerance, but they often give very poor oil solubilization, which makes them inadequate for EOR applications. The hydrophilic surfactants alkyldiphenyloxide disulfonate, C_{12-15}-15EO-sulfonate, C_{12} AOS, and Stepantan AS1246, were used for the initial screening as shown in Table 5.15. The initial aqueous solubility for surfactants was examined with a sodium chloride scan. However, these surfactants were too hydrophilic to solubilize Crude L. Consequently, they resulted in poor microemulsion phase behavior results, showing Type l.

Another approach for achieving the high salt tolerance and oil solubility for the formulation was to utilize ether sulfates. As a result of the advances made on the stability of ether sulfates, an alcohol ether sulfate was used as a component of the surfactant formulation in the phase behavior studies at 69 ºC with high salinities. Because of the high salinity requirement, the anionic surfactants needed to contain high EO levels. The background experiment, L-111, was performed using C_{12-15}-12EO-sulfate. Although the aqueous stability was good (around 19% TDS), this surfactant did not solubilize oil since the hydrophobe was too short. Previous phase behavior experiments suggested utilizing C_{12-15}-15EO-sulfonate as a co-surfactant in the formulation. The surfactant, C_{12-15}-15EO-sulfonate helped solubilize Crude L, but resulted in a viscous macroemulsions rather than the desired microemulsions (L-105 to L-108). The blend of 0.3% C_{12-15}-12EO-sulfate and 0.3% C_{12-15}-15EO-sulfonate in a 1:1 ratio was tested with 50% of Crude L (L-126) and it

exhibited excellent phase behavior results (solubilization ratio of 20 at optimum salinity) as shown in Figure 5.16 with high aqueous solubility (clear up to 19.75% TDS).

5.2.3 Aqueous solubility improvement

Co-solvents

Glycol ethers were identified as promising co-solvents by Jackson (2006). Sahni (2009) showed that TEGBE was the best co-solvent that gave the highest salt tolerance compared to the other glycol ethers. To handle very high salinity reservoir conditions, several hydrophilic surfactants were tested with TEGBE. Aqueous solubility experiments were performed with Alkyldiphenyloxide disulfonate, C_{12-15}-15EO-sulfonate, and C_{12-15}-9EO-sulfonate. It was observed that increasing the TEGBE concentration did not improve the aqueous stability at the extremely high salinity conditions shown in Figure 5.17.

Alcohol ethoxylate surfactant

Additional experiments were conducted to observe the effect of alcohol ethoxylates on aqueous solubility. Aqueous solubility tests were done in DI water with 0.5% surfactant and 1% alcohol ethoxylate at 69 ºC. The results are tabulated in Table 5.16. C_{12} AOS without any alcohol ethoxylate was cloudy at 18% NaCl, but the same surfactant with C_{13}-30EO and C_{12-15}-12EO showed improved aqueous solubility (clear up to 20%). Furthermore, the same alcohol ethoxylates when tested with Stepantan AS1246, which is a slightly heterogeneous C_{12} AOS, resulted in a similar observation. These results showed that the alcohol ethoxylate was more effective than the glycol ether as a solubilizer in conditions of extremely high salinity.

5.2.4 Phase behavior optimization

The results from phase behavior and aqueous solubility tests indicated that very hydrophilic surfactants including C_{12-15}-12EO-sulfate, C_{12-15}-15EO-sulfonate and C_{17}-

12EO-sulfate provided high salt tolerance. Also, the sodium carbonate without any surfactant was tested in L-109 to identify the effect of sodium carbonate with Crude L and viscous macroemulsions were observed. The experiment L-126 which included 0.3% C_{12-15}-15EO-sulfonate and 0.3% C_{12-15}-12EO-sulfate with 50% Crude L provided encouraging results. The formulation showed good phase behavior and aqueous solubility. However, the slope on the activity diagram shown in Figure 5.18 with different oil concentrations was too steep. Two approaches were taken in order to achieve a flat slope in the activity diagram. First, higher surfactant concentrations were tried in order to decrease the impact of the hydrophobic soap and different hydrophobe sulfates were investigated in order to provide added hydrophobicity to the ASP formulation and also to minimize chemical cost by replacing the sulfonate surfactant with a sulfate surfactant.

The L-130 experiment with 0.5% C_{17}-12EO-sulfate and 0.5% C_{12-15}-12EO-sulfate was conducted to fine-tune the L-126 formulation. A mixture of 0.5% C_{17}-12EO-sulfate and 0.5% C_{12-15}-12EO-sulfate without any co-solvent exhibited a high oil solubilization ratio and ultra low IFT even at low oil concentrations. Figures 5.19 to 5.23 show the phase behavior data for the best surfactant formulation at high salinity. The activity diagram shows a relatively flat slope as shown in Figure 5.24. The solubilization ratio and optimum salinity for the formulation are tabulated in Table 5.17. The formulation of C_{17}-12EO sulfate with C_{17}-12EO-sulfate resulted in better aqueous stability (21.0% TDS consisting of 1% Na_2CO_3 and 20.0% NaCl) than that with C_{12-15}-15EO-sulfonate (19.75% TDS consisting of 1% Na_2CO_3 and 18.75% NaCl).

The aqueous stability tests were done with SNF's Flopaam^{TM} 3230S polymer based on tests in reservoir cores (Slaughter, 2010). Table 5.18 is a summary of the phase behavior and aqueous solubility results with high salinity brine.

Table 5.1 Composition of Synthetic Brines

	F brine (ppm)	Synthetic Softened F brine (ppm)	Produced brine (ppm)	Softened produced water (ppm)	Reservoir brine (ppm)
Na^+	2719	3898	59970	77385	64893
K^+	64	64	Not determined	Not determined	500
Mg^{2+}	220	0	2153	0	2227
Ca^{2+}	665	0	11618	0	16578
Sr^{2+}	7	0	Not determined	Not determined	1300
Cl^-	4731	4731	118791	118791	136408
SO_4^{2-}	1830	1830	689	689	201
HCO_3^-	170	170	9	9	84
TDS	10406	10693	193230	196874	222191

*SSFB: Synthetic Softened F Brine
*SSPB: Synthetic Softened Produced Brine

Table 5.2 Summary of 0.5% surfactant screening data for 50% crude L with 2% TEGBE in SSFB

Exp. #	Primary surfactant structure	Solubilization ratio (cc/cc)	Optimum salinity Na_2CO_3 (wt%)	Aqueous stability limit (wt%)
L 001	C_{15+} bABS	33	2.75	1
L 002	C_{20-24} IOS	10	1.5	2
L 003	C_{16} bABS	19	0.5	0
L 005	C_{24-28} IOS	7	4.25	7
L 010	C_{16} Alkylaryl sulfonate	10	1.5	0
L 011	C_{15} Alkylaryl sulfonate	11	2.4	1
L 013	C_{19} Amphoteric	7	2.25	7
L 015	C_{16-17}-7PO 2EO Carboxylate	17	2.25	0
L 016	C_{16-17}-7PO 4EO Carboxylate	22	3.9	2

Table 5.3 Summary of co-surfactant screening data with C_{15+} ABS for 50% crude L with 2% TEGBE in SSFB

	Surfactant		Co-surfactant		Sol. Ratio	Opt. Sal.	Max Sol. Na_2CO_3 wt%
Exp. #	Structure	wt%	Structure	wt%	(cc/cc)	Na_2CO_3 wt%	Clear
L 027	C_{15+} bABS	0.50	C_{12-16} AOS	0.50	-	>7	7
L 028	C_{15+} bABS	0.50	C_{16-18} AOS	0.50	-	>7	7
L 029	C_{15+} bABS	0.50	C_{20-24} IOS	0.50	8	3.2	1
L 030	C_{15+} bABS	0.50	C_{15-18} IOS	0.50	5.7	6	6
L 031	C_{16-18} ABS	0.50	C_{20-24} IOS	0.50	~12	2.5-3	0
L 033	C_{15+} bABS	0.50	C_{16-17}-3PO-4EO Carboxylate	0.50	10	4.2	3
L 034	C_{15+} bABS	0.67	C_{20-24} IOS	0.33	10.5	2.7	1

Table 5.4 Summary of co-solvent screening data for 50% crude L

	Surfactant		Co Surfactant		Sol. Ratio	Opt. Sal.	Max Sol. Na_2CO_3 wt%	Brine
Exp. #	Structure	wt%	Structure	Wt %	(cc/cc)	Na_2CO_3 wt%		
L 001	C15+ bABS	0.50	TEGBE	2.00	19	3.75	1	SSFB
L 023	C15+ bABS	0.50	DGBE	2.00	-	-	1	SSFB
L 024	C15+ bABS	0.50	IBA	2.00	-	-	0	SSFB
L 025	C15+ bABS	0.50	t-pentanol	2.00	-	-	0	SSFB
L 026	C15+ bABS	0.50	SBA	2.00	-	-	0	SSFB

Table 5.5 Summary of alcohol ethoxylates screening data for crude L

	Surfactant		Solvent		Max Sol. Na_2CO_3 wt%	Brine
Exp. #	Name (structure)	wt%	Name (structure)	Wt %		
L 046	C15+ bABS	0.50	C_{12-15}-12EO	0.20	All cloudy	SSFB
L 047	C15+ bABS	0.50	TDA-18EO	0.20	All cloudy	SSFB
L 048	C15+ bABS	0.50	TDA-12EO	0.20	All cloudy	SSFB
L 049	C15+ bABS	0.50	TDA-6EO	0.20	All cloudy	SSFB
L 051	C15+ bABS	0.50	TDA-30EO	0.20	0	SSFB

Table 5.6 Summary of phase behavior data for 50% crude L in SSFB

	Surfactant		Co-surfactant		Solvent/Co Surfactant		Sol. Ratio	Opt. Sal.	Max Sol. Na_2CO_3 wt%
Exp. #	Structure	wt%	Structure	wt%	Co-solvent	Wt %	(cc/cc)	Na_2CO_3 wt%	Clear
L 055	C_{24-28} IOS	0.50	C_{15+} bABS	0.25	TEGBE	2.00	13	1.75	5
L 056	C_{24-28} IOS	0.85	C_{15+} bABS	0.40	TEGBE	2.00	-	3.5	4
L 060	C_{24-28} IOS	0.50	C_{15+} bABS	0.25	TDA 30EO	0.20	19	2.5	3
L 061	C_{24-28} IOS	0.50	C_{15+} bABS	0.25	C_{16-18} 28EO	0.2	-	3.75	2.5
L 062	C_{24-28} IOS	0.25	C_{15+} bABS	0.125	TDA 30EO	0.10	-	2	4
L 063	C_{24-28} IOS	0.375	C_{15+} bABS	0.125	TDA 30EO	0.15	-	2.9	-
L 068	C_{24-28} IOS	0.50	C_{15+} bABS	0.25	TEGBE	1.40	15	1.55	3.5
L 069	C_{24-28} IOS	0.50	C_{15+} bABS	0.25	TDA 30EO	0.30	23	3.45	3.5

Table 5.7 Summary of phase behavior data with Guerbet alkoxy sulfate for 50% crude L in SSFB

	Surfactant		Co-surfactant			wt%	Solubilizer	wt %	Sol. Ratio	Opt. Sal.	Max Sol.	Oil %	Comments
Exp #	Structure	Wt%	Structure	Wt%	Co-Solvent				(cc/cc)	wt%	%		
L-001 (G)	C-28-7PO-2EO Sulfate	0.30	C_{20-24} IOS (A)	0.30	TDA-30EO	0.30	Aerosol MA-80-I	0.30	35	2.75	3.50	50	Gel forms
L-002 (G)	C-28-7PO-2EO Sulfate	0.30	C_{20-24} IOS (A)	0.30	TDA-30EO	0.30	Aerosol MA-80-I	0.30	11	2.80	3.50	40	Gel forms
L-003 (G)	C-28-7PO-2EO Sulfate	0.30	C_{20-24} IOS (A)	0.30	TDA-30EO	0.30	Aerosol MA-80-I	0.30	6	2.85	3.50	30	Gel forms
L-004 (G)	C-28-7PO-2EO Sulfate	0.30	C_{20-24} IOS (A)	0.30	TDA-30EO	0.30	Aerosol MA-80-I	0.30	17	3.00	3.50	20	Gel forms
L-005 (G)	C-28-7PO-2EO Sulfate	0.30	C_{20-24} IOS (A)	0.30	TDA-30EO	0.30	Aerosol MA-80-I	0.30	4	3.10	3.50	10	Gel forms
L-006 (G)	C-32-7PO-6EO Sulfate	0.30	C_{20-24} IOS (A)	0.30	TDA-30EO	0.30	-	-	127	2.00	>3.5	50	Gel forms
L-007 (G)	C-32-7PO-6EO Sulfate	0.30	C_{20-24} IOS (A)	0.30	TDA-30EO	0.30	-	-	8	3.00	>3.5	20	Low IFT type 1 gel formed at high oil %
L-008 (G)	C-28-7PO-2EO Sulfate	0.30	C_{20-24} IOS (A)	0.30	-	-	Aerosol MA-80-I	0.60	-	-	-	20,50	Forming Gel
L-009 (G)	C-28-7PO-2EO Sulfate	0.30	C_{24-28} IOS (B)	0.30	TDA-30EO	0.80	-	-	12	-	-	20	Gel forms
L-010 (G)	C-32-7PO-6EO Sulfate	0.30	C_{20-24} IOS (A)	0.30	TDA-30EO	0.275	-	-	16.1	2-3	3.0	50	High oil solubilization ratio at high oil concentration
L-011 (G)	C-32-7PO-6EO Sulfate	0.30	C_{20-24} IOS (A)	0.30	TDA-30EO	0.275	-	-	4	3	3.0	20	Poor oil solubilization ratio at high oil concentration
L-012 (G)	C-28-7PO-2EO Sulfate	0.30	C_{24-28} IOS (B)	0.30	TDA-30EO Sulfate	0.30	-	-	10.2	3.25-4	0.00	20	Poor aqueous stability
L-013 (G)	C-28-7PO-2EO Sulfate	0.30	C_{24-28} IOS (B)	0.30	TDA-30EO Sulfate	0.30	-	-	15-20	1.5-2.5	0.00	50	Poor aqueous stability
L-014 (G)	C-32-7PO-6EO Sulfate	0.30	C-28-7PO-6EO Sulfate	0.30	TDA-30EO	0.60	-	-	-	-	-	20	All Formed Gel
L-015 (G)	C-32-7PO-6EO Sulfate	0.30	C-28-7PO-6EO Sulfate	0.30	TDA-30EO	1.00	-	-	-	-	-	20	Gel forms

Table 5.7 Summary of phase behavior data with Guerbet alkoxy sulfate for 50% crude L in SSFB (Cont.)

	Surfactant		Co-surfactant			wt%	Solubilizer	wt%	Sol. Ratio	Opt. Sal.	Max Sol.	Oil %	Comments
Exp #	Structure	Wt%	Structure	Wt%	Co-Solvent				(cc/cc)	wt%	%		
L-016 (G)	C-32-7PO-6EO Sulfate	0.30	C-28-7PO-6EO Sulfate	0.30	TDA-30 Sulfate	0.50	-	-	0.5	-	-	20	Gel forms Type I
L-017 (G)	C-28-7PO-2EO Sulfate	0.30	C_{24-28} IOS (B)	0.30	TDA-30 Sulfate	0.80	-	-	4	3-3.5	>4.00	20,50	Gel formed
L-018 (G)	C-32-7PO-6EO Sulfate	0.30	C_{20-24} IOS (C)	0.30	TDA-30EO	0.30	Aerosol MA-80-I	0.40	66	1.1	-	50	Solubilizer
L-018 (G)	C-32-7PO-6EO Sulfate	0.30	C_{20-24} IOS (C)	0.30	TDA-30EO	0.30	Aerosol MA-80-I	0.40	37	1.4	-	40	Solubilizer
L-018 (G)	C-32-7PO-6EO Sulfate	0.30	C_{20-24} IOS (C)	0.30	TDA-30EO	0.30	Aerosol MA-80-I	0.40	40	1.48	-	30	Solubilizer
L-018 (G)	C-32-7PO-6EO Sulfate	0.30	C_{20-24} IOS (C)	0.30	TDA-30EO	0.30	Aerosol MA-80-I	0.40	30	2.25	-	20	Solubilizer
L-018 (G)	C-32-7PO-6EO Sulfate	0.30	C_{20-24} IOS (C)	0.30	TDA-30EO	0.30	Aerosol MA-80-I	0.40	17	2.3	-	10	Solubilizer

Table 5.8 Berea core properties for core flood L-7

Rock Type	Berea
Mass (g)	1200.04
Porosity	0.199
Length (cm)	29.06
Diameter (cm)	5.05
Area (cm^2)	20.07
Temperature (°C)	69
Pore volume (ml)	116.2

Table 5.9 Permeability and relative permeability values of Berea core L-7

Absolute brine permeability, k_{brine} (md)	587
Oil permeability, k_{oil} (md)	506
Water permeability, k_{water} (md)	20
Relative oil permeability, k_{ro}	0.862
Relative water permeability, k_{rw}	0.04

Table 5.10 Saturation data for the Berea core L-7

Initial oil saturation, S_{oi}	0.65
Residual oil saturation, S_{orw}	0.37

Table 5.11 Viscosity data at 69°C and 10 sec^{-1}

Brine viscosity (cp)	0.48
Crude L viscosity (cp)	3
ASP slug viscosity (cp)	13.6
Polymer drive viscosity (cp)	14.9

Table 5.12 Alkali surfactant polymer slug data L-7

Pore Volume Injected (PV)	0.3
C_{32}-7PO-6EO-sulfate	0.30%
C_{20-24} IOS (A)	0.30%
TDA 30EO	0.10%
MA-80-I	0.40%
PV*C	18
Sodium Carbonate (ppm)	25000
Total Dissolved solid (ppm)	35000
Floppam 3330S (ppm)	3000
Front Adv. Rate [ft/day]	2
Viscosity [cP @ 10s-1]	13.6

Table 5.13 Polymer drive data for L-7

Pore Volume Injected (PV)	2.5
Total Dissolved solid (ppm)	12500
Floppam 3330S (ppm)	2500
Front Adv. Rate [ft/day]	2
Viscosity [cP @ 10s-1]	14.9

Table 5.14 Core flood results for L-7

S_{orc} [%]	1.1
Oil Recovery [%]	97.1
Oil Breakthrough, [PV]	0.2
Emulsion Breakthrough, [PV]	0.78
Surf. Retention [mg/g]	Not measured

Table 5.15 Initial aqueous solubility tests with DI water, 0.5% surfactant, NaCl scan

Order	Chemical description	Aqueous limitation
AQ 14	Alkyldiphenyloxide disulfonate (C_{16})	over 20% clear
AQ 15	C_{12-15} 15EO Sulfate	over 20% clear
AQ 16	C_{12} AOS	up to 16% clear
AQ 17	C_{12} AOS(C9-CH(OH)-CH2-CH2-SO3- (~75%) & C9-CH=CH-CH2-SO3- (~25%)	up to 16% clear

Table 5.16 Aqueous solubility test in DI water, 0.5% surfactant with 1% alcohol ethoxylate

Order	Chemical description	Alcohol ethoxylate	16% NaCl	18% NaCl	20% NaCl
AQ 16-1	C_{12} AOS	None	clear	cloudy	cloudy
		C_{13}- 30EO	clear	clear	clear
		C_{12-15}-12EO	clear	clear	clear
		iC_{10}-14EO	clear	cloudy	cloudy
AQ 17-1	(Stepantan AS1246) C_{12} AOS (C_9-CH(OH)-CH2-CH2-SO3- (~75%) & C_9-CH=CH-CH2-SO3- (~25%)	None	clear	cloudy	cloudy
		C_{13}- 30EO	clear	clear	clear
		C_{12-15}-12EO	clear	clear	clear
		iC_{10}-14EO	clear	cloudy	cloudy

Table 5.17 Solubilization ratio and optimum salinity for L-130 oil scan with sodium chloride scan

Exp. #	Formulation	Oil %	Sol.Ratio (cc/cc)	Optimum Salinity (% Total TDS)
L-130	0.5% BASF RD 4032(C17-12EO sulfate 0.5% Neodol 25-12EO sulfate 1.0% Na_2CO_3	50	16	17.50%
		40	17	19.10%
		30	11	20.40%
		20	9	21.00%
		10	5	22.60%

Table 5.18 Summary of surfactant screening results at high salinity

	Surfactant		Co-surfactant		Solvent Co Surfactant		Oil %	Sol. Ratio	Opt. Sal.	Max Sol. NaCl wt%	Brine	Comments
Exp. #	Name (structure)	wt%	Name (structure)	wt%	Cosolvent	Wt %		(cc/cc)	NaCl wt%	Clear		
L-AQ-1	C24-28 IOS (A)	0.5	TDA-30 EO	.5-5%	TEGBE	2.00	50	-	-	Phase separation	SSPB	Only AQ test
L-AQ-2	C24-28 IOS (A)	0.5	C16-17 0PO 7EO Carboxylate	.5-5%	TEGBE	2.00	50	-	-	Phase separation	SSPB	Only AQ test
L-AQ-3	C24-28 IOS (A)	0.5	-		TEGBE	2.00	50	-	-	Phase separation	SSPB	TDA-30 scan (.5-5%), only AQ test
L-AQ-4	C24-28 IOS (A)	0.5	TDA-30	0.50	TEGBE	2-7%	50	-	-	Phase separation	SSPB	TEGBE scan (2-7%), only AQ test
L-AQ-5	-	-	-	-	-	-	50	-	-	Phase separation	SSPB	Salt Precipitation test, only AQ test
L-AQ-6	C24-28 IOS (A)	0.5	C10 14EO	1-3%	-	-	50	-	-	Phase separation	SSPB	non-ionic scan (1-3%), only AQ test
L-AQ-7	C24-28 IOS (A)	0.5	TDA-30EO	1-3%	-	-	50	-	-	Phase separation	SSPB	non-ionic scan (1-3%), only AQ test
L-AQ-8	C24-28 IOS (A)	0.5	TDA-18EO	1-3%	-	-	50	-	-	Phase separation	SSPB	non-ionic scan (1-3%), only AQ test
L-AQ-9	C24-28 IOS (A)	0.5	Cetyl Betaine	1-3%	-	-	50	-	-	Phase separation	SSPB	non-ionic scan (1-3%), only AQ test
L-AQ-10	C24-28 IOS (A)	0.5	Dowfax 8390	1-3%	-	-	50	-	-	Phase separation	SSPB	non-ionic scan (1-3%), only AQ test
L-AQ-11	C24-28 IOS (A)	0.5	C16-17 9PO sulfonate	0.5	TEGBE/TDA-30EO	1.5/.5	50	-	-	Phase separation	SSPB	Only AQ test
L-AQ-12	C16-17 9PO Sulfonate	0.5	C10 14EO	2	Dowfax 8390	1.5	50	-	-	Phase separation	SSPB	Only AQ test
L-AQ-13	C16-17-9EO glyceryl Sulfonate	0.5	-	-	-	-	50	-	-	Phase separation	SSPB	Only AQ test
L-AQ-14	Dowfax 8390	0.5	-	-	-	-	50	-	-	Over 20%	DI	TDS tolerance scan (2-20% NaCl)
L-AQ-15	C12-15 15EO sulfonate	0.5	-	-	-	-	50	-	-	Over 20%	DI	TDS tolerance scan (2-20% NaCl)
L-AQ-16	Petrostep C5	0.5	-	-	-	-	50	-	-	16-18%	DI	TDS tolerance scan (2-20% NaCl)

Table 5.18 Summary of surfactant screening results at high salinity (Cont.)

	Surfactant		Co-surfactant		Solvent Co Surfactant		Oil %	Sol. Ratio	Opt. Sal.	Max Sol. NaCl wt%	Brine	Comments
Exp. #	Name (structure)	wt%	Name (structure)	wt%	Cosolvent	Wt %		(cc/cc)	NaCl wt%	Clear		
L-AQ-17	Stepantan AS1246	0.5	-	-	-	-	50	-	-	16-18%	DI	TDS tolerance scan (2-20% NaCl)
L 074	C12-15 15EO sulfonate	0.30	-	-	TEGBE	0.60	50	-	-	19%	DI	@ 1% Na2CO3, at 18% type3,
L 075	Dowfax 8390	0.30	-	-	-	-	50	-	-	21%	DI	@ 1% Na2CO3, all type 1
L 076	Cetyl Betaine	0.30	-	-	-	-	50	-	-	21%	DI	@ 1% Na2CO3, All type 1
L 071	Dowfax 8390	0.30	-	-	-	-	50	-	-	Cloudy @ 19.7%	SSPB	@ 1% Na2CO3, All type 1
L 072	Cetyl Betaine	0.30	-	-	-	-	50	-	-	25%	SSPB	@ 1% Na2CO3, All type 1 viscous
L 081	Dowfax 8390	0.30	C9 AOS	0.1	TEGBE	1.00	50	6	20.70%	21%	SSPB	@ 1% Na2CO3,
L 082	Cetyl Betaine	0.30	C9 AOS	0.1	TEGBE	1.00	50	-	-	Phase separation	SSPB	@ 1% Na2CO3, All type1, viscous
L 097	C12-15 15EO sulfonate	0.20	C12-15 9EO sulfonate	0.1	-	-	50	-	-	Phase separation	SSPB	@ 1% Na2CO3, type2
L 098	C12-15 15EO sulfonate	0.10	C12-15 9EO sulfonate	0.2	-	-	50	-	-	Phase separation	SSPB	@ 1% Na2CO3, type2
L 099	C12-13 12EO glyceryl sulfonate	0.30	-	-	-	-	50	-	-	Phase separation	SSPB	@ 1% Na2CO3, Not oil soluble
L 100	C12-15 7EO glyceryl sulfonate	0.30	-	-	-	-	50	-	-	Phase separation	SSPB	@ 1% Na2CO3, Not oil soluble
L 102	Dowfax 8390	0.30	-	-	TEGBE	0.30	50	-	all type 2	21.95%	DI	@ 1% Na2CO3
L 103	Dowfax 8390	0.30	-	-	TEGBE	0.20	50	8	21.50%	23.20%	DI	@ 1% Na2CO3
L 104	Dowfax 8390	0.30	-	-	TEGBE	0.10	50	12	22.30%	23%	DI	@ 1% Na2CO3
L 105	C12-15 15EO sulfonate	0.30	-	-	TEGBE	0.30	50	-	-	-	DI	@ 1% Na2CO3, macroemulsion
L 106	C12-15 15EO sulfonate	0.20	C12-15 9EO sulfonate	0.1	TEGBE	0.30	50	-	-	-	DI	@ 1% Na2CO3, macroemulsion

Table 5.18 Summary of surfactant screening results at high salinity (Cont.)

	Surfactant		Co-surfactant		Solvent Co Surfactant		Oil %	Sol. Ratio	Opt. Sal.	Max Sol. NaCl wt%	Brine	Comments
Exp. #	Name (structure)	wt%	Name (structure)	wt%	Cosolvent	Wt %		(cc/cc)	NaCl wt%	Clear		
L 107	C12-15 15EO sulfonate	0.30	-	-	-	-	50	-	-	20%	DI	@ 1% Na2CO3, macroemulsion
L 108	C12-15 15EO sulfonate	0.20	C12-15 9EO sulfonate	0.1	-	-	50	-	-	19%	DI	@ 1% Na2CO3, Macroemulsion
L 109	Na2CO3	1.00	-	-	-	-	50	-	-	-	DI	@ 1% Na2CO3, Macroemulsion
L 110	Na2CO3	1.00	-	-	TEGBE	0.75	50	-	-	-	DI	@ 1% Na2CO3, , Macroemulsion
L 111	C12-15 12EO sulfate	0.30	-	-	-	-	50	-	-	19%	DI	@ 1% Na2CO3
L 113	C12-15 12EO sulfate	0.30	C20-24 IOS (A)	0.1	-	-	50	-	-	14%	DI	@ 1% Na2CO3
L 114	C12-15 12EO sulfate	0.30	C15-18 IOS	0.1	-	-	50	-	-	15%	DI	@ 1% Na2CO3
L 115	C12-15 12EO sulfate	0.30	C16-17 7PO sulfate	0.1	-	-	50	-	-	14%	DI	@ 1% Na2CO3
L 117	Dowfax 8390	0.30	C12-15 12EO sulfate	0.30	-	-	50	7	17.80%	17%	DI	@ 1% Na2CO3
L 118	Dowfax 8390	0.30	C15-18 IOS	0.1	-	-	50	-	-	20%	DI	@ 1% Na2CO3, narrow type 3 window
L 119	Dowfax 8390	0.30	C12-15 15EO sulfonate	0.30	-	-	50	8	18.00%	16%	DI	@ 1% Na2CO3
L 120	Dowfax 8390	0.30	-	-	TDA 30EO	0.10	50	4	16.50%	19%	DI	@ 1% Na2CO3
L 121	C12-15 15EO sulfonate	0.30	C15-18 IOS	0.1	-	-	50	-	-	14%	DI	@ 1% Na2CO3
L 122	C12-15 15EO sulfonate	0.30	C12-15 12EO sulfate	0.30	-	-	50	20	15.50%	21%	DI	@ 1% Na2CO3
L 123	C_{17}-12EO-sulfate	0.30	-	-	-	-	50	-	-	18%	DI	@ 1% Na2CO3
L 124	C_{17}-12EO-sulfate	0.30	C12-15 15EO sulfonate	0.10	-	-	50	-	-	19%	DI	@ 1% Na2CO3
L 125	C_{17}-12EO-sulfate	0.30	C12-15 15EO sulfonate	0.30	-	-	50	-	-	20%	DI	@ 1% Na2CO3
L 126	C12-15 15EO sulfonate	0.30	C12-15 12EO sulfate	0.30	-	-	50	20	14.70%	19.75%	DI	@ 1% Na2CO3
L 126	C12-15 15EO sulfonate	0.30	C12-15 12EO sulfate	0.30	-	-	40	10	18.00%	19.75%	DI	@ 1% Na2CO3

Table 5.18 Summary of surfactant screening results at high salinity (Cont.)

	Surfactant		Co-surfactant		Solvent Co Surfactant		Oil %	Sol. Ratio	Opt. Sal.	Max Sol. NaCl wt%	Brine	Comments
Exp. #	Name (structure)	wt%	Name (structure)	wt%	Cosolvent	Wt %		(cc/cc)	NaCl wt%	Clear		
L 126	C12-15 15EO sulfonate	0.30	C12-15 12EO sulfate	0.30	-	-	30	8	20.20%	19.75%	DI	@ 1% Na2CO3
L 126	C12-15 15EO sulfonate	0.30	C12-15 12EO sulfate	0.30	-	-	20	-	-	19.75%	DI	@ 1% Na2CO3, all type 1
L 126	C12-15 15EO sulfonate	0.30	C12-15 12EO sulfate	0.30	-	-	10	-	-	19.75%	DI	@ 1% Na2CO3, all type 1
L 130	C_{17}-12EO-sulfate	0.50	C12-15 12EO sulfate	0.50	-	-	50	16	17.50%	21%	DI	@ 1% Na2CO3
L 130	C_{17}-12EO-sulfate	0.50	C12-15 12EO sulfate	0.50	-	-	40	17	19.10%	21%	DI	@ 1% Na2CO3
L 130	C_{17}-12EO-sulfate	0.50	C12-15 12EO sulfate	0.50	-	-	30	11	20.40%	21%	DI	@ 1% Na2CO3
L 130	C_{17}-12EO-sulfate	0.50	C12-15 12EO sulfate	0.50	-	-	20	9	21.00%	21%	DI	@ 1% Na2CO3
L 130	C_{17}-12EO-sulfate	0.50	C12-15 12EO sulfate	0.50	-	-	10	5	22.60%	21%	DI	@ 1% Na2CO3

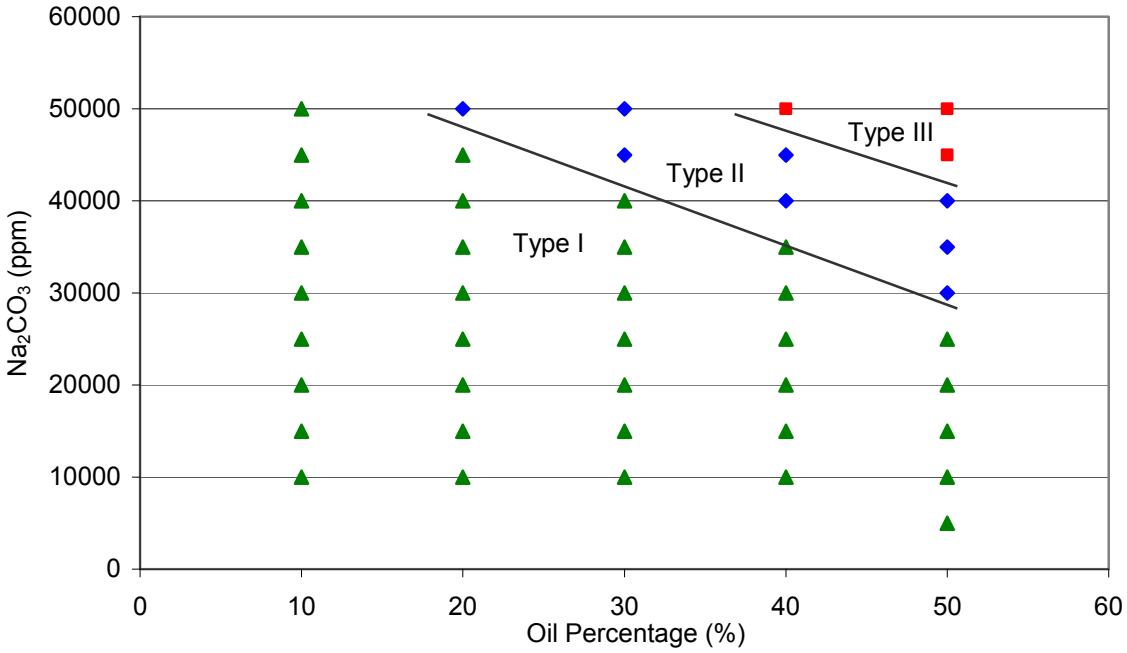

Figure 5.1 Activity Diagram for L-069 formulation

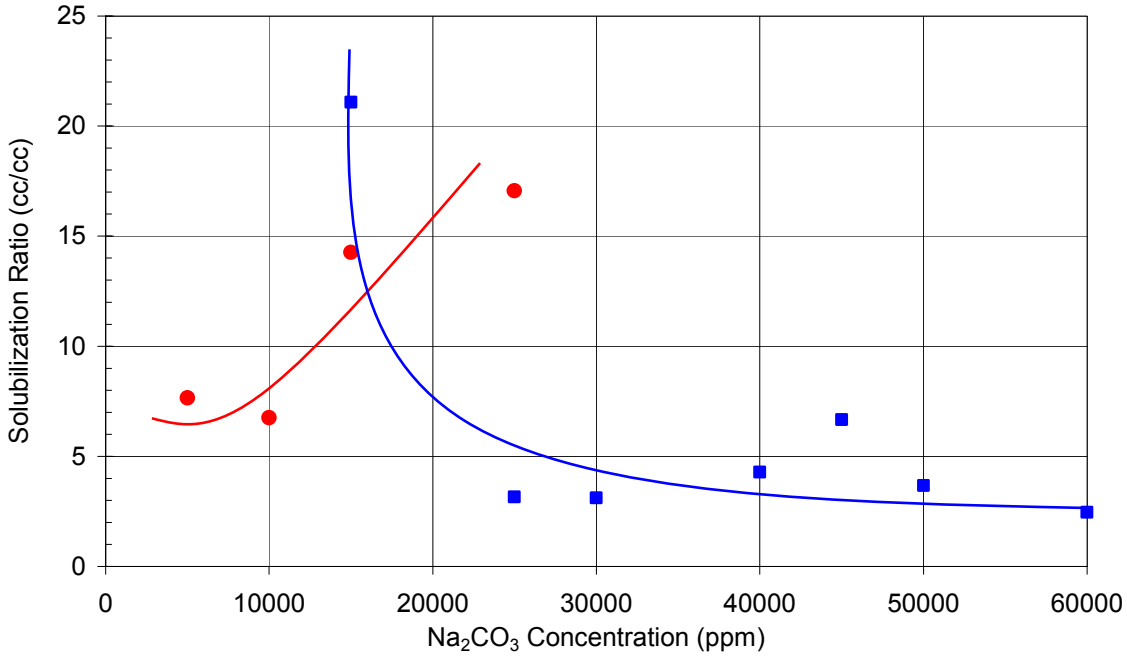

Figure 5.2 Solubilization ratios with 50% crude L after 93 days. L-055: 0.5% C_{24-28} IOS, 0.25% C_{15+} ABS and 2% TEGBE in SSFB

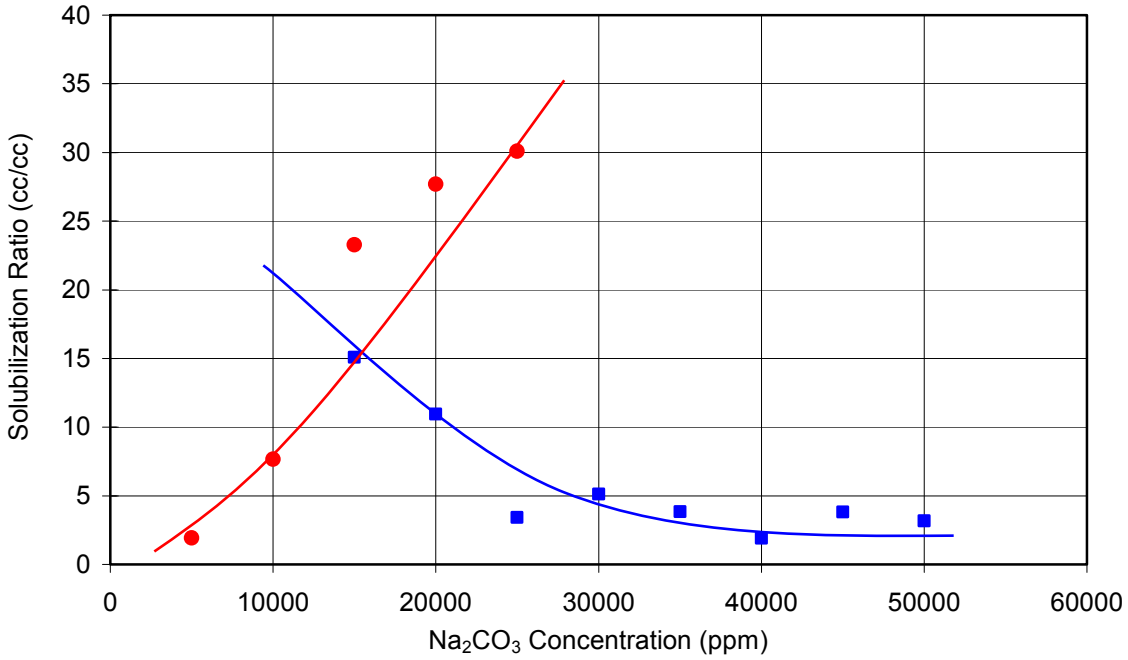

Figure 5.3 Solubilization ratios with 50% crude L after 98 days. L-068: 0.5% C_{24-28} IOS, 0.25% C_{15+} ABS and 1.4% TEGBE in SSFB

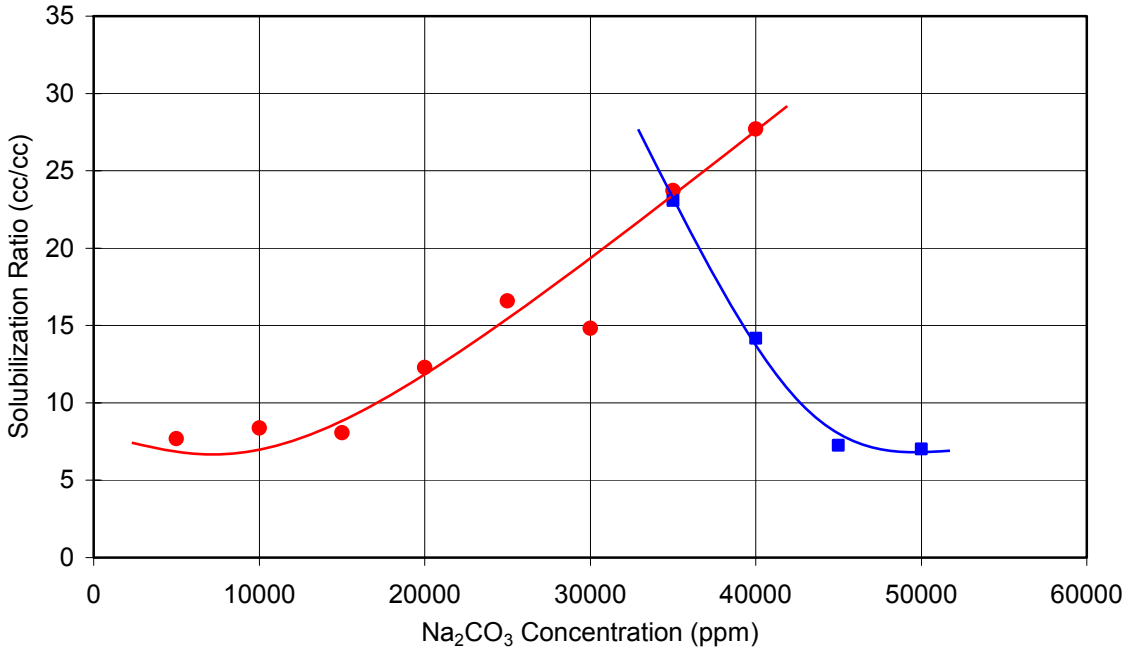

Figure 5.4 Solubilization ratios with 50% crude L after 38 days. L-069: 0.5% C_{24-28} IOS, 0.25% C_{15+} ABS and 0.3% TDA 30EO in SSFB

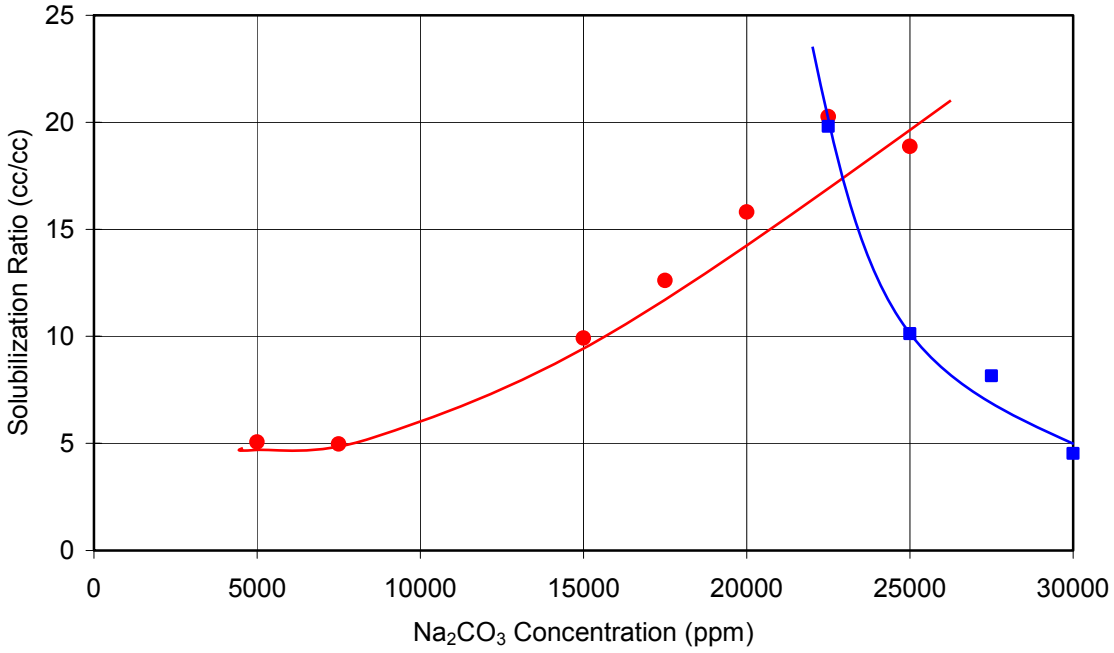

Figure 5.5 Solubilization ratios with 10% crude L after 141 days. L-018(G): 0.3% C_{32}-7PO-6EO Sulfate, 0.3% C_{20-24} IOS, 0.1% C_{13}-30EO, 0.4% Aerosol MA-80) in 1% NaCl

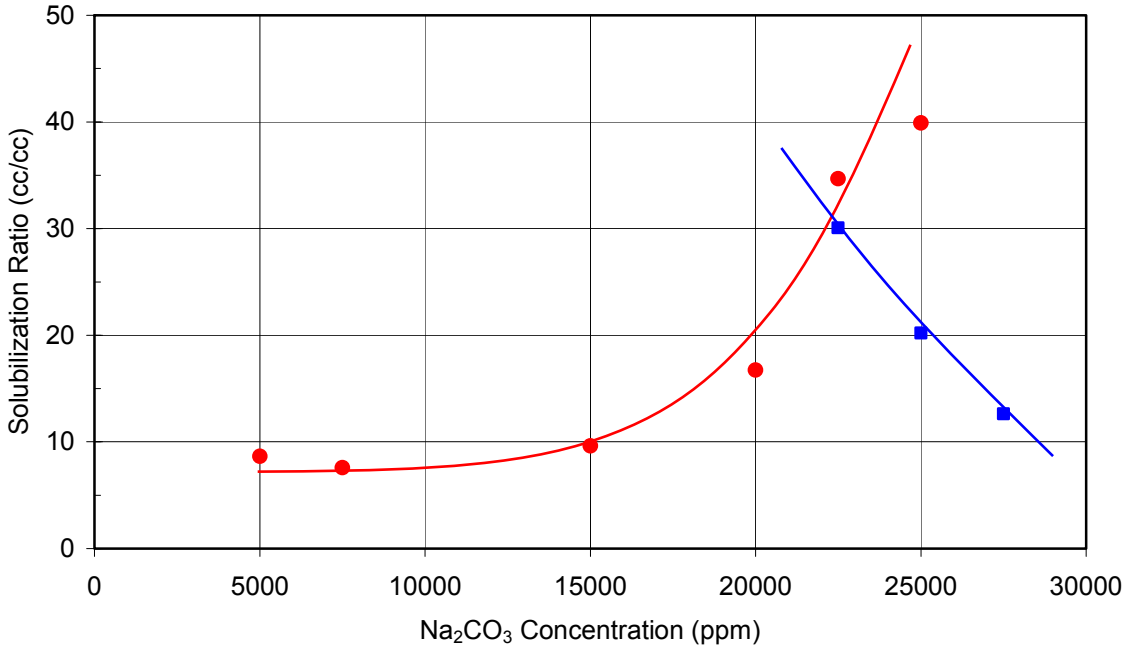

Figure 5.6 Solubilization ratios with 20% crude L after 141 days. L-018(G): 0.3% C_{32}-7PO-6EO Sulfate, 0.3% C_{20-24} IOS, 0.1% C_{13}-30EO, 0.4% Aerosol MA-80) in 1% NaCl

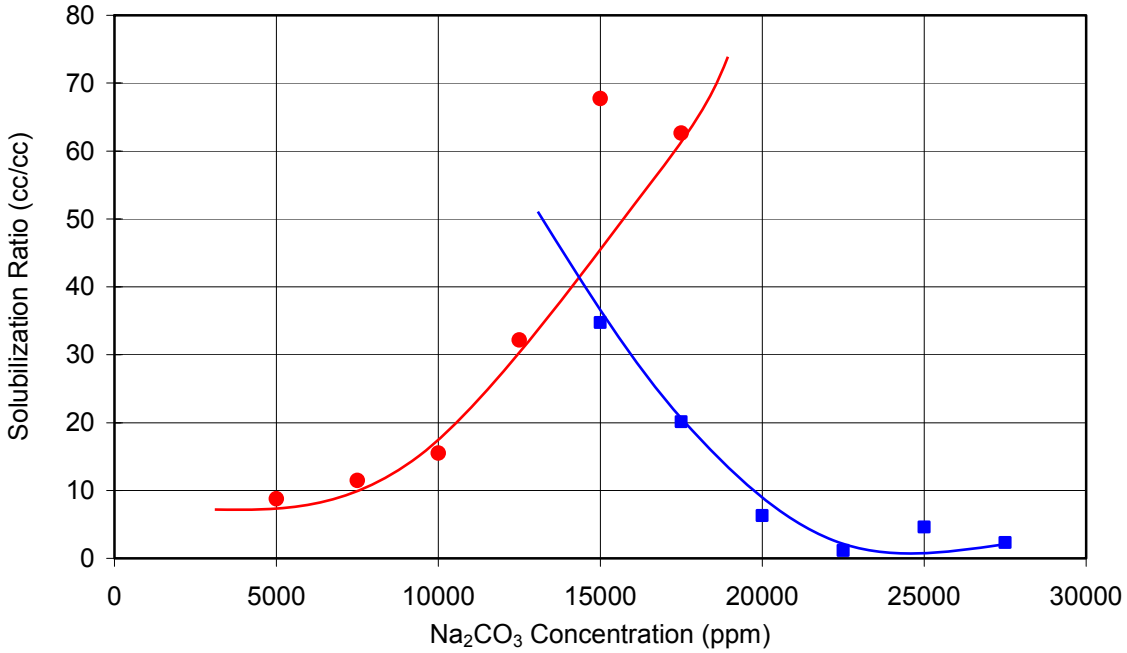

Figure 5.7 Solubilization ratios with 30% crude L after 141 days. L-018(G): 0.3% C_{32}-7PO-6EO Sulfate, 0.3% C_{20-24} IOS, 0.1% C_{13}-30EO, 0.4% Aerosol MA-80) in 1% NaCl

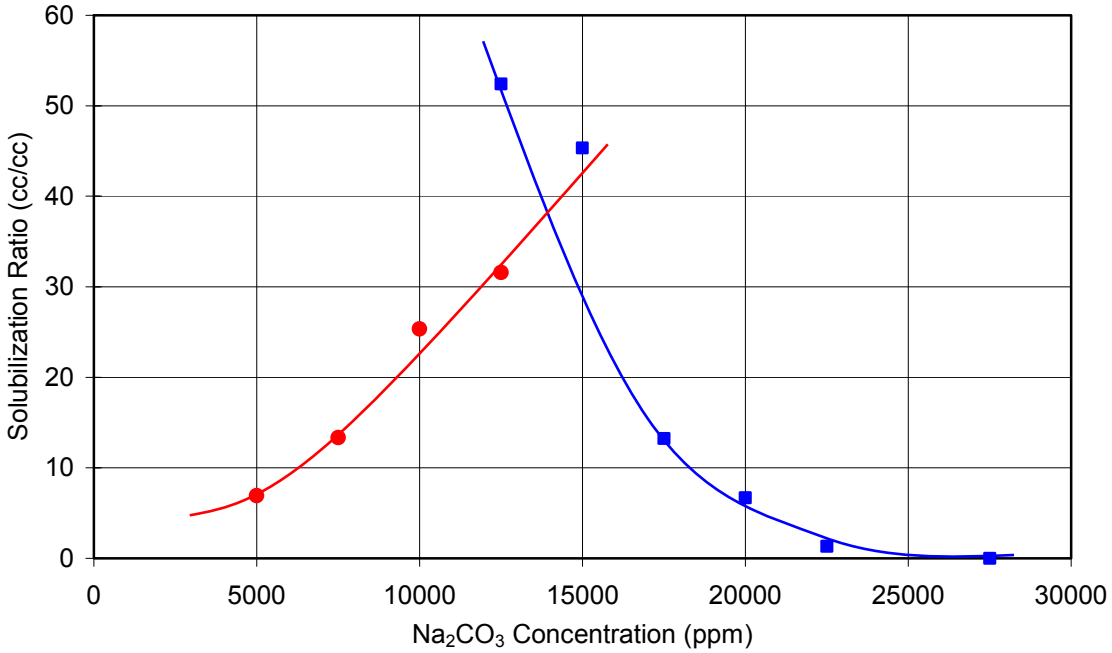

Figure 5.8 Solubilization ratios with 40% crude L after 141 days. L-018(G): 0.3% C_{32}-7PO-6EO Sulfate, 0.3% C_{20-24} IOS, 0.1% C_{13}-30EO, 0.4% Aerosol MA-80) in 1% NaCl

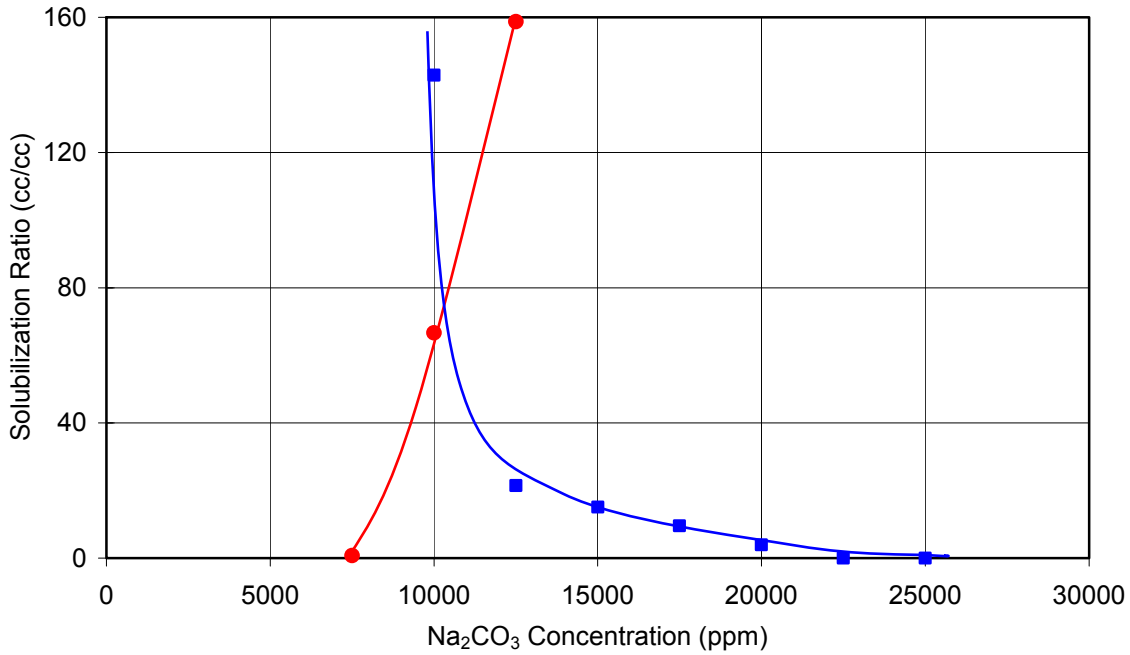

Figure 5.9 Solubilization ratios with 50% crude L after 141 days. L-036(1): 0.3% C_{32}-7PO-6EO Sulfate, 0.3% C_{20-24} IOS, 0.1% C_{13}-30EO, 0.4% Aerosol MA-80) in 1% NaCl

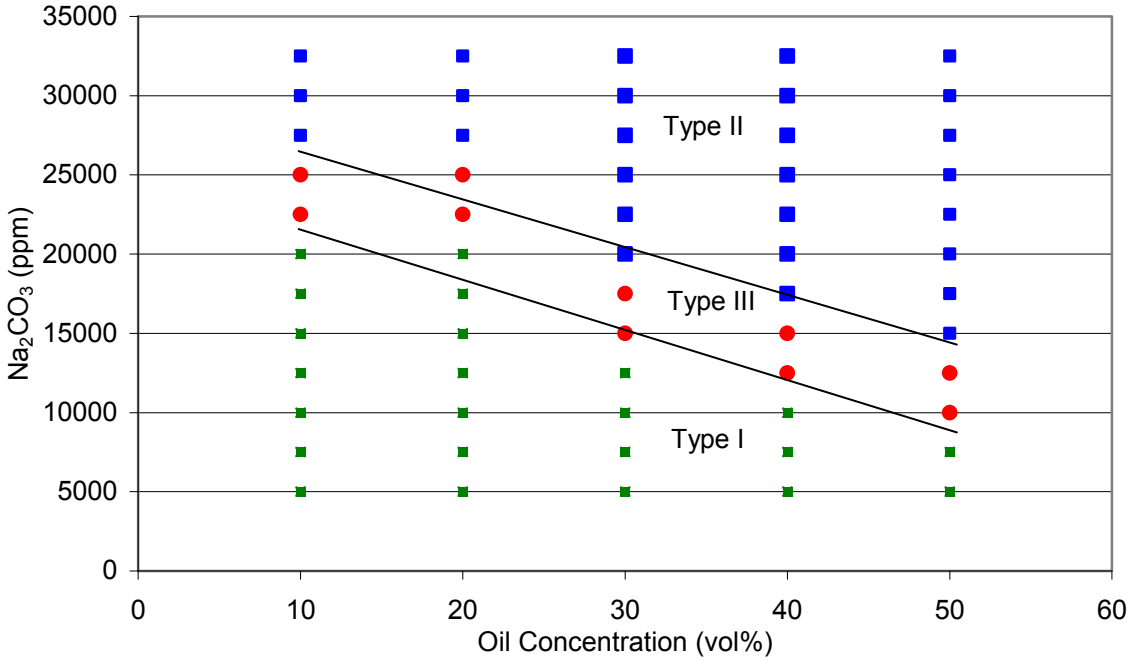

Figure 5.10 Activity diagram for 0.3% C_{32}-7PO-6EO Sulfate, 0.3% C_{20-24} IOS, 0.1% C_{13}-30EO, 0.4% Aerosol MA-80) in 1% NaCl with crude L

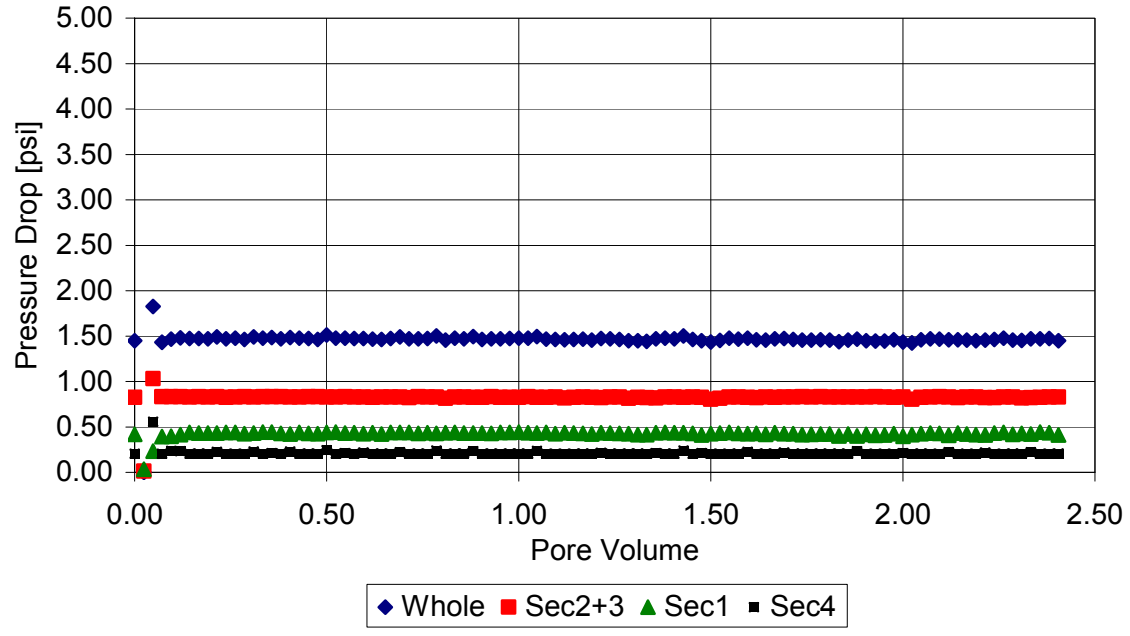

Figure 5.11 L-7 Brine Flood pressure

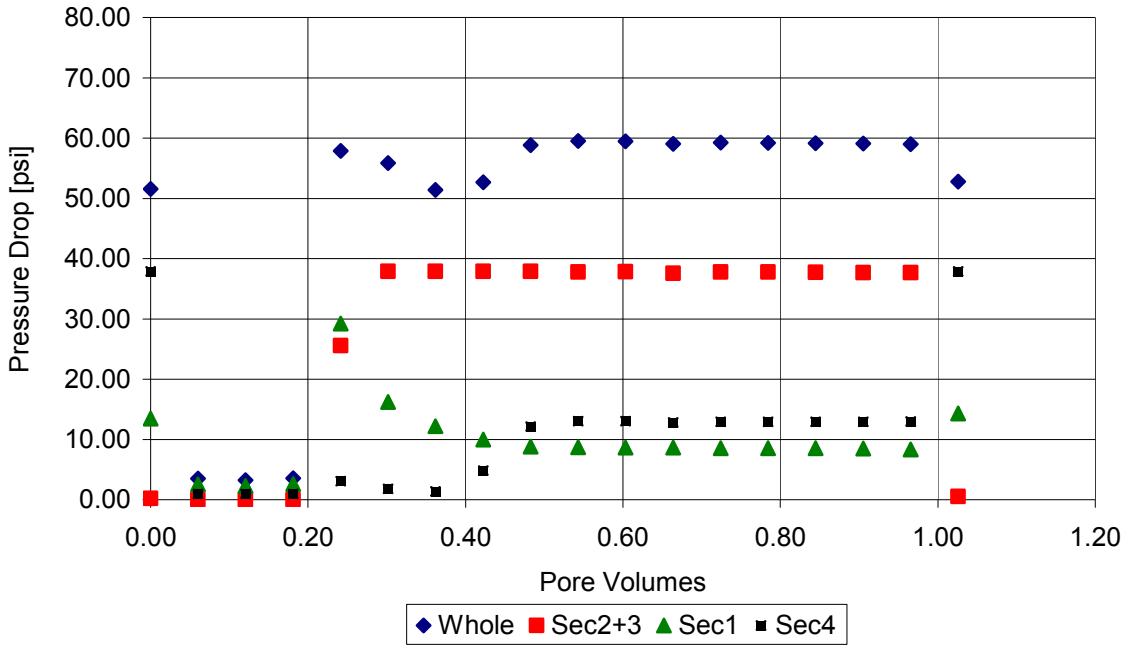

Figure 5.12 L-7 Oil Flood pressure

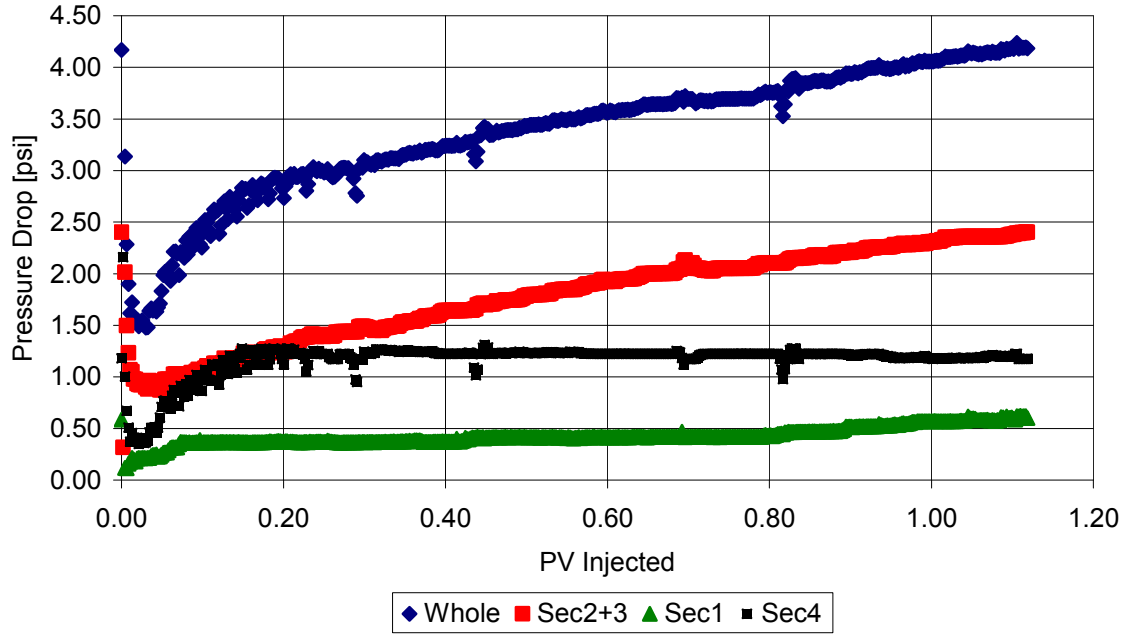

Figure 5.13 L-7 Water Flood pressure

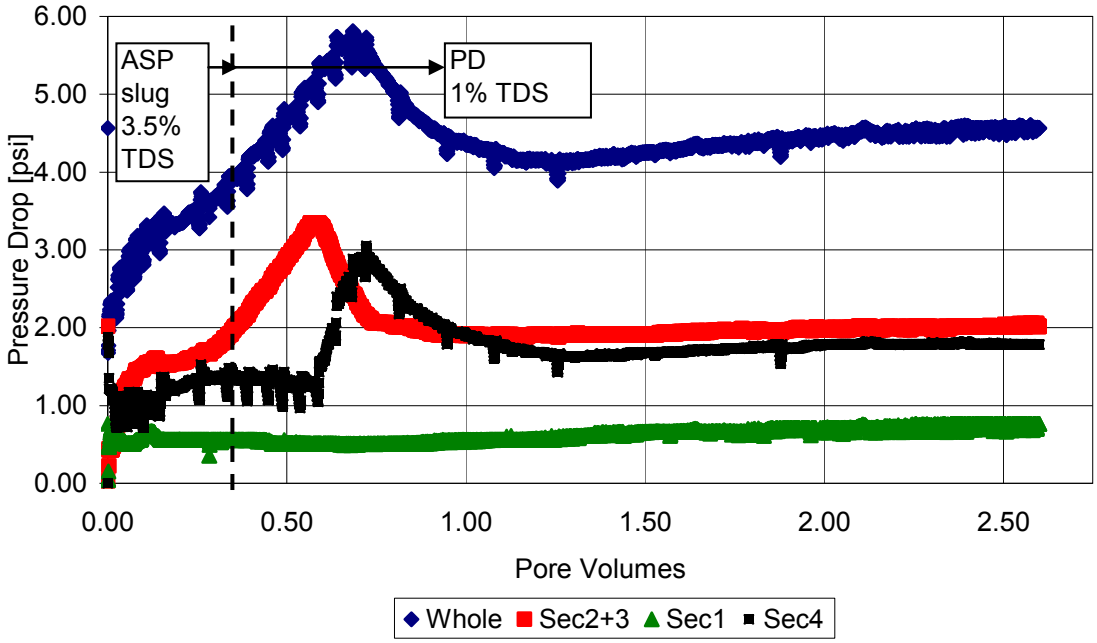

Figure 5.14 L-7 ASP Pressure

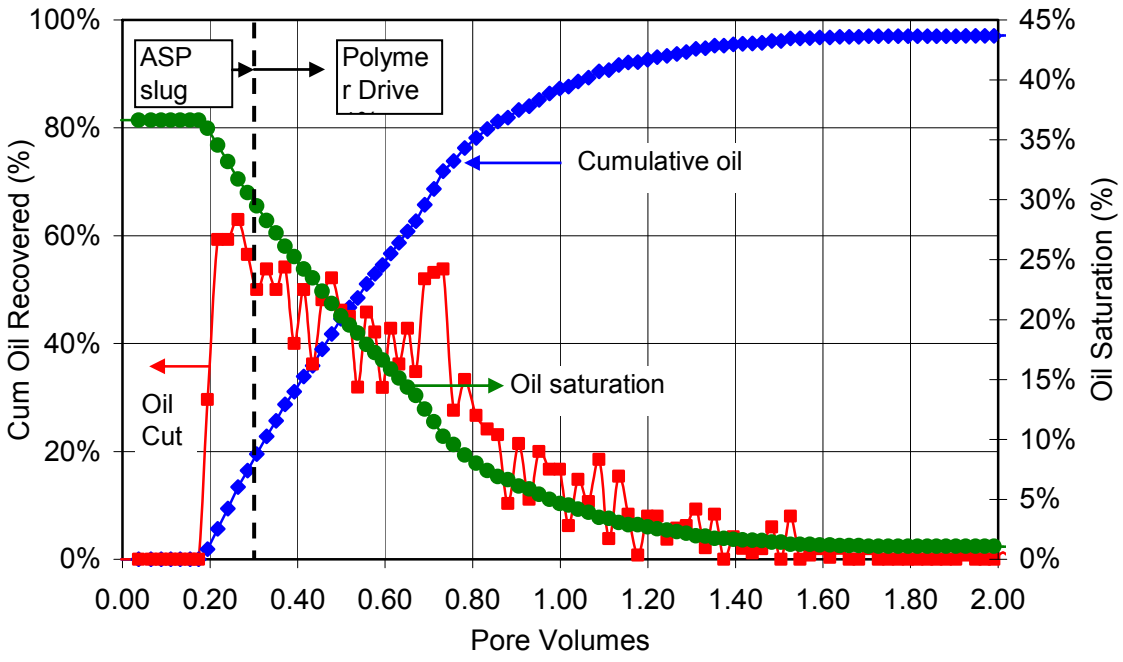

Figure 5.15 L-7 Oil Recovery

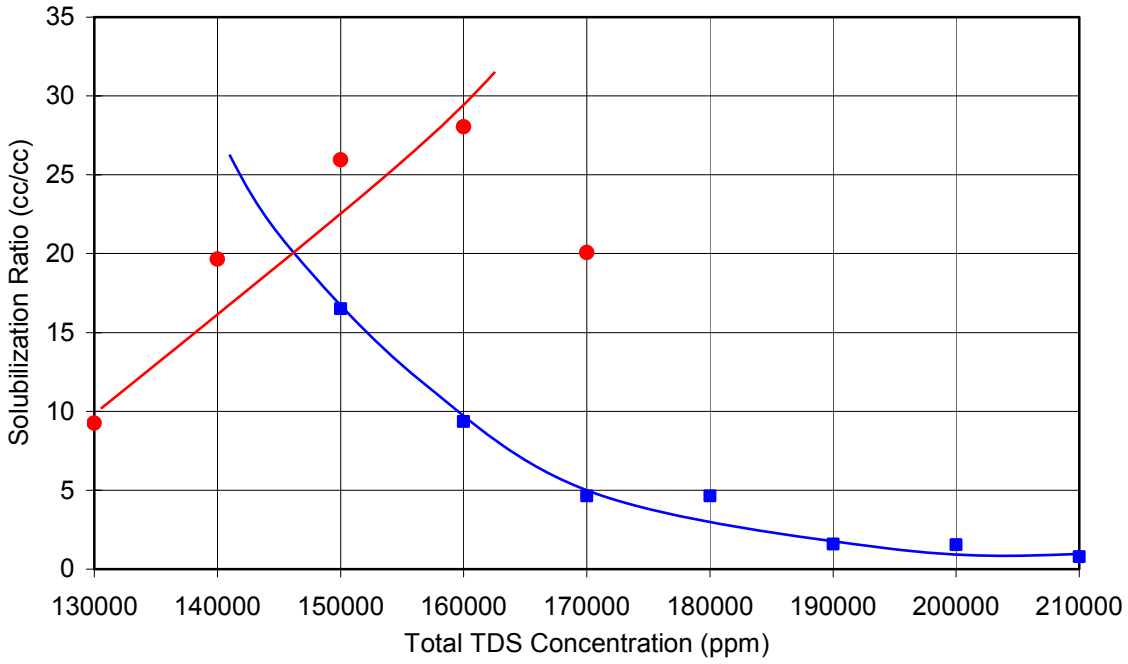

Figure 5.16 Solubilization ratios with 50% crude L after 11 days. L-126: 0.3% C_{12-15}-15EO-sulfonate and 0.3% C_{12-15}-12EO-sulfate in DI (1% Na_2CO_3 and NaCl scan)

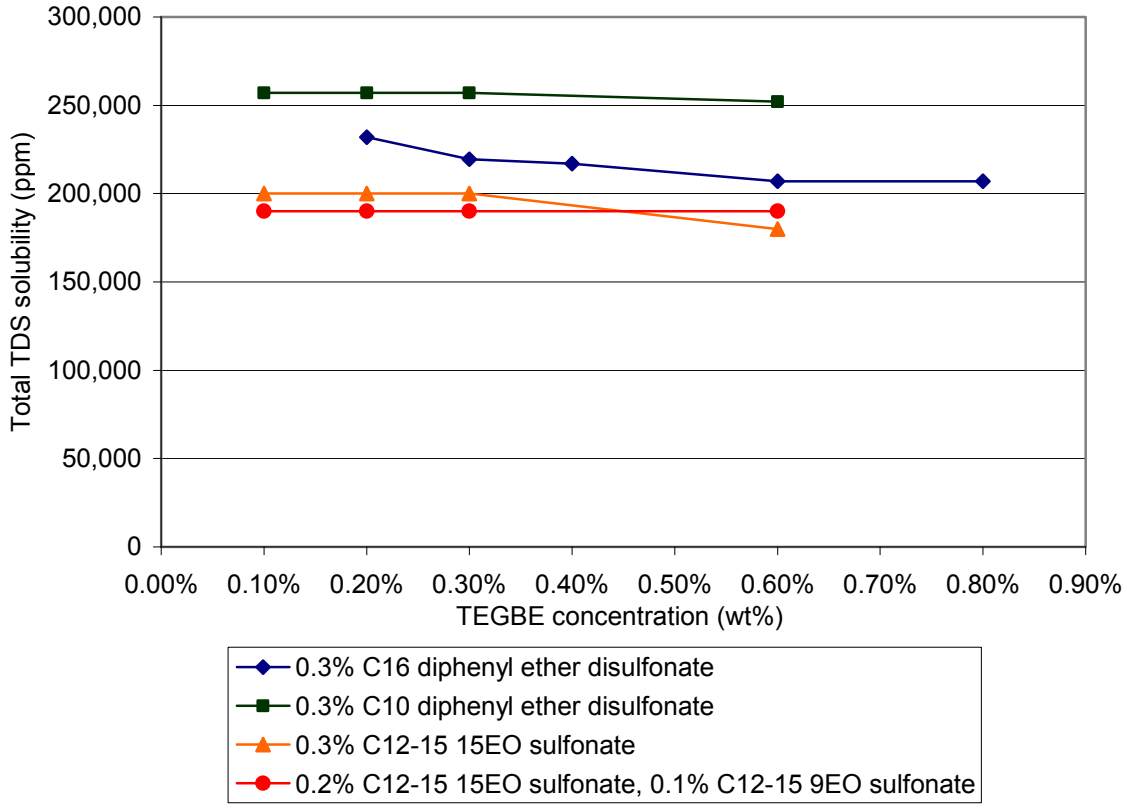

Figure 5.17 Effect of TEGBE concentrations on aqueous stability with 1% Na_2CO_3 at high salinity brine

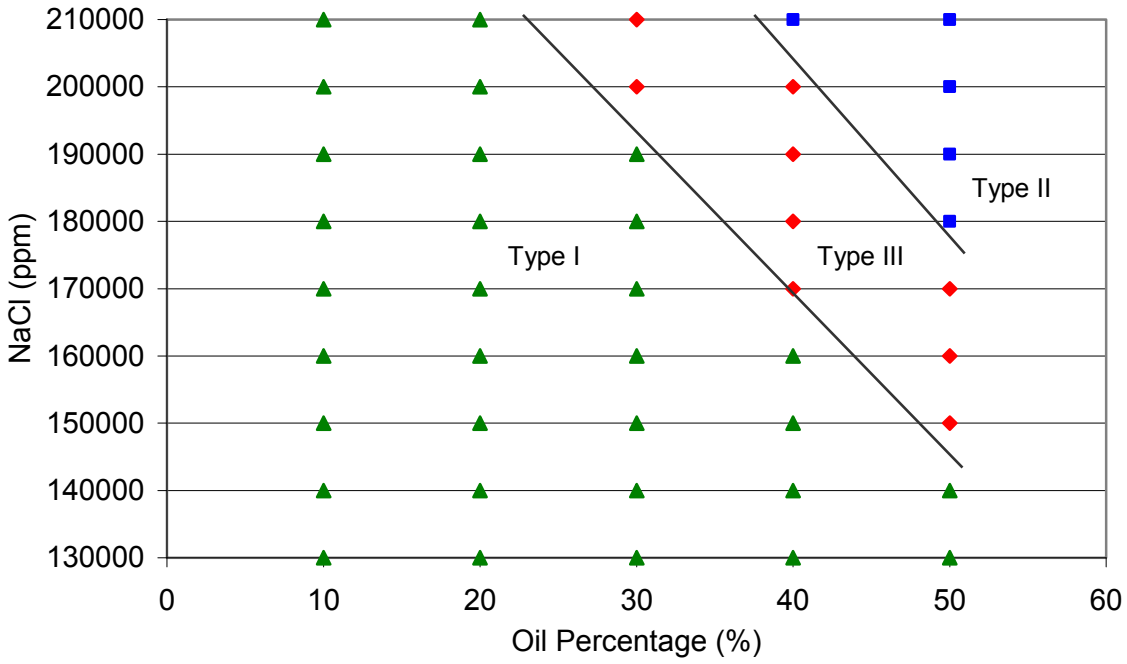

Figure 5.18 Activity diagram for 0.3% $C_{12\text{-}15}$-15EO-sulfonate and 0.3% $C_{12\text{-}15}$-12EO-sulfate with crude L

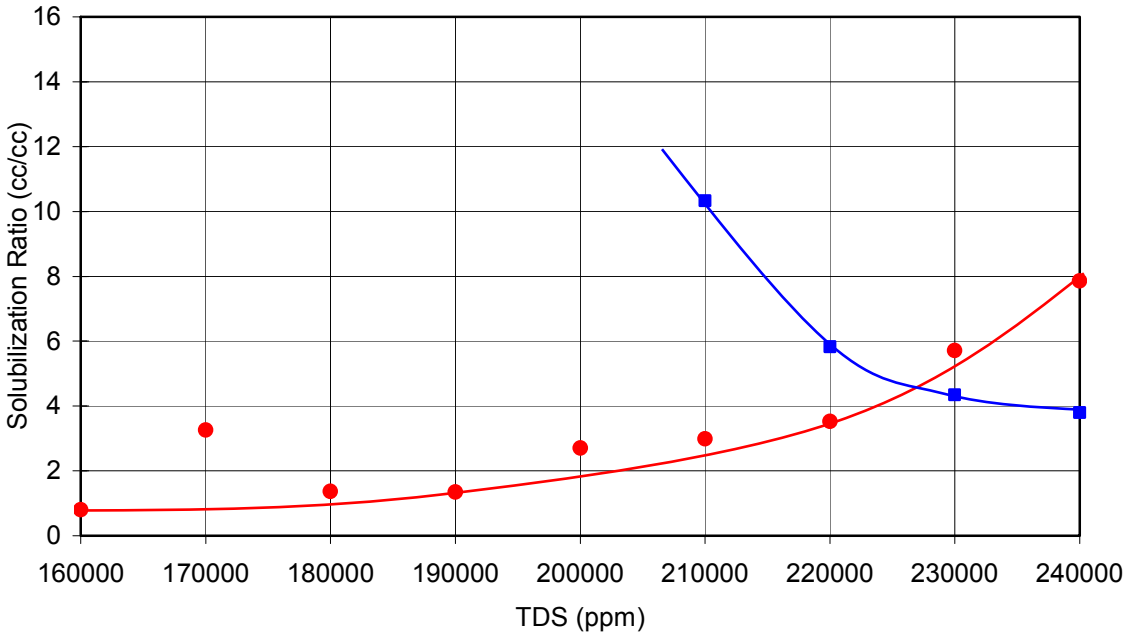

Figure 5.19 Solubilization ratios with 10% crude L after 9 days. L-130: 0.5% C_{17}-12EO-sulfate and 0.5% $C_{12\text{-}15}$-12EO-sulfate in DI (1% Na_2CO_3 and NaCl scan)

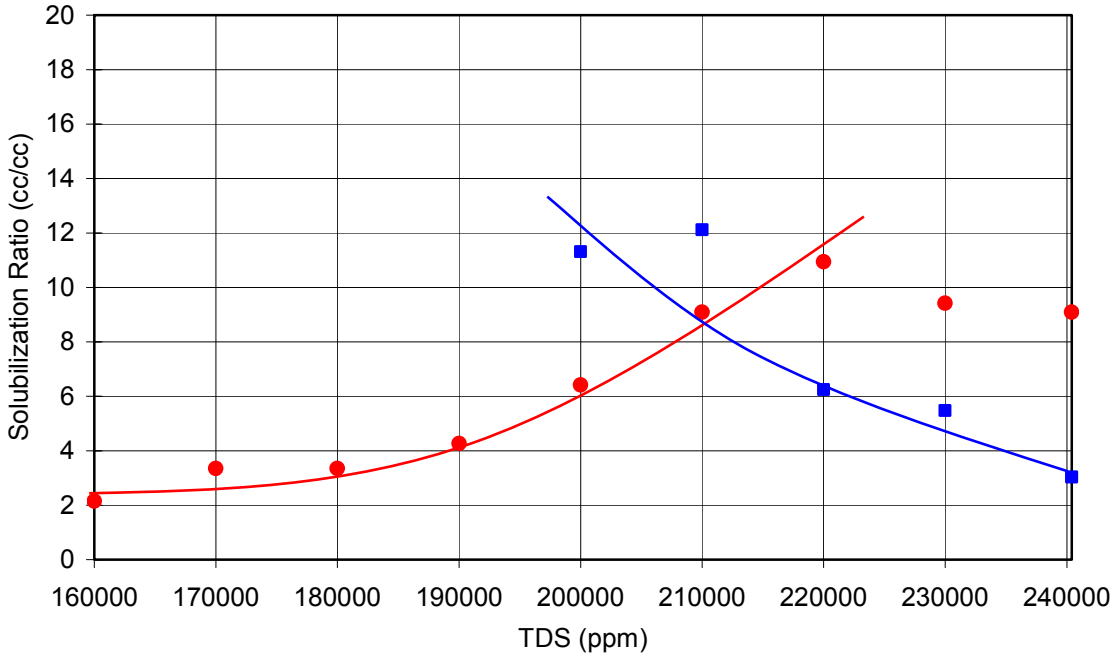

Figure 5.20 Solubilization ratios with 20% crude L after 9 days. L-130: 0.5% C_{17}-12EO-sulfate and 0.5% $C_{12\text{-}15}$-12EO-sulfate in DI (1% Na_2CO_3 and NaCl scan)

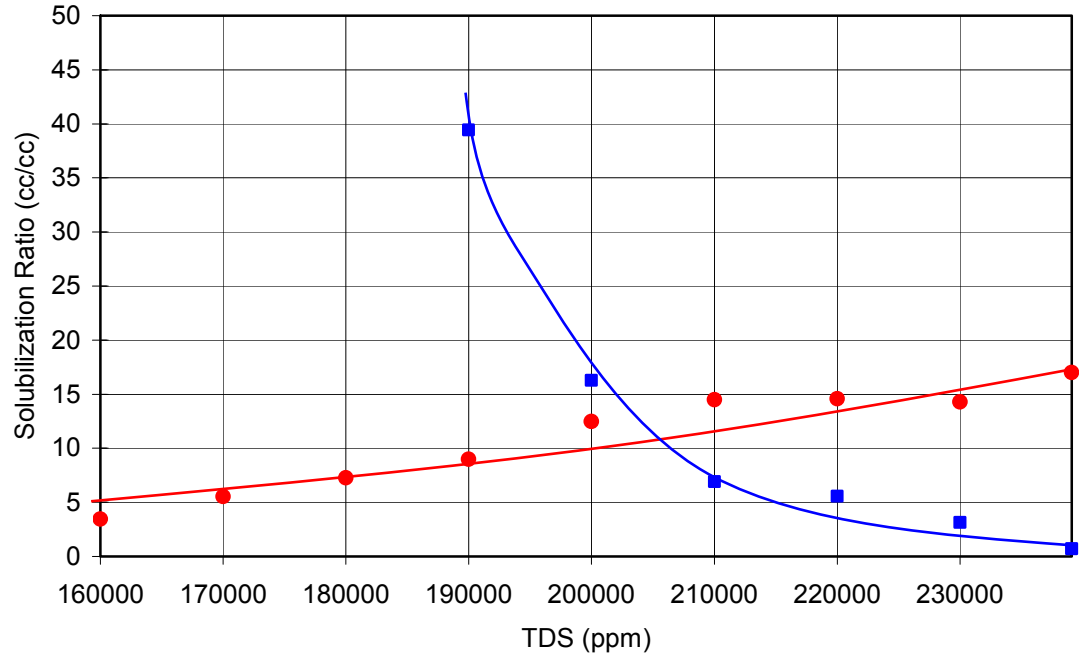

Figure 5.21 Solubilization ratios with 30% crude L after 9 days. L-130: 0.5% C_{17}-12EO-sulfate and 0.5% $C_{12\text{-}15}$-12EO-sulfate in DI (1% Na_2CO_3 and NaCl scan)

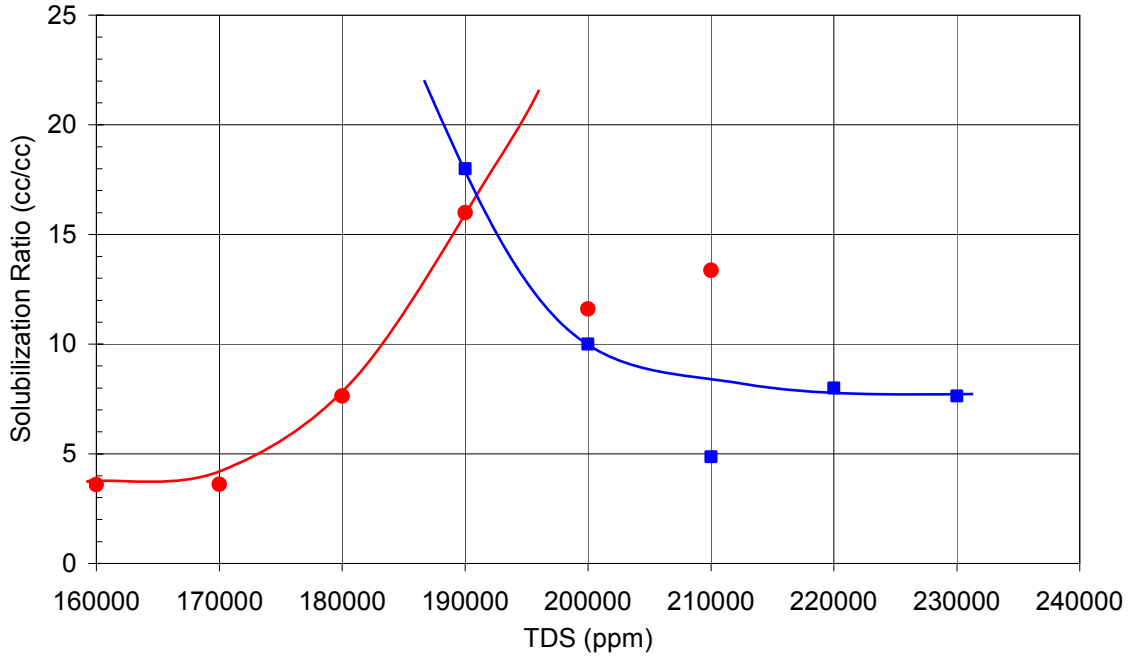

Figure 5.22 Solubilization ratio plot of phase behavior with 40% crude L after 9 days. L-130: 0.5% C_{17}-12EO-sulfate and 0.5% C_{12-15}-12EO-sulfate in DI (1% Na_2CO_3 and NaCl scan)

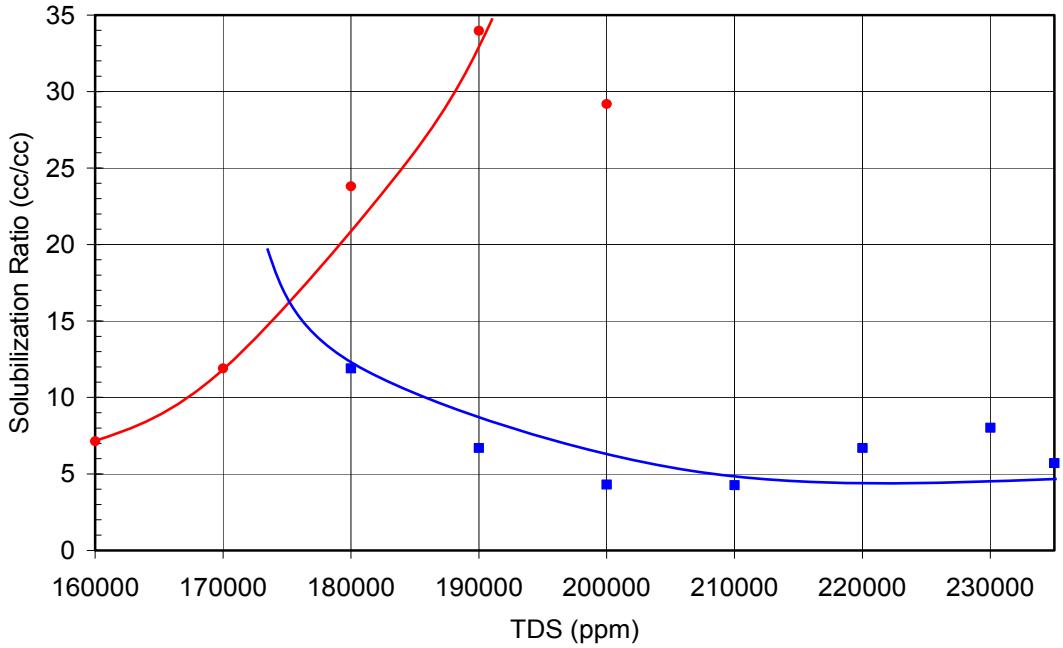

Figure 5.23 Solubilization ratio with 50% crude L after 9 days. L-130: 0.5% C_{17}-12EO-sulfate and 0.5% C_{12-15}-12EO-sulfate in DI (1% Na_2CO_3 and NaCl scan)

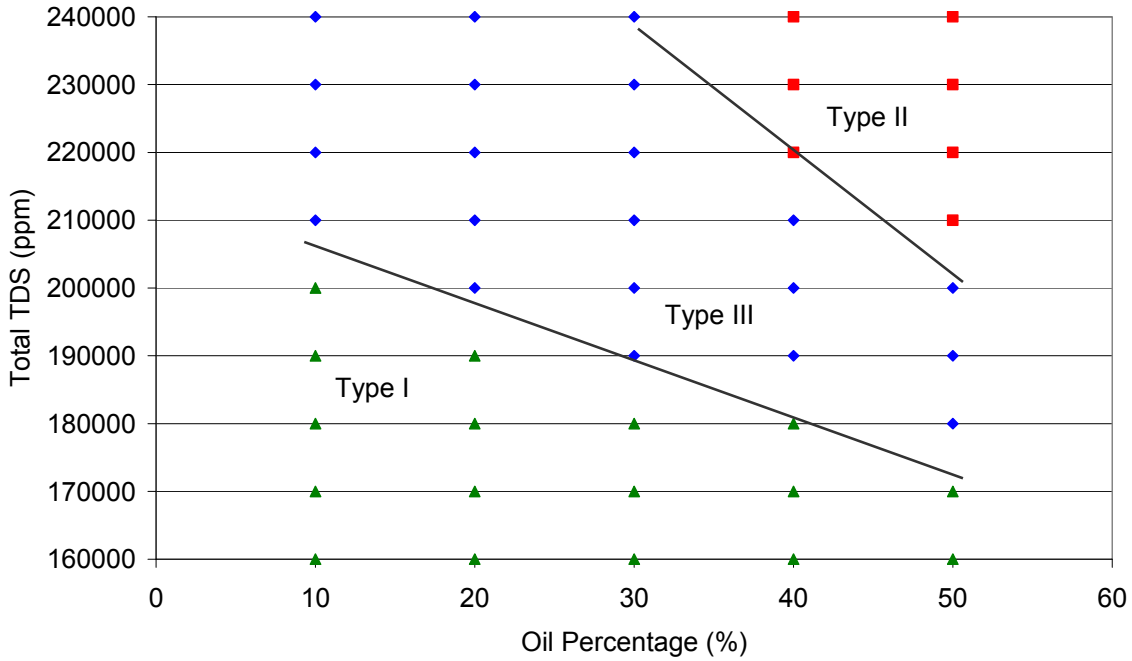

Figure 5.24 Activity diagram for 0.3% C_{17}-12EO-sulfate and 0.3% $C_{12\text{-}15}$-12EO-sulfate with crude L

CHAPTER 6: SUMMARY AND CONCLUSIONS

This chapter summarizes the key concepts applied and observations made from research on the development of surfactant formulations for two different crude oils. Improvements made to the surfactant formulation to achieve the desired phase behavior and aqueous stability are summarized. An important conclusion of this research is that surfactants with very large hydrophobes are sometimes needed even for light crude oils.

Both new and commercial surfactants were evaluated by phase behavior experiments. Alkyl benzene sulfonate (ABS) surfactants showed high solubilization ratios and low optimal salinity because of high hydrophobicity. However, aqueous solubility of high molecular weight ABS surfactants is limited unless high concentrations of co-solvent or co-surfactant are used. Internal olefin sulfonates (IOS) surfactants with a high carbon number were found to be promising surfactants, but also have limited aqueous solubility by themselves.

Guerbet alkoxy sulfate (GAS) surfactants and mixtures of GAS surfactants and IOS surfactants with large hydrophobes showed the best results. These GAS surfactants exhibited many desirable features due to their very large hydrophobes and mid chain branched structures. Another advantage of these surfactants is that the carbon chain length and the number of PO/EO groups in the molecule can be tailored to the oil to optimize performance.

Several co-solvents, non-ionic surfactants and sacrificial surfactants were used for improving aqueous solubility of the primary surfactants. Among alcohols and glycol ethers, TEGBE showed the best results. Also, the performance and structural features of non-ionic alcohol ethoxylate surfactants were evaluated as co-solvents. Before testing alcohol ethoxylates as a co-solvent, cloud points were considered. The main benefit the

alcohol ethoxylates offered was that only low concentrations can result in the same or better aqueous solubility enhancement when compared to alcohol and glycol ether co-solvents. Also, faced with the difficulty of reducing the co-solvent concentration for extremely large hydrophobe surfactants, sacrificial surfactants were introduced to provide temporary aqueous solubility. Thus, the use of Aerosol MA-80 was suitable for verifying the surfactant performance in core flood experiments.

This study included testing the best formulations with a core flood experiment for a reactive crude and a core flood experiment for a non-reactive crude. For core flood M-9, a 0.3 PV ASP slug containing 0.25% C32-7PO-6EO-sulfate, 0.25% C20-24 IOS, 0.25% TEGBE, and 0.4% Aerosol MA-80 was injected with 2000 ppm FP3630S followed by 2 PV of polymer drive with 1150 ppm FP3630S. The oil recovery was 97.9% and the final residual oil saturation was 0.008. The surfactant retention was only 0.01 mg/g of rock. For core flood (L-7) using the reactive crude, a 0.3 PV ASP slug containing 0.3% C32-7PO-6EO sulfate, 0.3% C20-24 IOS, 0.1% TDA-30EO, and 0.4% Aerosol MA-80 was injected with 3000 ppm FP3330S followed by a 2.5 PV of polymer drive with 2500 ppm FP3330S. The oil recovery was 97.1% and the final residual oil saturation was 0.011. These core floods successfully verified the efficacy of using large hydrophobe surfactants for recovering both reactive and non-reactive crudes.

This research amply demonstrates that by proper selection of the surfactant structures and the use of correct additives such as co-solubilizers, it is possible to develop cost effective ASP formulations under very different conditions. Large branched hydrophobes with appropriate PO and EO levels and the sulfate group were used as a new class of robust surfactants. In addition, the advantages of non-ionic surfactants as co-solvents or co-solubilizers was demonstrated for both a non-reactive crude oil and a reactive crude oil. Finally, a mixture of C1215-12EO sulfate and C17-12EO sulfate

surfactants with sodium carbonate alkali showed excellent phase behavior with an optimum salinity of about 200,000 ppm of the reactive crude oil.

BIBLIOGRAPHY

Abe, M., Schechter, D., Schechter, R.S., Wade, W.H., Weerasooriya, U., and Yiv, S. "Microemulsion Formation with Branched Tail Polyoxyethelene Sulfonate Surfactants," *JCIS*, Vol.114, No. 2, 342-356, 1986

Adkins, S., Liyanage, P. J., Arachchilage, G. W. P., Mudiyanselage, T., Weerasooriya, U., and Pope, G. A. "A New Process for Manufacturing and Stabilizing High-Performance EOR Surfactants at Low Cost for High-Temperature, High-Salinity Oil Reservoirs", SPE 129923 presented at SPE IOR Symposium, Tulsa, OK, 25-28 April, 2010.

Aoudia, Mohamed. "Optimum Microemulsions Formulated with Propoxylated Guerbet Alcohol and Propoxylated Tridecyl Alcohol Sodium Sulfates," Journal of Dispersion Science and Technology 16(2), 1995.

Austad, Tor and Milter, Jess "Surfactant Flooding in Enhanced Oil Recovery," Surfactants: Fundamentals and Applications in the Petroleum Industry, Cambridge University Press, October, 1998.

Bourrel, M. and Schechter, R. S. "Microemulsions and Related Systems," Marcel Dekker, Inc., New York, NY, 1988.

Dwarakanath, V., Chaturvedi, T., Jackson, A.C., Malik, T., Siregar, A., and Zhao, P. "Using Co-Solvents to Provide Gradients and Improve Oil Recovery during Chemical Flooding in a Light Oil Reservoir," SPE 113965, paper presented at the SPE/DOE IOR Symposium, April 2008.

Falls, A.H., Thigpen, D.R., Nelson, R.C., Ciaston, J.W., Lawson, J.B., Good, P.A., Ueber, R.C., and Shahin, G.T. "A Field Test of Co-Surfactant Enhanced Alkaline Flooding," SPE 24117, August 1994.

Flaaten, A.K. "Experimental study of Microemulsion Characterization and Optimization in Enhanced Oil Recovery: A Design Approach for Reservoirs with High Salinity and Hardness," M.S. Thesis, University of Texas at Austin, December 2007.

Flaaten, A.K., Nguyen, Q.P., and Pope, G.A.: "A Systematic Laboratory Approach to Low-Cost, High-Performance Chemical Flooding," SPE 113469, paper presented at SPE IOR Symposium, Tulsa, OK, April 2008.

Gogarty, W.B. and Tosch, W.C. "Miscible-Type Waterflooding: Oil Recovery with Micellar Solutions," Journal of Petroleum Technology, December 1968, 1407-1414.

Green, D. W. and Willhite, G.P. "Enhanced Oil Recovery," SPE Textbook Series, Henry L. Doherty Memorial Fund of AIME, Society of Petroleum Engineers, Richardson, Texas, Volume 6, 1998.

Healy, R. N., Reed, R. L., and Stenmark, D. K. "Multiphase Microemulsion Systems," *SPEJ* (June 1976), 147.

Hirasaki, G.J., Miller, C.A., and Puerto, M. "Recent Advances in Surfactant EOR," IPTC 115386, presented at the IPTC held in Kuala Lumpur, December 2008.

Hsieh, W.C. and Shah, D.O. "The Effect of Chain Length of Oil and Alcohol as well as Surfactant to Alcohol Ratio on the Solubilization, Phase Behavior and Interfacial Tension of Oil/Brine/Surfactant/Alcohol Systems," SPE 6544, 1977.

Huh, C. "Interfacial Tensions and Solubilizing Ability of a Microemulsion Phase that Coexists with Oil and Brine," Journal of Colloid and Interface Science (September 1979), 408.

Jackson, A.C. "Experimental Study of the Benefits of Sodium Carbonate on Surfactants for Enhanced Oil Recovery," M.S Thesis, University of Texas at Austin, December 2006.

Jayanti, S., Britton, L.N., Dwarakanath V., and Pope, G.A. "Laboratory Evaluation of Custom Designed Surfactants to Remediate NAPL Source Zones," Environmental Science and Technology, 5491-5497, 2002.

Jennings, H.Y, Jr. "A Study of Caustic Solution-Crude Oil Interfacial Tensions," *SPEJ*, June, 197-202, 1975.

Labrid, Jean. "The Use of Alkali Agents in Enhanced Oil Recovery Processes," Institut Francais du Petrole, Rueil-Malmaison, France. Critical Reports on Applied Chemistry, Vol. 33, 1991.

Lake, L. W. "Enhanced Oil Recovery," Prentice-Hall, Upper Saddle River, NJ, 1989.

Levitt, D.B. "Experimental Evaluation of High Performance EOR Surfactants for a Dolomite Oil Reservoir," M.S. Thesis, University of Texas, December 2006.

Levitt, D.B., and Pope, G.A. "Selection and Screening of Polymers for Enhanced Oil Recovery," SPE 113845, SPE IOR Symposium, Tulsa, OK, April 2008.

Levitt, D.B., Jackson, A.C., Heinson, C., Britton, L.N., Malik, T., Dwarakanath, V., and Pope, G.A. "Identification and Evaluation of High-Performance EOR Surfactants," SPE 100089-PA, *SPE Reservoir Evaluation and Engineering,* 12(2), April, 2009, 243-253.

Liu, Q., Dong, M., Ma, S. and Tu, Y. "Surfactant enhanced alkaline flooding for western Canadian heavy oil recovery," Colloids Surf., A FIELD Full Journal Title:Colloids and Surfaces, A: Physicochemical and Engineering Aspects, 293(1-3): 63-71. 2007.

Maerker, J.M. and Gale, W.W. “Surfactant Flood Process Design for Loudon,” SPERE, 36-44, 1992.

Milton J.R "Surfactants and Interfacial Phenomena," John Wiley & Sons, Hoboken, NJ, 2004.

Nelson, R.C. and Pope, G. A. “Phase Relationships in Chemical Flooding,” SPE 6773, ATCE in Denver, CO. October, 1977.

Nelson, R.C., Lawson, J. B., Thigpen, D. R. and Stegemeier, G. L. “Co-Surfactant Enhanced Alkaline Flooding,” SPE 12672, 1984.

Pope, G. A., Wu, W., Narayanaswamy, G., Delshad, M., Sharma, M. M., and Wang P. "Modeling Relative Permeability Effects in Gas-Condensate Reservoirs With a New Trapping Model," SPE Reservoir Evaluation and Engineering, 171-178, April 2000.

Sanz, C. A. and Pope, G. A. “Alcohol-Free Chemical Flooding: From Surfactant Screening to Coreflood Design,” SPE 28956, SPE Symposium on Oilfield Chemistry, San Antonio, TX, February, 1995.

Sahni, V. "Experimental Evaluation of Co-Solvents in Development of High Performance Alkali/Surfactant/Polymer Formulations for Enhanced Oil Recovery," M.S. Thesis, University of Texas, December 2009.

Sahni, V., Dean, R. M., Britton, C., Kim, D.H., Weerasooriya, U., and Pope, G.A., "The Role of Co-Solvents and Co-Surfactants in Making Chemical Floods Robust," SPE 130007, presented at SPE IOR Symposium, Tulsa, OK, 25-28 April, 2010.

Salter, S.J. “The Influence of Type and Amount of Alcohol on Surfactant-Oil-Brine Phase Behavior and Properties,” SPE 6843, presented at the SPE Annual Meeting, Denver, CO, 1977.

Slaughter W.S. "Stability of Polymers used for Enhanced Oil Recovery," M.S. Thesis, University of Texas, May 2010.

Sorbie, Kenneth “Polymer Improved Oil Recovery,” Blackie and Son Ltd, Glasgow, 1991.

Stegemeier, G.L. ‘‘Mechanisms of Entrapment and Mobilization of Oil in Porous Media,’’ *Improved Oil Recovery by Surfactant and Polymer Flooding*, D.O. Shah and R.S. Schechter (eds.), Academic Press, New York City (1977) 55–91.

Talley, L.D., "Hydrolytic Stability of Alkylethoxy Sulfates," SPE 14912, 1988

Trogus, F.J., Sophany, T., Schechter R. S., and Wade, W.H. "Static and Dynamic Adsorption of Anionic and Nonionic Surfactants," SPE 6004-PA, October 1977.

Varadaraj, R., Bock, J., Valint, P., Jr., Zushma, S. and Thomas, R., "Fundamental interfacial properties of alkyl-branched sulfate and ethoxy sulfate surfactants derived from Guerbet alcohols," *Journal of Physical*, Chemistry, 95(4): 1671-6, 1991.

Labrid, Jean. “The Use of Alkali Agents in Enhanced Oil Recovery Processes,” Institut Francais du Petrole, Rueil-Malmaison, France. Critical Reports on Applied Chemistry, Vol. 33, 1991.

Wessen, L.L and Harwell, J.H., "Dilute Surfactant Adsorption in Porous Media," in Surfactants: Fundamentals and Applications in the Petroleum Industry, Schramm, L.L., ed., Cambridge University Press, New York, 2000.

Winsor, P. A. “Solvent Properties of Amphiphilic Compounds,” Butterworths, London, 1954.

Wu, Y., Shuler, P., Blanco, M., Tang, Y., and Goddard, W.A. “A Study of Branched Alcohol Propoxylate Sulfate Surfactants for Improved Oil Recovery,” SPE 95404, 2005.

Yang, H., Britton C., Liyanage, P. J., Solairaj, S., Kim, D.H., Nguyen, Q., Weerasooriya U., and Pope, G.A. "Low-Cost, High-Performance Chemicals for Enhanced Oil Recovery," SPE 129978, presented at the SPE/DOE IOR Symposium, Tulsa, OK, April 2010

Zhao, P. "Developments of High-Performance Surfactants for Difficult Oils," M.S Thesis, University of Texas at Austin, December 2007.

Zhao, P., Jackson, A.C., Britton, C., Kim, D.H., Britton, L.N., Levitt, D.B., and Pope, G.A “Development of High-Performance Surfactants for Difficult Oils,” SPE 113432, presented at the SPE/DOE IOR Symposium, Tulsa, OK, April 2008.

Zhang, Leslie D. and Hirasaki, George J. “Favorable Attributes of Alkali-Surfactant-Polymer Flooding,” SPE 99744, IOR Symposium in Tulsa, OK. April, 2006.

Zhang, L. D. and Hirasaki, G. J. “Surface Chemistry of Oil Recovery from Fractured, Oil-Wet, Carbonate Formations,” *SPEJ*, 2004.

Zhang, R. and Somasundaran, P., "Advances in adsorption of surfactants and their mixture at solid/solution interfaces," *Adv. Colloid Interface Sci.*, Vol.123-126, 213-229, 2006.

VITA

Hyuntae Yang, the son of Nakso Yang and Youngjin Ahn was born in Seoul, Korea in October, 12, 1981. After graduating from Sang-Moon High school, Seoul in February, 2000, he entered Yonsei University. While he was an undergraduate, he had undergone two and half years of military service as a process engineer at defense industry in South Korea. There he earned a Bachelor of Science degree in Chemistry in February, 2008. In January of 2008 he was admitted to the Graduate School at The University of Texas at Austin for petroleum engineering.

Permanent address: Acrovista Apt B-2201, Seocho 4-Dong, Seocho-Gu,
Seoul, South Korea, 137-921

This thesis was typed by the author.